A Hitchhiker's Guide to Multiple Scattering

An Incomplete Collection of Mostly Steady-State Monoenergetic Neutral-Particle Problem Solutions

Exact Analytic, Monte Carlo and Approximate Solutions in Transport Theory

Eugene d'Eon
8i, Wellington, New Zealand

July 24, 2016

Contents

1 Introduction

The flow of neutral particles which interact with a background material but not with themselves is described in some generality by a linear kinetic, or transport, equation. This equation, while algebraically complex, has a very simple physical content; it is simply the mathematical statement of particle conservation in phase space. - Jerry Pomraning [1997].

1.1 What is this Document?

1.1.1 Brief Intro

This book is an incomplete, dynamic collection of solutions to *multiple scattering* problems. These solutions are gathered from many disciplines, including radiative transfer, neutron transport, and computer graphics. In addition to providing *Monte Carlo* solutions to most problems (in the form of explicit code together with numerical benchmark values), both exact and common approximate *deterministic* solutions are provided, wherever possible. We make no attempt to provide theory and derivations for any solution. Instead, this book is intended as a reference tool that collects as many known solutions as possible in one place under one notation. We also focus on so-called “model problems" in transport theory—those problems that are simple enough to attract attempts at exact analytic solutions. Pointers to other works that provide the missing theory and derivations are provided. Any collection of this kind will invariably be incomplete, but we will update and grow this collection over time.

1.1.2 Expanded Intro

This book is a collection of solutions to multiple scattering problems. We use the term “multiple scattering" to refer to non-trivial applications of both *linear transport theory* and the problem of *random flights*. Both of these mathematical disciplines study the motion (transport) of neutral particles (or energy). Particle transport is often subject to random absorption (capture) events, which cause particles to leave the system. Additionally, it is common for random scattering events in the medium (or at the boundaries) to cause particles to change direction during flight. We are interested in the statistics of motion of a limited class of such transport problems.

More precisely, in this book we consider *scattering problems* consisting of:

- Specifying the permissible positions and directions that particles may take, comprising the *phase space* (for example, infinite three-dimensional space with a continuous distribution of directions, or, left/right motion along a one-dimensional domain)
- Specifying a distribution of initial position(s) and direction(s) for the birth of particles, comprising the *source* (for example, a point source that emits isotropically, or a uniform distribution of parallel rays arriving at the surface of a slab)
- Specifying how free-path lengths between particle events are distributed after birth and after any scattering event. Particles may be absorbed, or otherwise exit the system, or change direction due to random scattering events in the medium or at a boundary between two differing regions of the medium. The nature of these (random or deterministic) deviations from straight motion needs to be specified. This is typically, but not always, achieved by assigning absorption and scattering coefficients, together with phase functions, to each element of phase space.

- Asking a question about some quantity of interest (such as “what is the escape probability of a particle arriving normally incident to an absorbing and scattering semi-infinite medium?”)

We limit our attention to *linear* scattering problems: particles do not interact with other particles in flight and do not alter the nature of the medium through which they move. Further, we are typically interested in problems where the quantities of interest include non-negligible contributions from particles that suffer multiple scattering events. In the absence of scattering or absorption, particles stream through vacua in a simple fashion and straightforward ray-tracing or analytical methods suffice to determine any quantity of interest. Similarly, for a medium that absorbs but does not scatter—the *reduced-intensity* (*uncollided/ballistic*) quantities are often trivial to acquire. In a medium that includes scattering it is occassionally useful to consider only the *single-scattering* component, but our most general interest lies in the more challenging (and more fun!) consideration of problems that permit any order of scattering to occur, hence the label “multiple scattering".

Once we have completely defined the properties of a scattering problem, we begin the core statistical analysis of considering a point particle with initial position and direction drawn randomly from the source distribution. The particle then undergoes an alternating sequence of straight displacements and scattering events. The distances between scattering events and the deviations in angle at each scattering event are random variables drawn from given distributions. The process is eventually terminated when the particle is randomly absorbed, or when the particle escapes the system (if finite).

In one form, such an analysis lies in a branch of mathematics known as random walk or random flight theory where it is common to ask questions such as “what is the probability density that a random flight ends its nth displacement at some radius r from its original position?". Closely related to random flight theory is the statistical analysis of the bulk transport of waves or particles through random media. Be it neutral particles such as neutrons, or approximate flow of electromagnetic energy, such as visible light, a valuable framework for simulating such bulk transport forms the mathematical physics discipline of linear transport theory. The random flight and transport theories differ in that the latter is typically only concerned with the total densities at some position and location, regardless of how many times any particle has previously scattered, whereas the random flight analysis typically asks direct questions about the Neumann series decomposition (the uncollided portion, the single scattering, double scattering, etc). However, the transport quantities are expressable as the sum of the random flight quantities, linking the two studies closely.

Further Reading

For more on the relationship between linear transport theory and random flights/walks, see [Guth and Inönü 1960]. See [Larsen and Vasques 2011] for deriving linear Boltzmann equations for non-exponential random flights.

Solutions to problems in linear transport theory are often found by solving integral- or integrodifferential-balance equations. These *linear transport equations* are at the heart of many applied disciplines of physics such as radiative transfer, neutron transport and also finds use outside of physics, such as in computer graphics for synthesizing realistic images of highly scattering materials such as human skin. Common to all of these applied studies is the supposition

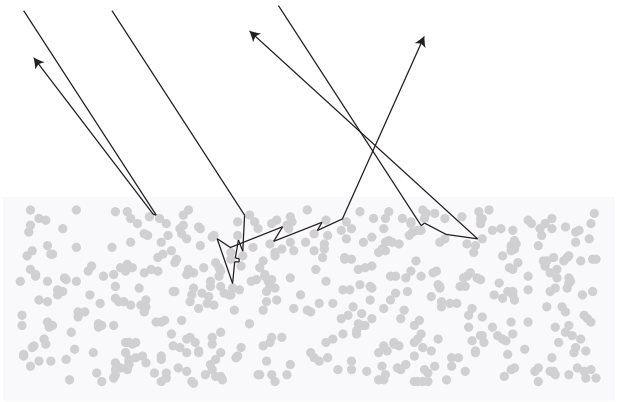

Figure 1: *The motion of individual particles or photons within random media can be quite complex when the medium and the particles interact. In practice it is often the case that a huge number of particles influence a sensor measurement of interest and so only the bulk behaviour is desired. In this case, a statistical* multiple scattering *problem can be solved, producing radiometric probability densities for finding particles flowing at any position and in any particular direction (in or around the medium). This avoids the burden of sampling random realizations of the medium and tracing through them (such as the example pictured here). This book is a collection of solutions to such multiple scattering problems.*

of some medium through which point particles or energy flow. The motion of these particles is subject to the random nature of this medium (Figure 1). Each of these applied fields begins with its own unique physics that govern the transport of the particular particle or wave through the medium of interest (such as visible light moving through water droplets in an atmosphere or neutrons interacting with molecules in a reactor). Once physics has be used to derive the distributions that govern the random flight of one particle, the physics ends and the transport theory begins. At this stage these many fields share much in common.

Despite significant overlap in transport theory mathematics across a wide variety of applied physics domains, most of the solutions gathered in this book are found directly in the literatures of these various fields as opposed to a common mathematical physics journal using common notation. For this reason, an expert in transport theory is someone who is keenly aware of much of this literature in all of these fields—a significant challenge. One aim of this book is to provide an incomplete map of some of this literature to aid the interested reader and encourage interdisciplinary awareness.

The underlying assumptions make the application of transport theory approximate in any field—particle/wave duality, interference and diffraction effects are neglected at some level. However, a purely particle interpretation of the multiple scattering of light (and other neutral particles) has long proven useful despite the underlying assumptions [Mishchenko 2013, Mishchenko 2014].

It is always possible (at least in principle) to randomly construct specific realizations of a given class of random media and to generate random flights explicitly within each realization via brute-force ray-tracing (Figure 1). The desired bulk transport quantities can be estimated by

averaging over many medium realizations, each with many random flights sampled within them. However, this procedure can be prohibitively costly. Often, the measurable quantity of interest is governed by a huge quantity of particles and the statistical expectation we seek can be attained more directly and efficiently from a solving a linear transport equation.

The application of transport-theoretic statistical models is a common and essential practice for making realistic computer generated imagery a tractable problem. A scattering volume (participating medium) is often used to reduce complexity when authoring scenes with optically-active material such as tissue and similar structures seen at a distant scale where explicit structure is not directly visible. For example, closely-resolved water droplets in a water fountain (Figure 2) must be explicitly modeled, whereas the same optical structures in a distant waterfall should almost certainly be replaced by a statistical scattering volume with some spatially-varying density that defines it apparent shape. Similarly, light transport within human skin can often be described by a volume scattering model [Tuchin 2007] but not when imaged so closely that the dielectric structures become clearly visible (Figure 2). Efficient, approximate analytic functions for describing the scattering in simplified geometries is also essential practice for rapidly synthesizing realistic images of human skin, for example. Indeed, the subsurface-scattering revolution in computer graphics can be arguably tied to the introduction of efficient analytic volume scattering functions inspired by the tissue optics literature [Jensen et al. 2001].

Simple, compact, mathematical solutions to multiple scattering problems are thus a powerful tool for accelerating image synthesis. This document, however, focuses solely on the mathematical solutions to abstract scattering problems (forgetting, for the most part, what particle is being considered). As such, it sits between theory and application as a Hitchhiker's guide for a reader who has a problem in mind within their field of interest (not necessarily graphics) and who wishes to find a solution to that problem. In most fields the simplicity of the "model problems" we consider here might seem only useful for educational purposes but their solutions continually find use as components of efficient approximate methods in computer graphics.

Even more specifically, when we speak of multiple scattering, we are (usually) referring to solutions to the equation (of many names):

$$\vec{\omega} \cdot \nabla L(\vec{x}, \vec{\omega}) = -\Sigma_t(\vec{x}, \vec{\omega})\, L(\vec{x}, \vec{\omega}) + \Sigma_s(\vec{x}, \vec{\omega}) \int_{4\pi} L(\vec{x}, \vec{\omega}') p(\vec{\omega}, \vec{\omega}') d\vec{\omega}' + Q(\vec{x}, \vec{\omega}). \qquad (1)$$

1.2 Why?

This is a subset of the author's personal notes on transport theory and releasing a public version is intended to serve several purposes:

- Most of the seminal texts on linear transport theory [Chandrasekhar 1960, Case et al. 1953, Davison 1957, Weinberg and Wigner 1958, Case and Zweifel 1967, Bell and Glasstone 1970, Williams 1971, Duderstadt and Martin 1979, van de Hulst 1980] are out of print, expensive to acquire, and lack recent developments. While in no way intended to replace these texts, we hope to provide a rough map of the set of solved linear transport problems—to help people find not only the solutions to solved problems, but also help people know exactly what has been solved. Solutions are provided in a compact form without derivation or theory—extensive references to articles that provide the missing theory and derivations are included to the author's best knowledge.

Figure 2: *Complex volumes of optically-active material viewed at different distances call for different representations in computer graphics. Distant (or not-directly-visible) explicit structure is often replaced by statistical models that describe bulk multiple-scattering behaviour. Indeed, the success of physically-based rendering hinges critically on our ability to author scenes described at the lowest level by statistical surface and volume scattering models.*

- Benchmark solutions are important, even in graphics. Most problems will come with at least one Monte carlo estimator of its solution. The Monte Carlo and deterministic solutions should help cross-check each other and help the reader check their own Monte Carlo code for correctness. The release of this document is, in part, a response to Peter Shirley's EGSR 2011 keynote where he asked the rendering community if anyone was willing to create and release trusted rendering benchmarks.
- Many readers in computer graphics simply need to know the final answer, and to have it provided concisely in one place in a familiar notation with numerical and graphical data to help the reader test that his implementation is accurate. We are unaware of any public

resource that fills this need and we hope to build something here that tries to.
- For the sheer fun of it. The rich beauty of the mathematics behind the deterministic solutions together with the powerful effectiveness and simplicity of the Monte Carlo method make for one heck of a fun sand box.

1.3 Computer Graphics Bias

Our interest in multiple scattering stems from its use in synthesizing realistic images of scenes that include translucent materials and atmospheric scattering. In computer graphics, Equation 1 is known as the *volume rendering equation* and it is used to model the scattering of light in *participating media*. Given this bias, we choose to mostly focus on:

- *linear* transport theory problems—luckily, today's lighting technical directors do not light the virtual sets of *Avatar 2* by placing a star and starting a fusion reaction, so we can always assume that the levels of heat created by the absorption events in the transport process don't measurably change the properties of the medium itself. We also assume that the photons never collide with each other. Thus, the transport equation and its solutions will remain strictly linear.
- *monoenergetic (gray, elastic, one-group)* problems—quantities will refer to light of a single energy/frequency and fluorescence will not be considered (colored images are made by solving the mono-energetic problem three or more times, at several independent wavelengths).
- *time-independent (steady-state, stationary)* problems—light sources are turned on and the distributions stabilize very quickly, so the temporal evolution of distributions is rarely of interest. However, a number of *time-resolved* solutions will be included because they provide deeper insight into the steady-state solutions and may be useful for creating steady-state appoximations.
- *conservative* or *absorbing* media. We will not consider *multiplying media*—the single scattering albedo of the material will never exceed 1.
- *scalar* radiative transfer–we typically will not consider polarization.
- phase-functions (scattering kernels) that are typically applied to visible light (and often *synthetic* scattering kernels—not measured ones)
- *no delay*—the scattering process is assumed to occur immediately with no delay (for time-dependent neutron transport problems, delay is an important aspect)

1.4 Revision History

This document will be updated as time permits and as more solutions become known. Please email me with any corrections and pointers to additional solutions and I will attempt to keep the document up to date.

- Version 0.1 - Jul 24, 2016 - *Initial release*

1.5 Organization

We begin in the next section with some notes regarding derivation of the transport equation, radiometric quantities, and scattering kernels. Problem descriptions and solutions will be presented in the remaining sections, with a section at the end for more detailed presentation of some common mathematical functions that appear repeatedly and were worth singling out.

Problems will be labeled in several ways:

- We will consider three universes for scattering phenomena: the *Rod Model* - a one dimensional domain where energy/particles can only travel in one of two discrete directions (left and right), *flatland*—a two-dimensional universe, and (most of the time) the traditional 3D universe.
- Some symmetry may divide the problems into groups (spherical symmetry, plane symmetry)
- The type of source function (isotropic point, delta point, isotropic plane, delta plane)
- The shape of the scattering volume (semi-infinite, slab, cube, sphere, disk)
- Boundary conditions (vacuum/index-matched, Fresnel)
- The character of scattering events (isotropic, forward-peaked)
- The type of media: classical (exponential) free path distributions, or generalized transport with non-exponential free paths

2 Ingredients of a Multiple Scattering Problem

In this section we briefly discuss the three transport equations that correspond to the three universes that we consider in this book (the Rod Model, Flatland, and classical 3D space). We also include several phase functions/scattering kernels and various useful related equations before mentioning the generalization of these transport equations to anisotropic media and to non-exponential/correlated/fractal random media.

2.1 Transport Quantities

We study multiple scattering with the goal of predicting some quantity. The quantities we most often seek to predict are radiance, fluence and albedo. These are ultimately determined by properties of the scattering problem under consideration. In Table 1 we summarize our notation for common transport quantities.

2.1.1 Radiance / Angular Flux / Specific Intensity

In our notation the angular radiometric quantity we seek, *radiance / angular-flux / specific intensity*, is denoted L. Radiance is a probability density in both position and solid angle such that the expected number of particles E flowing in some interval of time within a small volume of size dV containing position $\vec{x}$ considering only particles whose directions are contained within some small angular domain of solid angle $d\vec{\omega}$ containing direction $\vec{\omega}$ is proportional to

$$E = L(\vec{x}, \vec{\omega}) dV d\vec{\omega}. \tag{2}$$

2.1.2 Fluence / Scalar Flux

The *scalar flux / fluence* is formed by integrating the directionally-dependent quantity L over all directions and is denoted ϕ,

$$\phi(\vec{x}) = \int_{4\pi} L(\vec{x}, \vec{\omega}) d\vec{\omega}, \tag{3}$$

and is proportional to the total density of particles/energy *in flight* at position $\vec{x}$.

2.1.3 Assumptions

To simplify results, together with our bias towards time-independent problems, we typically assume an implicit unit particle velocity $v = 1$ and drop this quantity from most results.

Symbol	Description	Chandra60	Ishimaru78	Jensen01
ρ_s	*number density of interacting particles* [m^{-3}]	ρ	ρ	
σ_a	*absorption cross-section* [m^2]	σ	σ_a	
σ_s	*scattering cross-section* [m^2]	σ	σ_s	
$\sigma_t = \sigma_s + \sigma_a$	*extinction (total) cross-section* [m^2]		σ_t	
$\Sigma_a = \rho_s \sigma_a$	*absorption coefficient* [m^{-1}]	κ	$\rho\sigma_a$	σ_a
$\Sigma_s = \rho_s \sigma_s$	*scattering coefficient* [m^{-1}]	κ	$\rho\sigma_s$	σ_s
$\Sigma'_s = \Sigma_s(1-g)$	*reduced scattering coefficient* [m^{-1}]	κ		σ'_s
$\Sigma_t = \Sigma_s + \Sigma_a$	*extinction coefficient* [m^{-1}]			σ_t
$\Sigma'_t = \Sigma'_s + \Sigma_a$	*transport coefficient* [m^{-1}]		$\rho\sigma_{\mathrm{tr}}$	σ'_t
Σ_{eff}	*effective attenuation coefficient* [m^{-1}]		κ_d	σ_{tr}
α	*single-scattering albedo*	w_0	W_0	
s	*free distance*			
S(s)	*free path distribution*			
ℓ	*mean free path (MFP)* [m]			
$p(\vec{\omega}, \vec{\omega}')$	*phase function* [sr^{-1}]	p	p	p
g	*mean cosine of the scattering angle*			g
D	*diffusion constant* or *diffusion coefficient*		D	D
$L(\vec{x}, \vec{\omega})$	*radiance* [$\mathrm{W\,m^{-2}\,sr^{-1}}$]	$I(\vec{x}, \vec{\omega})$	$I(\vec{x}, \vec{\omega})$	$L(\vec{x}, \vec{\omega})$
$Q(\vec{x}, \vec{\omega})$	*source intensity*		$\varepsilon(\vec{x}, \vec{\omega})$	$Q(\vec{x}, \vec{\omega})$
$\phi(\vec{x})$	*fluence rate* [$\mathrm{W\,m^{-2}}$]			$\phi(\vec{x})$
η	*relative refractive index at interface*			
m	*surface roughness*			

Table 1: *Description of symbols for transport in a 3D universe*

2.2 Three Classical Transport Equations

There are two equivalent forms of linear transport equations, an integrodifferential form and an integral form.

2.2.1 Transport in a 3D Universe

We will typically consider transport processes that lead to the following balance equation:

$$\vec{\omega} \cdot \nabla L(\vec{x}, \vec{\omega}) = -\Sigma_t(\vec{x}, \vec{\omega})\, L(\vec{x}, \vec{\omega}) + \Sigma_s(\vec{x}, \vec{\omega}) \int_{4\pi} L(\vec{x}, \vec{\omega}') p(\vec{x}, \vec{\omega}, \vec{\omega}') d\vec{\omega}' + Q(\vec{x}, \vec{\omega}).$$

Often (in piece-wise homogeneous media) the *absorption coefficient* Σ_a and *scattering coefficient* Σ_s do not depend on position $\vec{x}$.

This form of the transport equation assumes that the *scattering kernel* (phase-function) p is a normalized probability distribution function (pdf) of directions:

$$\int_{4\pi} p(\vec{\omega}, \vec{\omega}') d\vec{\omega}' = 1. \tag{4}$$

Alternatively, we could instead have chosen that the scattering kernel integrate over the sphere to produce the single-scattering albedo α as in, for example, [Chandrasekhar 1960].

2.2.2 Transport in a 2D Universe (Flatland)

We will occasionally consider transport solutions to problems in flatland. The directional coordinate is then a scalar angle $\theta \in [0, 2\pi]$, the phase space is $\mathbb{R}^2 \times S^1$, and the balance equation is

$$\vec{\omega} \cdot \nabla L(\vec{x}, \theta) = -\Sigma_t(\vec{x}, \theta)\, L(\vec{x}, \theta) + \Sigma_s(\vec{x}, \theta) \int_0^{2\pi} L(\vec{x}, \theta') p(\theta, \theta') d\theta' + Q(\vec{x}, \theta).$$

Further Reading

There are limited number of flatland transport theory studies, to our knowledge. Pearson [1905], Kluyver [1906] and Rayleigh [1919] gave early seminal presentations on random flights in flatland. Watson describes random flights in flatland in section 13.48 of [Watson 1962]. Grosjean [1953] gives exact results for infinite medium random flights in k dimensions. Paasschens [1997] derives the time-resolved Green's function for isotropic scattering in an infinite flatland medium. Asadzadeh and Larsen [2008] derive diffusion and small-angle results for beam problems in flatland. Several recent works [Zoia et al. 2011a, Liemert and Kienle 2011] discuss exact solutions for exponential random flights in an infinite flatland medium. We [2014] recently derived exact and diffusion solutions for infinite medium point source problems in classical or generalized transport theory in flatland. Additional exact solutions have been presented for bounded media [Liemert and Kienle 2012b], layered media [Liemert and Kienle 2012a], and Caseology in flatland [Machida 2015].

2.2.3 Transport in a 1D Universe: The Rod Model / Two-Stream Approximation

We will occasionally consider transport solutions in a very simplified 1D domain (called the *rod model* or the *forward/backward* model). In radiative transfer the application of the rod model to approximately describe transport in a 3D universe is called the *two-stream* approximation.

The rod model is a useful domain for comparison, research and teaching of transport problems and is unique in that, for most problems, exact analytic solutions are known.

In the rod model particles are restricted to move along a one dimensional domain—the real line. We denote the pair of possible directions of motion as simply left ($-$) and right ($+$). The phase space is thus $\mathbb{R} \times \{+, -\}$ instead of the $\mathbb{R}^3 \times S^2$ in 3D. The quantity of interest most closely related to radiance $L(\vec{x}, \vec{\omega})$ is simply $L_+(x)$, where $L_+(x)dx$ is the expected number of particles in $[x, x + dx]$ moving to the right, and $L_-(x)$ similarly describes left moving particles.

Let $\Sigma_t(x)\,\Delta + o(\Delta)$ be the probability of experiencing an interaction with the medium when traversing a distance of Δ in the rod where the *interaction coefficient* $\Sigma_t(x) = \Sigma_a(x) + \Sigma_s(x)$ is the sum of the absorption and scattering coefficients. Let the phase function be derived from $\{F(x), B(x)\}$ with $F(x) \geq 0$, $B(x) \geq 0$ such that $F(x)$ is the fraction/probability of energy arriving at the scatterer that continues *forward* in the direction of original motion, and $B(x)$ is the portion that reflects *backward* in the opposite direction. The single scattering albedo is thus $\alpha(x) = \Sigma_s(x)/\Sigma_t(x) = F(x) + B(x)$, the remaining energy is absorbed.

The rod model transport equation is a coupled pair of differential equations [Wing 1962]

$$\pm \frac{dL_\pm}{dx} = -\Sigma_t(x) L_\pm(x) + \Sigma_t(x) F(x) L_\pm(x) + \Sigma_t(x) B(x) L_\mp(x) + Q_\pm(x) \tag{5}$$

where the change in radiance on the left is related to the absorption, the incoming source due to scattering, and the anisotropic source term $Q_{\pm}$, which emits general amounts of light in either direction. Because the domain of directions is discrete (two directions) the transport equations are a discrete pair of differential equations, not an integro-differential equation.

Further Reading

The study of multiple scattering in a simplistic 1D domain dates back at least as far as Pearson's [1905] study of random walks and its first application to neutron transport was reportedly due to Fermi [Placzek 1941]. The two-stream approximation in radiative transfer was introduced by Schuster [1905]. In neutron transport the rod model has been an invaluable tool for benchmarking Monte Carlo and other codes and also for education [Wing 1962, Hoogenboom 2008] and it sees continued used in evaluating new solutions—see the recent work of Zoia et al. [2011c, 2011b] who also note many practical applications of the rod model in real world problems. We [2014] recently derived exact and diffusion solutions for infinite medium point source problems in classical or generalized transport theory in a rod.

2.2.4 Derivation

We will not include derivation of the transport equation here. Excellent references on this topic include [Bell and Glasstone 1970, Williams 1971, Duderstadt and Martin 1979, Prinja and Larsen 2010]. For an excellent review of the derivation and discussion of the integral form, see Prinja and Larsen [2010].

Further Reading

Ancient history of the transport equation:

- The linear transport equation can be found as a linearization of Boltzmann's equation [Boltzmann 1878, Williams 1971]
- The birth of transport theory is sometimes attributed to two early works prior to the 1900s, [Lommel 1889, Chwolson 1890]
- See Mishchenko's 125th radiative transfer anniversary review [Mishchenko 2013] for further detail

2.2.5 Existence, Uniqueness, Nonnegativity and Smoothness of Solutions

A rigourous investigation of the existence and uniqueness of solutions to linear transport equations was presented by Case and Zweifel [1963]. The solutions are strictly non-negative. The smoothness of the solutions is a complicated and not universally well-understood aspect (see [Kellogg 1974] or [Prinja and Larsen 2010]).

2.2.6 Linearity

Because the transport equations (and random flight problems) we consider are linear, the solution to any problem where the total source can be expressed as a linear combination of separate sources can be written as the same linear combination of solutions to separate problems, one for each source in the combination. Taken further, the solution to any problem with a source that is not a point source can be formed as an integral or convolution of a Green's function solution with the source function.

2.3 Scattering Kernels (Phase-Functions)

Scattering kernels are normalized probability distribution functions (PDFs) that define how a particle's direction changes during a scattering interaction with a volumetric element of the medium (distributions for scattering at media boundaries are defined separately). Given some incoming direction $\vec{\omega}_i$ the scattering kernel $p(\vec{\omega}_i, \vec{\omega}_o)$ is defined such that the probability that the particle will be deflected into a set of directions of solid angle $d\vec{\omega}$ about $\vec{\omega}_o$ is $p(\vec{\omega}_i, \vec{\omega}_o)d\vec{\omega}$. This is typically rotationally-invariant (i.e. there is no dependence on any laboratory coordinate frame—outgoing scattering directions are symmetric relative to any incoming direction and so the kernel is often defined as a function of deflection cosine $u = \vec{\omega}_i \cdot \vec{\omega}_o$. This type of scattering occurs in an *isotropic random media* (and has nothing to do with an isotropic scattering kernel). When the distribution of scattering deflections is tied in some way to some laboratory frame, then the medium is said to be an *anisotropic random media* (see section 2.7).

Here we list a variety of analytic scattering kernels for isotropic random media and include some relevant quantities and sampling methods for these kernels. All kernels will satisfy the same normalization condition for any incoming direction $\vec{\omega}$:

$$\int_{4\pi} p(\vec{\omega}, \vec{\omega}')d\vec{\omega}' = 1 \tag{6}$$

which is equivalent to

$$2\pi \int_{-1}^{1} p(u)du = 1. \tag{7}$$

in the case of isotropic random media ($\cos\theta = u$). The *mean cosine of deflection* g is:

$$g = 2\pi \int_{-1}^{1} p(u)udu. \tag{8}$$

The coefficients A_k of expansion into *Legendre polynomials* $P_k(x)$ are important quantities found via:

$$p(u) = \frac{1}{4\pi} \sum_{k=0}^{\infty} A_k P_k(u), \tag{9}$$

and

$$A_k = 2\pi(2k+1) \int_{-1}^{1} p(u)P_k(u)du. \tag{10}$$

The normalization condition (Equation 6) is equivalent to $A_0 = 1$.

2.3.1 Isotropic Scattering

In a medium with isotropic scattering all outgoing directions are equally likely:

$$p(\vec{\omega}, \vec{\omega}') = \frac{1}{4\pi}. \tag{11}$$

The mean cosine is $g = 0$ and expansion coefficients $A_{k>0} = 0$. Deflection cosines can be randomly sampled with

$$u(\xi) = 2\xi - 1 \tag{12}$$

where ξ is a random number drawn uniformly from $[0, 1)$.

Spherical particles with perfect mirror surfaces produce isotropic scattering (in a far-field (parallel) sense, assuming geometrical optics). Isotropic scattering is often a reasonable approximation for the scattering of thermal neutrons.

MC Code and Mathematica Validation (github):
code/scatteringevents

2.3.2 Linearly Anisotropic Scattering (Eddington)

Linearly anisotropic scattering (also known as the Eddington phase function) is the linear combination of a constant function and a cosine function:

$$p(u) = \frac{1 + bu}{4\pi} \tag{13}$$

where parameter b controls forward and backward scattering and must satisfy $-1 \leq b \leq 1$. The mean cosine g is $b/3$. The expansion coefficients are: $A_0 = 1, A_1 = b, A_{k>1} = 0$. Deflection cosines can be randomly sampled with

$$u(\xi) = \frac{\sqrt{b^2 + 4b\xi - 2b + 1} - 1}{b} \tag{14}$$

where ξ is a random number drawn uniformly from $[0, 1)$.

MC Code and Mathematica Validation (github):
code/scatteringevents

2.3.3 Rayleigh Scattering

The normalized Rayleigh scattering kernel [Chandrasekhar 1960] is typically written:

$$p(u) = \frac{3\left(u^2+1\right)}{16\pi}, \tag{15}$$

a special case of the more general,

$$p(u) = \frac{3\left(3\gamma+(1-\gamma)u^2+1\right)}{16\pi(2\gamma+1)} \tag{16}$$

where $\gamma = \rho_0/(2-\rho_0)$ accounts for the effect of molecular anisotropy and ρ_0 is the depolarization factor.

The mean cosine g is 0. The expansion coefficients are: $A_0 = 1, A_1 = 0, A_2 = \frac{1}{2}, A_{k>3} = 0$. Deflection cosines can be randomly sampled with

$$u(\xi) = \frac{1-\left(-4\xi+\sqrt{16(\xi-1)\xi+5}+2\right)^{2/3}}{\sqrt[3]{-4\xi+\sqrt{16(\xi-1)\xi+5}+2}} \tag{17}$$

where ξ is a random number drawn uniformly from $[0,1)$.

MC Code and Mathematica Validation (github):
code/scatteringevents

2.3.4 Henyey-Greenstein

$$p(u) = \frac{1-g^2}{4\pi\left(g^2-2gu+1\right)^{3/2}} \tag{18}$$

with mean cosine parameter $-1 < g < 1$, and expansion coefficients $A_k = (2k+1)g^k$. Deflection cosines can be randomly sampled with

$$u(\xi) = -\frac{-2\xi^2\left(g^3+g\right)+2\xi(g-1)\left(g^2+1\right)+(g-1)^2}{((2\xi-1)g+1)^2} \tag{19}$$

where ξ is a random number drawn uniformly from $[0,1)$.

Further Reading
Originally presented by [Henyey and Greenstein 1941]. Often chosen for convenient expansion coefficients. The HG phase function does not posses a Fokker-Planck limit [Pomraning 1992]. Limitations of HG for use in tissue are described by [Mourant et al. 1998, Flock et al. 1987, Marchesini et al. 1989]. Generalizations of Henyey-Greenstein in flatland have been derived in several works [Davis et al. 1993, Heino et al. 2003, Davis 2006] (see Section 2.5).

MC Code and Mathematica Validation (github):
code/scatteringevents

2.3.5 Kagiwada-Kalaba / Ellipsoidal

The Kagiwada-Kalaba [1967] (also known as ellipsoidal [Sobolev 1975]) scattering kernel is given by

$$p(u) = \frac{b}{2\pi(1-bu)\log\left(\frac{b+1}{1-b}\right)} \tag{20}$$

with parameter $-1 < b < 1$, mean-cosine $g = \frac{1}{b} - \frac{2}{\log\left(\frac{b+1}{1-b}\right)}$, and expansion coefficients

$$A_1 = 3g \tag{21}$$

$$A_2 = \frac{5}{2}\left(\frac{3}{b^2} - \frac{6}{b\log\left(\frac{b+1}{1-b}\right)} - 1\right) \tag{22}$$

$$A_3 = \frac{7\left(b\left(\frac{8b^2-30}{\log\left(\frac{1}{1-b}\right)+\log(b+1)} - 9b\right) + 15\right)}{6b^3} \tag{23}$$

$$A_4 = \frac{3\left(9b^4 - 90b^2 + \frac{10\left(11b^2-21\right)b}{\log\left(\frac{1}{1-b}\right)+\log(b+1)} + 105\right)}{8b^4}. \tag{24}$$

Deflection cosines can be randomly sampled with

$$u(\xi) = \frac{1-(b+1)\left(\frac{b+1}{1-b}\right)^{-\xi}}{b} \tag{25}$$

where ξ is a random number drawn uniformly from $[0,1)$.

MC Code and Mathematica Validation (github):
code/scatteringevents

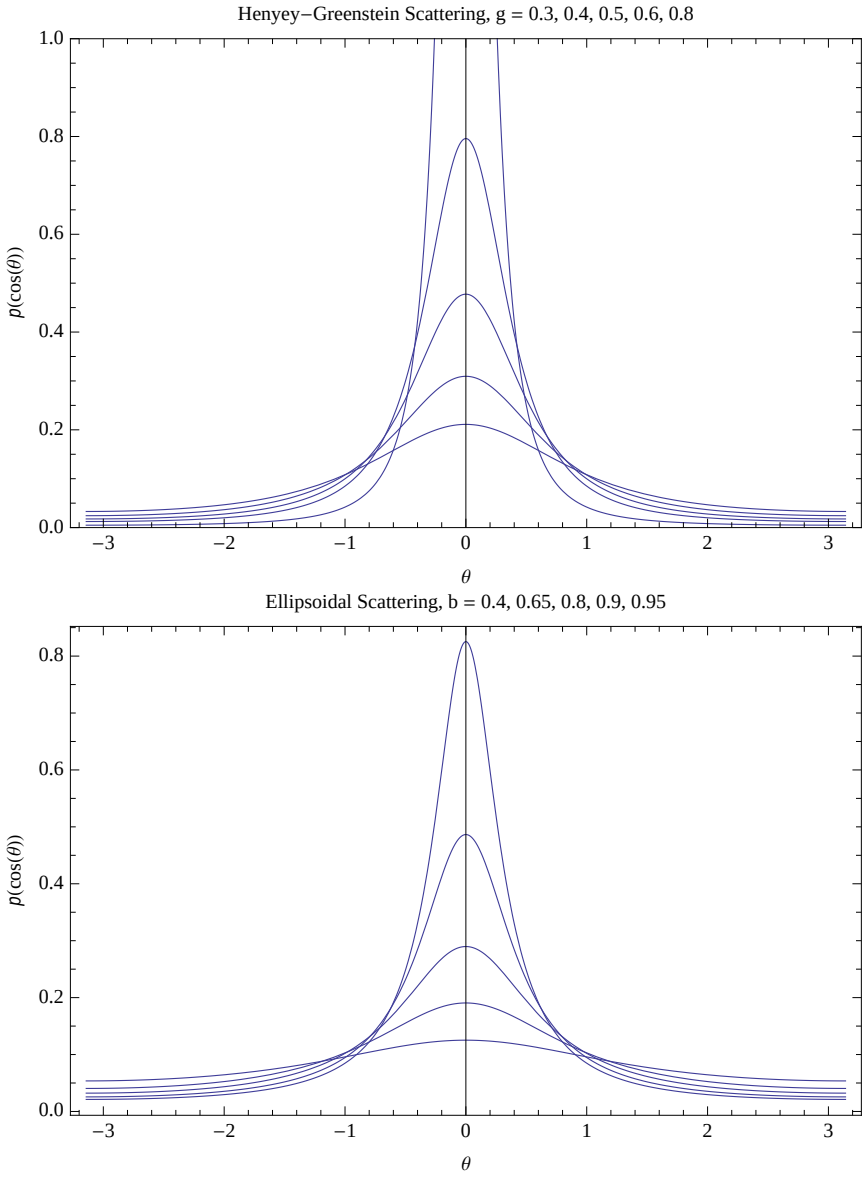

Figure 3: *Henyey-Greenstein vs Ellipsoidal*

2.3.6 Binomial

The forward binomial scattering kernel [Kaper et al. 1970] is given by:

$$p(u) = \frac{2^{-n-2}(n+1)(u+1)^n}{\pi} \tag{26}$$

with parameter $n \geq 0$, mean-cosine $g = \frac{n}{2+n}$, and expansion coefficients

$$A_1 = 3g = \frac{n}{2+n} \tag{27}$$

$$A_{k>1} = (2k+1)\frac{\prod_{j=0}^{k-1} n-j}{\prod_{j=2}^{k+1} n+j} \tag{28}$$

which can be also computed by the recurrence

$$A_{k>1} = \left(\frac{2k+1}{2k-1}\right)\left(\frac{n+1-k}{n+1+k}\right)A_{k-1}. \tag{29}$$

Deflection cosines can be randomly sampled with

$$u(\xi) = \left(\xi 2^{n+1}\right)^{\frac{1}{n+1}} - 1 \tag{30}$$

where ξ is a random number drawn uniformly from $[0,1)$. The binomial kernel is always 0 for the perfectly-backward direction, so two binomial kernels are often combined (with one rotated to face the opposite direction).

MC Code and Mathematica Validation (github):
code/scatteringevents

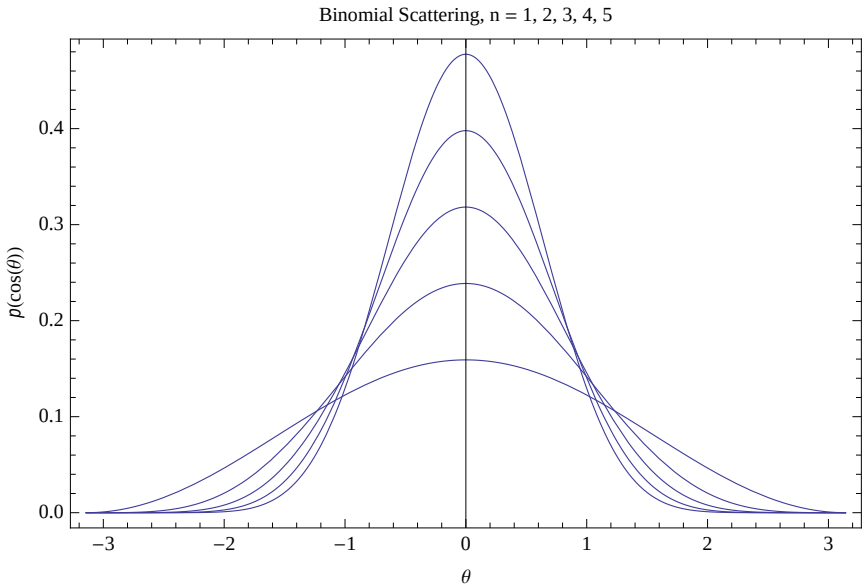

Figure 4: *Binomial phase function.*

2.3.7 Gegenbauer

The generalized Henyey-Greenstein scattering kernel known as the Gegenbauer kernel [Reynolds and McCormick 1980] is given by

$$p(u) = \frac{aG\left(G^2 - 2Gu + 1\right)^{-a-1}}{\pi\left((1-G)^{-2a} - (G+1)^{-2a}\right)} \tag{31}$$

with parameter $-1 < G < 1$ and $a > 0$. The mean-cosine of scattering deflections is

$$g = \frac{(G+1)^{2a}\left(-2aG + G^2 + 1\right) - (1-G)^{2a}\left(2aG + G^2 + 1\right)}{2(a-1)G\left((1-G)^{2a} - (G+1)^{2a}\right)}. \tag{32}$$

The order 1 Legendre expansion coefficient is

$$A_1 = 3g. \tag{33}$$

The phase function can be expanded in terms of Gegenbauer polynomials which can be computed using a reccurence relation. Deflection cosines can be randomly sampled with

$$u(\xi) = \frac{-\left(\xi(1-G)^{-2a} - (\xi-1)(G+1)^{-2a}\right)^{-1/a} + G^2 + 1}{2G} \tag{34}$$

where ξ is a random number drawn uniformly from $[0, 1)$.

MC Code and Mathematica Validation (github):
code/scatteringevents

2.3.8 Liu

A scattering kernel introduced by Liu [1994] to provide better similarity to Mie scattering results is given by:

$$p(u) = \frac{(2m+1)\varepsilon(u\varepsilon+1)^{2m}}{2\pi\left((\varepsilon+1)^{2m+1} - (1-\varepsilon)^{2m+1}\right)} \tag{35}$$

with anisotropy parameter m, a positive integer and a characteristic factor ε. The mean-cosine of scattering deflections is

$$g = \frac{(2m\varepsilon + \varepsilon + 1)(1-\varepsilon)^{2m+1} + (\varepsilon+1)^{2m+1}(2m\varepsilon + \varepsilon - 1)}{2(m+1)\varepsilon\left((\varepsilon+1)^{2m+1} - (1-\varepsilon)^{2m+1}\right)}. \tag{36}$$

The order 1 Legendre expansion coefficients is

$$A_1 = 3g \tag{37}$$

The remaining coefficients are fairly complex, but closed-form. Deflection cosines can be randomly sampled with

$$u(\xi) = \frac{\left((\xi-1)(\varepsilon-1)(1-\varepsilon)^{2m} + \xi(\varepsilon+1)^{2m+1}\right)^{\frac{1}{2m+1}} - 1}{\varepsilon} \tag{38}$$

where ξ is a random number drawn uniformly from $[0, 1)$.

MC Code and Mathematica Validation (github):
code/scatteringevents

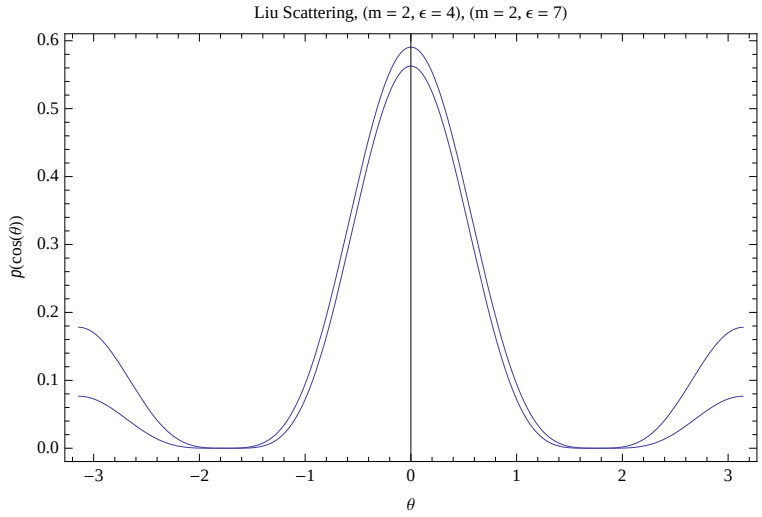

Figure 5: *Liu phase function.*

2.3.9 Spherical Gaussian (von-Mises-Fischer)

A spherical Gaussian (vMF) scattering kernel was recently introduced by [Gkioulekas et al. 2013]

$$p(u) = \frac{k e^{ku} \operatorname{csch}(k)}{4\pi} \tag{39}$$

with anisotropy parameter k. The mean-cosine of scattering deflections is

$$g = \coth(k) - \frac{1}{k}. \tag{40}$$

Low order Legendre expansion cofficients are

$$A_1 = 3g \tag{41}$$

$$A_2 = \frac{5\left(k^2 - 3k\coth(k) + 3\right)}{k^2} \tag{42}$$

$$A_3 = \frac{7\left(k\left(k^2+15\right)\coth(k) - 3\left(2k^2+5\right)\right)}{k^3} \tag{43}$$

$$A_4 = \frac{9\left(k^4 + 45k^2 - 5\left(2k^2+21\right)k\coth(k) + 105\right)}{k^4}. \tag{44}$$

Deflection cosines can be randomly sampled with

$$u(\xi) = \frac{\log\left(e^{-k}(1-\xi) + e^{k}\xi\right)}{k} \tag{45}$$

where ξ is a random number drawn uniformly from $[0, 1)$.

MC Code and Mathematica Validation (github):
code/scatteringevents

2.3.10 Anli-Gungor

See [Anli et al. 2005].

2.3.11 Explicit/General Legendre Polynomial Expansions

A scattering kernel may be expressed directly as a Legendre polynomial expansion (due to how it is computed, or measured). Such expansions fall out of a wave-theory derivation of scattering from dielectric [Chu and Churchill 1955] or conducting [Born and Wolf 2002] spherical scattering particles.

Coveyou [1965] gives an importance sampling scheme for general Legendre expanded phase functions. Peterson [1983] discusses efficient sample generation for directional distributions that arise from n-fold application of a given symmetric kernel on the sphere.

2.3.12 Computer Graphics Literature

It is common for papers in the computer graphics literature to refer to the mean-cosine of deflection g for a scattering process without further specifying the complete phase function. It is likely the case that Henyey-Greenstein is assumed (for no good reason). It is the case that classical diffusion approximations rely only on the mean-cosine g. However, it is also important to remember that there are an uncountably infinite number of valid phase functions for every mean-cosine g (for example, see Figure 6). Gkioulekas et al. [2013] provide strong evidence for the importance of supporting a generality of phase functions beyond just Henyey-Greenstein in image synthesis.

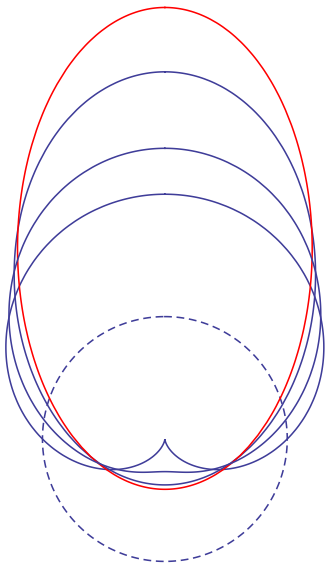

Figure 6: *The solid lines are all scattering kernels defined above with a mean cosine $g = 1/3$. The dashed line is a reference isotropic scattering kernel.*

2.4 Similarity Relations, Condensed-History Acceleration, Rescaling

It is common practice (for both deterministic and Monte Carlo methods) to make a modification to the transport process—essentially replacing the original medium with one having slightly different properties—in order to more easily or more efficiently compute some transport quantity of interest.

A certain class of such methods that involves changing the phase function, single-scattering albedo and mean free path in concert is referred to as *similarity relations* [van de Hulst 1980, Wyman et al. 1989, van de Hulst and Graaff 1996], and seeks to exploit relationships between two media with different properties such that transport within these media is as similar as possible under certain circumstances. This can allow, for example, mapping of general anisotropic scattering to a close-as-possible isotropic medium, where deterministic solutions are approximations are much simpler to derive or evaluate.

The most common similarity relation is the mapping to isotropic scattering, where the *reduced scattering coefficient* Σ_s' is defined as

$$\Sigma_s' = \Sigma_s(1-g). \tag{46}$$

Altering the properties of the original medium during Monte Carlo random walks as an acceleration scheme is also common, where it is even common to alter the phase function and other properties after each collision in a single random walk. This relates to a larger class of Monte Carlo acceleration methods sometimes referred to as *condensed-history* (CH) schemes where one or more free-paths and scattering events are approximated and randomly sampled together as a single step.

There are some beautiful *rescaling* properties of the transport process that produce, in limited cases, useful relationships between transport quantities within one medium as the absorption level is varied [Kienle and Patterson 1996].

Further Reading

- The condensed-history (CH) idea dates back to Berger [1963] for charged particles. He used a fixed sampling distance s between successive collisions for all events (user-defined) and the scattering kernel was adjusted to represent multiple scattering using the Goudsmit-Saunderson (GS) PDF [Goudsmit and Saunderson 1940].
- [Goudsmit and Saunderson 1940] - angular moments only for multiple anisotropic scattering after distance s
- [Lewis 1950] - spatial moments (averaged angularlly) for multiple anisotropic scattering after distance s
- [Davison 1957] - similarity relations from early neutron transport
- [van de Hulst 1980] - observed similarities between scattering in slabs with low absorption
- [Fleck and Canfield 1984] - proposed jumping to the surface of the largest sphere contained within a homogeneous region containing the current position, using a diffusion approximation to estimate the adjusted sample weight (thereby simulating an arbitrary number of collisions in one step)
- [Wyman and Patterson 1988] - replacement of a continuous phase function with one having discrete angles, preserving moments
- [Wyman et al. 1989] - similarity relations for alteration of the scattering cross section as well as the phase function
- [Larsen 1992] - proof that CH is a solution to the transport equation in the limit of small step size, proposed higher order method and indicated possibility of even lower error by splitting the translation and scattering steps apart
- [Ballinger et al. 1992] - The response history Monte Carlo method: don't use analytic CH for low energy electrons, because of errors, instead just compute CH functions with MC analog sampling
- [Baro et al. 1995] random hinge method
- [Kawrakow and Bielajew 1998] - comparison of previous and proposal of new electron CH method
- [Cooper 2000] - propose diffusion solution for angular distribution leaving the Fleck / Canfield sphere samplings instead of cosine distribution in angle.
- [Fomenko et al. 2000] Recurrence relation method to evaluate time-resolved green's function for 30 anisotropic scattering events in one step
- [Tolar Jr and Larsen 2001a] moment condensed history (MCH) - spatio-angular moments for multiple anisotropic scattering after travelling distance s and a CH method to satisfy those exact moments
- [Tolar Jr and Larsen 2001b] - transport condensed history (TCH)
- [Franke and Prinja 2005] - discrete angle CH
- [Bhan and Spanier 2007] - Study of Lewis, GS and Larsen Tolar CH methods for photon transport in biological tissue
- [Densmore et al. 2008] - improved diffusion-based sphere-exitance sampling for the [Fleck and Canfield 1984] approach
- [Zhao et al. 2014] - algorithm for determining moment-preserving similarity relations with consideration of smoothness of rendered images and render performance

2.5 Scattering Kernels / Phase Functions in Flatland

The phase space for transport in flatland has an angular component in correspondence with points on the unit circle, S^1, parametrized by angle $\theta \in [-\pi, \pi)$.

Phase function normalization in flatland is found via

$$\int_{-\pi}^{\pi} p(\theta) d\theta = 1. \tag{47}$$

Isotropic Scattering in Flatland Isotropic scattering in Flatland is given by

$$g(\theta) = \frac{1}{2\pi}. \tag{48}$$

2.5.1 Henyey-Greenstein Scattering in Flatland

Davis derived a generalization of Henyey-Greenstein scattering for Flatland [Davis et al. 1993, Davis 2006],

$$p(\theta, g) = \frac{1}{2\pi} \frac{1 - g^2}{1 + g^2 - 2g\cos\theta}, \tag{49}$$

which satisfies

$$\int_{-\pi}^{\pi} p(\theta) \cos(n\theta) d\theta = g^n, \tag{50}$$

analagous to the 3D kernel (Sec 2.3.4). This phase function is sampled via

$$\theta_s = 2\tan^{-1}\left(\frac{1-g}{1+g}\tan\left[\frac{\pi}{2}(1-2\xi\right]\right) \tag{51}$$

where ξ is a random number drawn uniformly from $[0, 1)$.

2.6 Scattering Kernels / Phase Functions in the Rod Model

A completely general scattering kernel in the rod domain is a tuple $\{F, B\}$. A complete description of all possible anisotropic media in rods can be formed by specifying the single scattering albedo α and a quantity analagous to the mean-cosine of scattering:

$$g = \frac{\Sigma_t F - \Sigma_t B}{\Sigma_s} = \frac{F - B}{\alpha} \tag{52}$$

where, just like in 3D, $|g| \leq 1$, $g = 0$ is isotropic scattering, and $g > 0$ is forward scattering, etc.

Further Reading

see [Sharma 2015] for an in depth review of scattering phase functions for light scattering.

2.7 Anisotropic Random Media (Asymmetric Scattering)

A common pair of assumptions in scattering problems are

- The probability of experiencing an absorption or scattering collision when traversing through some small element of the volume is independent of the incoming direction,
- The outgoing distribution of scattered angles is relative only to the incoming direction and not a function of any external frame of reference (the scattering kernel is *symmetric*)

This leads to the absorption and scattering coefficients being independent of the incoming direction and to the scattering kernel being expressed as a function of the dot product between the incoming and outgoing directions, $p(\vec{\omega}_i \cdot \vec{\omega}_o)$. This form of scattering media is sometimes referred to as *isotropic random media* (not to be confused with isotropic scattering kernels).

In the more general case where interaction events and scattering deflections are tied in some way to an absolute frame of reference for the system/media, the absorption and scattering coefficients depend on the incoming direction, the phase function remains written $p(\vec{\omega}_i, \vec{\omega}_o)$ and the media is sometimes referred to as *anisotropic random media (asymmetric scattering)*.

2.7.1 Relation to Underlying Physics

Figure 7 illustrates a physical motivation for considering the use of anisotropic random media.

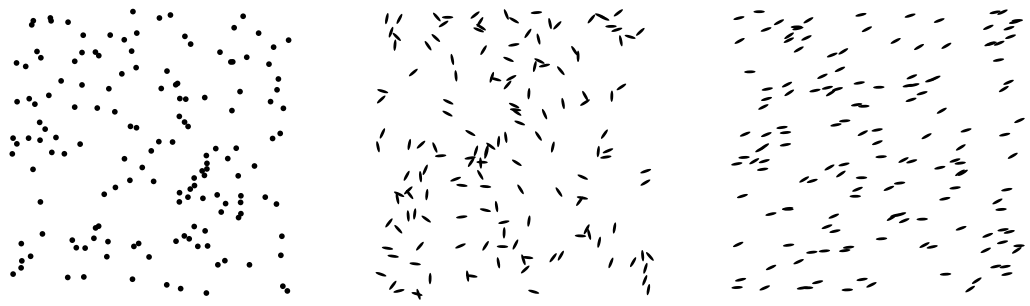

(a) isotropic random media (b) isotropic random media (c) anisotropic random media

Figure 7: *For a collection of reflecting/refracting particles in a medium that scatter and absorb light under a geometrical optics approximation, the shapes and orientations of those particles will determine the overall character of the scattering. In the case (a) that the particles themselves are isotropic in shape, the scattering is certainly symmetric. In the case (b) that the particles are anisotropic in shape but are isotropically oriented in the medium, the convolution of the orientation distribution with the reflectance distribution is symmetric. However, if (c) there is an angularly-anisotropic random orientation of anisotropically-shaped scattering particles, the scattering, absorption and phase function will be a function of incident angle in an external frame of reference for the system. In this particular example of stretched particles (c), the distribution of free paths is longer for flights moving similar to the direction that the particles are stretched in, and shorter for paths orthogonal to the direction of stretching.*

Further Reading

We don't currently include anisotropic media scattering problems in this book, but hope to in the future. Scattering in anisotropic random media has been studied for some time [Kuščer and Summerfield 1969]. It has seen successful application in the study of light transport in tree canopies [Ganapol and Myneni 1992b, Ganapol and Myneni 1992a] and for transport of radionuclides in fractured rock [Williams 1992]. In these plane-parallel problems the discrete eigenvalues no longer occur in conjugate pairs and the rigorous asymptotic diffusion term satisfies an equation that includes an adjective flow term [Cassell and Williams 1992]. The generalization of Caseology for anisotropic 1D media was explored by Furfaro and Ganapol [2007]. The ADO numerical solution method has also been extended to 1D anisotropic media [Picca et al. 2012, Picca and Furfaro 2013]. The transport of visible light through biological tissue exhibits clear features of anisotropic media transport, due to the alignment of the cellular structures (especially collagen) that give rise to much of the scattering [Nickell et al. 2000, Weyrich et al. 2006]. Anisotropic media was introduced to graphics by Jakob et al. [2010]. It was recently shown how the popular Smith model for random surface scattering can be formulated as a new form of anisotropic random media, which leads to tractable calculation of all order microsurface scattering [Heitz et al. 2015].

2.8 Non-Classical Transport

In this section we discuss generalizations of classical transport theory.

In any theory of transport, the fundamental ingredients are: the nature of absorption and scattering events (the *medium interactions*) together with the distribution of free-path lengths between the medium interactions. In the generalizations we discuss here, absorption and scattering processes remain identical to the classical case, but the distributions of distances between medium interactions (the *free-path distributions*) are extended to permit any normalized PDF on $[0,\infty)$. Classical transport is included in the general theories as the special case that the free-path distribution is an exponential distribution.

In classical heterogeneous media where the *density* of scattering particles is non-uniform the distribution of path lengths between scattering events will be non exponential. We consider a distinct form of transport here where, due to the *correlation between scattering events* (even for a homogeneous medium of uniform density), non-exponential free paths arise.

2.8.1 The Free-Path Distribution of Random Flights

The free-path distribution $S(s)$ of a random flight is a normalized distribution for selecting free path lengths s between particle interaction events within the homogeneous medium:

$$\int_0^\infty S(s)ds = 1, \tag{53}$$

where the *mean free path* (if finite) is

$$\ell = \int_0^\infty sS(s)ds. \tag{54}$$

Further Reading

Heavy-tailed free-path distributions, such as the Levy distribution, produce well-defined random flights with several interesting properties. Because there is no finite mean free path, the transport process has no characteristic length and looks the same at all scales (i.e. is fractal). This requires a new form of "anomalous" diffusion theory [Metzler and Klafter 2000].

2.8.2 Exponential Free-Paths (Classical Transport)

A fundamental assumption of classical transport theory is that the locations of the medium interactions (the scattering centres) are uncorrelated. This means that any particle in classical transport theory determines its future one microstep at a time, rolling independent dice to decide whether or not it should scatter or absorb in the next microstep, with no memory of previous events. In moving through some region of a homogeneous medium with interaction coefficient Σ_t, we assign a probability of $\Sigma_t\Delta + o(\Delta)$ to interact with the medium when traversing a path segment of length Δ. The distance s that a particle has travelled unscattered since the last scattering event (or birth) has no influence on its probability to scatter or absorb when passing along path segment Δ (see Figure 8).

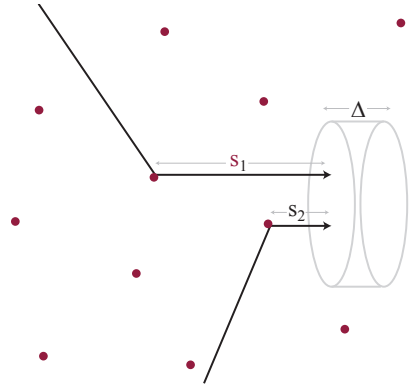

Figure 8: *In classical transport theory both particles traversing through the small volume segment of thickness Δ have identical chances of experiencing a collision within Δ. Having arrived at the surface of Δ, no memory of distance s to the previous medium interaction has any influence on the particle's future when passing through Δ. The generalized transport theories described in this section introduce a dependence on s to the transport coefficient $\Sigma_t(s)$. In the general theory the two particles with free path parameters $s_1 \neq s_2$ can have different scattering and absorption probabilities when passing through Δ.*

This classical first-principles assumption of non-correlated scattering leads to an exponential distribution of free-path lengths between events with one free parameter, ℓ, the mean free path,

$$S(s) = \frac{1}{\ell} e^{-s/\ell} = \Sigma_t e^{-s\Sigma_t}. \tag{55}$$

An additional consequence is that the *attenuation/extinction function* $X(s)$ for the medium is also exponential (the Beer-Lambert law)

$$X(s) = 1 - \int_0^s S(s')ds' = e^{-s\Sigma_t}. \tag{56}$$

This assumption has largely dominated 100 years of transport theory. The last decade has seen the emergence of several theoretical and applied approaches to lifting this assumption in order to extend the utility of transport theory methods to cover a broader range of problems.

2.8.3 Motivation for Non-Exponential Free-Paths (Generalized Transport)

The non-correlated scattering-center assumption of classical transport limits the accuracy for the theory to accurately approximate transport in random media such as that illustrated in Figure 9 (b) where the dots illustrate the locations in the medium that give rise to absorption or scattering and are negatively correlated in their relative positions.

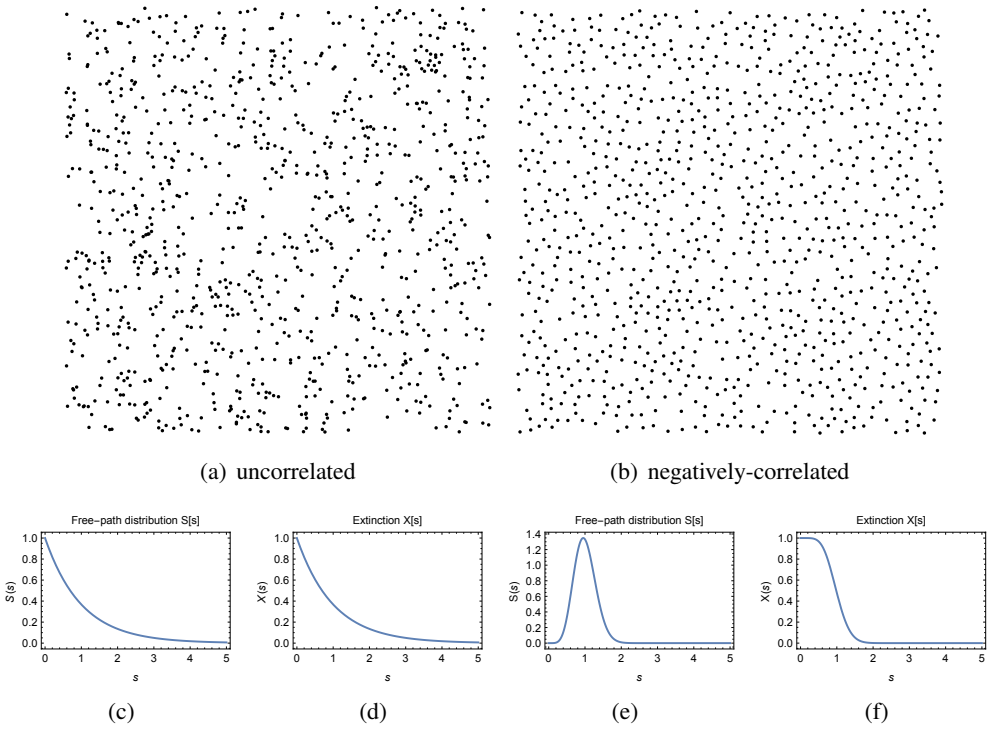

(a) uncorrelated (b) negatively-correlated

(c) (d) (e) (f)

Figure 9: *Classical transport theory assumes infinitesimal scattering centers with completely uncorrelated positions (a), leading to a free-path distribution (c) (and extinction law (d)) that is exponential. However, it is likely that in any real medium some correlation between scattering particles exists (b) leading to non-exponential (generalized) transport. In example (b) the scattering particles are negatively correlated and there is very little chance of scattering at a position that is very close to the previous scattering event. This yields a free-path distribution (e) that begins at 0 and peaks near the mean-free-path, and an extinction law (f) that is flat for distances s that are small compared to the mean free path.*

Evidence for the correlation of scattering particles in optics and atmospheric sensing have led researchers [Kostinski 2001, Davis and Marshak 2004] to extend transport theory to better predict bulk transport in such media. In a class of nuclear reactors known as "pebble bed" reactors, the correlated positions of the pebbles have likewise motivated similar lines of research [Larsen and Vasques 2011, Vasques and Larsen 2013]. Also, in computer graphics, measurement of the statistics of random flights through complex dielectric media (such as a bowl of glass Buddha statues) has produced non-exponential free path statistics. Generalized rendering methods with non-exponential free paths and extinction have been proposed to approximate the bulk transport in such media resulting in significant reductions in computation time with negligible visible change [Moon et al. 2007].

2.8.4 The Extension of Larsen and Vasques

In this section we briefly discuss aspects of a formal generalization of transport theory by Larsen and Vasques [2011], extending transport theory to include non-exponential free paths. A new fundamental quantity that makes no appearance in classical theory is s, the *distance a particle has travelled since birth or its previous scattering event* in the medium. To account for correlated scattering centers, such as those illustrated in Figure 9 (b), memory of s must influence the scattering probabilities for all positions along the free path. In Figure 8, classical theory assigns identical collision probabilities to both particles when traversing Δ. In the new generalized theory, if we suppose that the medium consists of negatively-correlated scattering centres, we see that the distance s_2 of the second particle is much smaller than the average distance between scattering center, and so we expect that the particle with free-path s_2 would experience a lower probability to experience a collision or absortion within Δ compared to a particle having travelled free-path length s_1.

Larsen and Vasques [2011] show that the linear-Boltzmann-equation framework of classical transport theory can be extended directly to produce any desired free path distribution $S(s)$ by redefining the transport/interaction coefficients Σ_t to depend on s,

$$\Sigma_t(s) = \frac{S(s)}{X(s)}, \tag{57}$$

the ratio of the free-path distribution to the source extinction function. What was previously a fundamental property of the medium, Σ_t, is now a function of the free-path distribution. Only in the case of classical transport (where $S(s)$ is an exponential) is $\Sigma_t(s)$ a constant [Larsen and Vasques 2011],

$$\Sigma_t(s) = \frac{S(s)}{X(s)} = \frac{\frac{1}{\ell}\mathrm{e}^{-s/\ell}}{\mathrm{e}^{-s/\ell}} = \frac{1}{\ell}, \tag{58}$$

the inverse mean free path.

A generalized transport medium is completely characterized by

- The free-path distribution $S(s)$
- The single-scattering albedo α
- The scattering kernel/phase function.

2.8.5 The Generalized Linear Boltzmann Equation (GLBE)

Larsen and Vasques [2011] presented a complete formulation of transport theory based on the above extension of random flights with several additional assumptions:

- The single-scattering albedo is not dependent on s.
- The scattering kernel/phase function is not dependent on s.

The resulting generalized linear Boltzmann equation is

$$\frac{\partial L}{\partial s}(\vec{x},\vec{\omega},s) + \vec{\omega}\cdot\nabla L(\vec{x},\vec{\omega},s) + \Sigma_t(s)L(\vec{x},\vec{\omega},s) = \\ = \delta(s)\alpha\int_{4\pi}\int_0^\infty p(\vec{\omega},\vec{\omega}')\Sigma_t(s')L(\vec{x},\vec{\omega}',s')ds'd\vec{\omega}' + \delta(s)\frac{Q(\vec{x})}{4\pi} \tag{59}$$

where the angular flux / radiance L now depends on s. The total radiance is found by accumulating the radiances due to particles of all previous step distances s via

$$L(\vec{x},\vec{\omega}) = \int_0^\infty L(\vec{x},\vec{\omega},s)ds. \tag{60}$$

The appearance of s in $L(\vec{x},\vec{\omega},s)$ decomposes the fundamental quantity of transport into a "spectra" of particles with differing free path parameters, s. This decomposition is required in order to understand the evolution of the transport quantities throughout the system and over time.

The aspect of absorption in the theory of Larsen and Vasques is worthy of attention. Once the assumptions of classical transport are adopted, it is impossible to distinguish between a medium where the scattering and absorption events are caused by the same underlying process (e.g., collisions with one class of particle that both absorbs and scatters) and a medium where absorption is caused by a different underlying process than the one causing scattering (like tissue, where scattering is mainly due to small fluctuations in index of refraction of the cellular structures, and absorption is mainly due to chromophores like melanin and hemoglobin). Indeed, the following three physical scenarios lead to identical classical transport theory predictions:

- The flight of particles through a vacuum colliding with a single class of particles, which both absorb and scatter (Figure 10a)
- The flight of particles through a vacuum colliding with two classes of particles, one purely scattering, and the other purely absorbing, with no correlation between their positions (Figure 10b)
- The flight of particles subject to the scattering from purely scattering particles embedded in a base material with continuous Beer-Lambert absorption (Figure 10c).

For the generalized theory of Larsen-Vasques, the GLBE essentially requires that absorption is caused by the same process as scattering. The GLBE accurately describes transport in the first two analogous cases (Figure 10d,e) but does not accurately encompass transport through Beer-Lambert-absorbing jello with negatively correlated mirror spheres (Figure 10f) because the single scattering albedo then becomes dependent upon s.

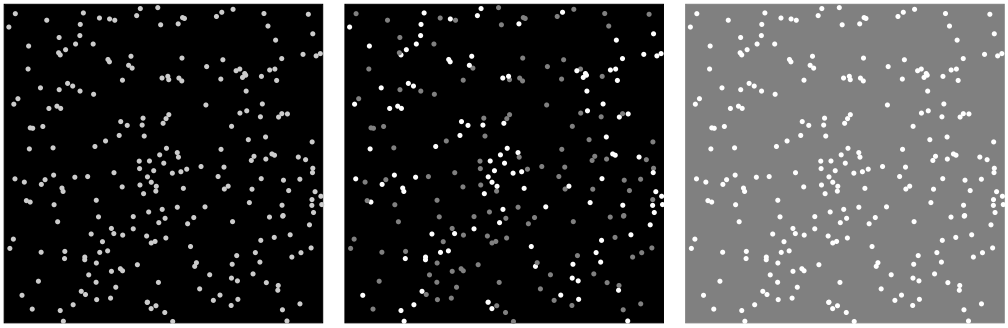

(a) Grey particles in vacuum

(b) Mixture of purely absorbing and purely scattering particles

(c) Purely Scattering particles in Beer-Lambert-absorbing continuum

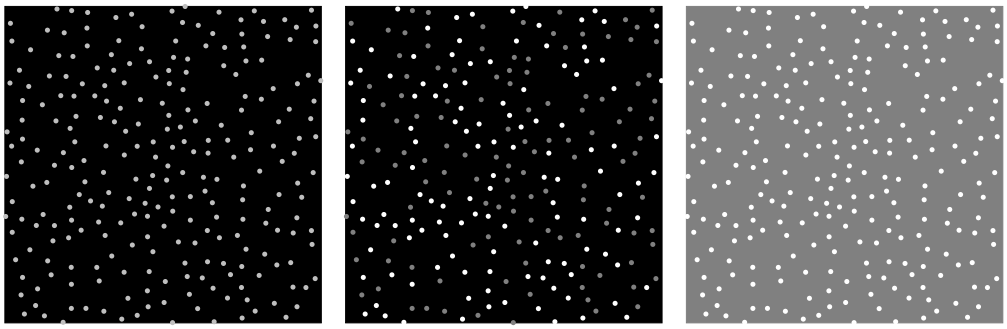

(d) Grey particles in vacuum

(e) Mixture of purely absorbing and purely scattering particles

(f) Purely Scattering particles in Beer-Lambert-absorbing continuum

Figure 10

We refer the reader to [Larsen and Vasques 2011] for more information on the derivation of this generalized theory and to [Vasques and Larsen 2013] for its extension to describe anisotropic random media (asymmetric scattering).

Further Reading

This has not been the only proposed extension of Σ_t for non-classical transport. [Myneni et al. 1991] consider $\Sigma_t(\vec{x}', \vec{x}'')$ where the transport coefficient depends on the last two scattering positions, in order to produce a transport model capable of exhibiting coherent backscattering (the opposition effect).

2.8.6 Monte Carlo Estimators for Generalized Linear Transport

Despite the complexity of Equation 59, Monte Carlo estimators for generalized transport problems are quite similar to the classical case.

Forward and adjoint analog estimators begin with source/detector sampling and repeated alternation of free-path sampling, using $S(s)$, followed by random sampling to select absorption vs

scattering, and phase-function sampling in the latter case. Estimation of the collision densities in the medium are analagous to the classical case using the collision estimator.

In *classical* media, fluence and radiance are trivially computed from the analogous collision density because the two quantities are proportional (by a factor of the constant Σ_t). Here, however, the estimation of fluence and radiance within the medium is more challenging, because knowledge of the collision density at a location is not sufficient to determine the fluence or radiance there. It is possible to formulate next-event estimators for the fluence and radiance quantities using the source-extinction function $X(s)$. It is important to remember that $X(s)$ only applies to densities leaving a birth or collision and does not apply generally to radiance at any location like in the classical case.

To expand further on the subtlety between collision densities and radiance/fluence (energy density of particles *in flight*): there are different physical reasons for wanting to predict a collision density vs fluence or radiance within a medium. For example, if collision events were the source of heat or other derivative phenomena of interest (like reaction rates), the collision density may be the desired quantiy. This is different (and not proportional to) the quantity that would be measured by inserting a tiny directional or omni-directional "camera" sensor whose signal is proportional to the radiance/fluence. What were two proportional quantities in classical transport are now two very different quantities and even have differing diffusion asymptotics [d'Eon 2014, d'Eon 2016]. Scalar and angular flux are the only measurable quantities exiting a medium, so for BRDF/BSDF and BSSRDF derivations, radiance/scalar-flux and its integral remain the desired quantity of prediction.

Further Reading

There is a large body of work studying simulation of correlated transport, correlated distributions and their relation to real world measurements/processes:

- [Metropolis et al. 1953] metropolis shuffling algorithm for efficient dart throwing of sphere packings
- [Percus and Yevick 1958] Percus Yevick distributions for sphere packings (blue noise)
- [Wertheim 1963] exact solution of Percus-Yevick distributions
- [Baxter 1967] method of solution for Percus-Yevick distributions
- [Smith and Henderson 1970] solution of dart throwing sphere packing (blue noise) in terms of Percus-Yevick hard-sphere radial distribution
- [Perram 1975] new numerical solution to Percus-Yevick hard-sphere radial distributions
- [Ishimaru and Kuga 1982] observation of non-exponential attenuation
- [Tsang and Ishimaru 1984] second-order multiple scattering approximation for accounting for backscattering enhancement of random discrete scatterers
- [Kuga and Ishimaru 1984] retroreflection from an ensemble of spherical particles
- [Nigmatullin 1986] realization of a transfer equation in a fractal medium (porous structure)
- [Jakeman and Tough 1987] K-distributions and non classical transport
- [Zurk et al. 1995] application of the Metropolis shuffling algorithm for dart throwing/sphere packing
- [Davis and Marshak 1997] Applied Levy stable time resolved solutions instead of Gaussian (classical diffuion) solutions for clouds.

- [Tsang et al. 1998] application of the Metropolis shuffling algorithm for dart throwing/sphere packing
- [Tsang et al. 2000] looks at sitcky particle sizes and correlations and uses a advanced statistical theory to derive attenuations
- [Kostinski 2001] Super poissoidian model yields slower than exponential attenuation. Considers beam moving through slab with spatial correlations between finding scatterers in two adjacent volume elements.
- [Borovoi 2002] criticism of [Kostinski 2001]
- [Kostinski 2002] reply to [Borovoi 2002]
- [Giusto et al. 2003] high density medium with correlations can be described by equivalent classical medium, but with a complex index of refraction
- [Zaccanti et al. 2003] Measurement of effective scattering, absorption and phase function laws as the volume density of scatterers becomes large the and independent scattering assumption is not fulfilled. The phase function changes with high density.
- [Guéron and Mazzolo 2003] "chord length distributions across packings—random or not—of equal hard disks have a universal divergence which is proportion to $n_c/\sqrt{l}$ for small chords, where n_c is the mean number of contacts."
- [Davis and Marshak 2004] enhanced mean-free-paths and wider-than-exponential free-path distributions (optical media with spatial correlations)
- [Guérin et al. 2006] effective medium theory for random aggregates of small spherical particles that account for the finite size of the embedding volume
- [Olson et al. 2006] analysis of chord length distributions in discs and spheres without intersection
- [Moon et al. 2007] first use of non-exponential free path transport in graphics
- [Ji and Martin 2007] simulation of dense sphere packings, slightly non exponential chord lengths, proposal of linear-exponential free-path distributions
- [Ziya Akcasu and Corngold 2007] Volterra functional calculus, methods to determine the mean flux and its variance over all realizations of some random random medium
- [Olson 2008] chord length distributions in ordered and disordered packing of hard disks and spheres - dilute media: power law is independent of structure, but with higher density packing, it changes a lot - the tails follow power law distributions instead of exponentials.
- [Reinert et al. 2010] heterogeneous binary mixtures
- [Frank et al. 2010] existence, uniqueness, and asymptotic diffusion of non-exponential random flights of the form [Larsen and Vasques 2011]
- [Larsen and Vasques 2011] Generalized linear boltzmann equation for non-exponential random flights
- [Griesheimer et al. 2011] analyzes non-exponential step length distributions in materials with inclusions
- [Golse 2012] Lorentz gas transport, estimation of free-path distributions
- [Svensson et al. 2013] Holy random walks: analytic diffusion derivation for quenched disorder and media with void spacings
- [Tramontana et al. 2013] super and sub-exponential attenuations using Wright functions.
- [Vasques and Larsen 2013] Generalized linear boltzmann equation for non-exponential random flights within anisotropic media

- [Larsen and Clark 2013] link between particle distributions and non-Beer-Lambert extinction
- [Savo et al. 2014] measurement of the fractal dimension of transport in highly disordered media that violates the classical assumptions of transport theory
- [d'Eon 2014] Rigorous-, classical- and Grosjean-modified-diffusion approximations for infinite media problems in arbitrary dimension with general free-path distribution
- [Davis and Xu 2014] Generalized transport with power law extinction
- [Frank et al. 2015] Diffusion and SPN solutions are exact transport solutions of non-classical transport with appropriate selection of the free-path distribution
- [Xu et al. 2016] markov chain formalism in plane parallel media with polarization

3 Boundaries

Applied transport theory is typically concerned with finite or semi-infinite problems involving at least one boundary between two types of differing media (one typically a vacuum). Boundaries can sometimes lead to additional scattering and absorption events and their properties need to be specified. In this section we briefly list several boundary conditions that arise later in volume scattering problems (biased heavily from a computer graphics perspective).

3.1 Lambertian Reflector

Isotropic reflectance from an opaque surface (Lambertian reflectance) is a common approximation for diffuse reflectance in many fields.

Sampling random reflections from a Lambertian reflector with diffuse albedo R_d can be done by sampling an azimuthal direction uniformly $\phi \in [0, 2\pi]$ and a vector component along the surface normal direction with

$$z = \sqrt{\xi} \tag{61}$$

where ξ is a random number drawn uniformly from $[0, 1]$. In a coordinate frame where the surface normal points outward along the z axis, the reflected direction is $(\sqrt{1-z^2}\cos(\phi), \sqrt{1-z^2}\sin(\phi), z)$ and the particle weight is reduced by a factor of R_d to accomodate the absorption.

3.2 Fresnel Reflection

Light encountering a boundary between two dielectric media of differing index of refraction will lead to some portion F_R of the energy being reflected into the mirror-reflection direction, and the remaining energy F_T refracting into the material across the boundary at an angle governed by Snell's law. When entering a less dense medium, total internal reflection can occur.

3.2.1 Snell's Law

For refraction at a smooth boundary between two dielectrics with refraction indicies η_i and η_t the incident and exitant angles measured to the boundary normal, θ_i and θ_t, respectively, satisfy Snell's law

$$\eta_i \sin\theta_i = \eta_t \sin\theta_t. \tag{62}$$

Reflection Vector For some unit incoming direction $\vec{\omega}_i$, the unit reflected direction $\vec{R}$ given unit surface normal $\vec{N}$ is computed via (assuming $\vec{\omega}_i \cdot \vec{N} > 0$)

$$\vec{R} = -\vec{\omega}_i + 2\vec{N}(\vec{N} \cdot \vec{\omega}_i). \tag{63}$$

Refraction Vector The unit refracted direction $\vec{T}$ is computed via

$$\vec{T} = \vec{N}\left(-\sqrt{1 - \frac{\eta_i^2\,(1 - (\vec{\omega}_i \cdot N)^2)}{\eta_t^2}}\right) - \frac{\eta_i(\vec{\omega}_i - \vec{N}\vec{\omega}_i \cdot \vec{N})}{\eta_t}. \tag{64}$$

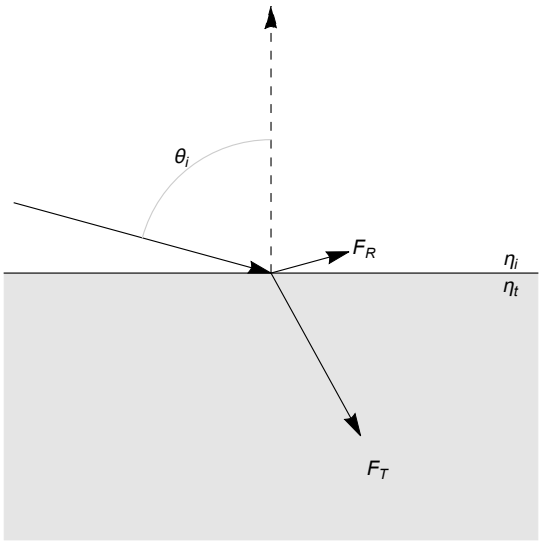

Figure 11: *Notation for Fresnel interaction at a boundary between two dielectric media (reflection F_R and transmission F_T).*

3.2.2 Smooth Dielectric

Fresnel reflectance F_R from a dielectric with incidence angle θ_i (less than the critical angle) and with index of refraction η_t is [Born and Wolf 2002]

$$F_R(\theta_i) = \frac{1}{2}\left(\frac{\left(\eta\cos(\theta_i) - \sqrt{1-\eta^2\sin^2(\theta_i)}\right)^2}{\left(\eta\cos(\theta_i) + \sqrt{1-\eta^2\sin^2(\theta_i)}\right)^2} + \frac{\left(\cos(\theta_i) - \eta\sqrt{1-\eta^2\sin^2(\theta_i)}\right)^2}{\left(\cos(\theta_i) + \eta\sqrt{1-\eta^2\sin^2(\theta_i)}\right)^2}\right) \tag{65}$$

where θ_i is the angle measured to the surface normal and η_i is the index of refraction of the incident medium, with the relative index of refraction $\eta = \eta_t/\eta_i$ (see Figure 11). Equivalently,

$$F_R(\theta_i) = \begin{cases} \frac{1}{2}\frac{(g-c)^2}{(g+c)^2}\left(\frac{(c(g+c)-1)^2}{(c(g-c)+1)^2}+1\right), & \eta^2 - 1 + c^2 \geq 1 \\ 1, & \eta^2 - 1 + c^2 < 1 \end{cases} \tag{66}$$

$$c = \cos\theta_i \tag{67}$$

$$g = \sqrt{\eta^2 - 1 + c^2}. \tag{68}$$

For normal incidence $\theta_i = 0$

$$F_R(0) = \frac{(\eta_i - \eta_t)^2}{(\eta_i + \eta_t)^2}. \tag{69}$$

	$F_R(\theta_i)$					
η	$\theta_i = 0$	$\theta_i = 0.2$	$\theta_i = 0.5$	$\theta_i = 1$	$\theta_i = 1.2$	$\theta_i = 1.5$
0.5	0.111111	0.111752	0.283268	1	1	1
0.7	0.0311419	0.0312467	0.0387004	1	1	1
0.9	0.00277008	0.00277588	0.00309559	0.0452967	1	1
0.99	0.0000252519	0.0000252954	0.0000275606	0.000184621	0.00132454	1
1.01	0.0000247519	0.0000247928	0.0000269003	0.000160946	0.000962525	0.143225
1.1	0.00226757	0.0022707	0.0024255	0.00987357	0.0376234	0.507226
1.4	0.0277778	0.0277999	0.0288139	0.0611806	0.135736	0.657913
2	0.111111	0.111145	0.112621	0.15019	0.222786	0.6834

Table 2: *Fresnel dielectric reflectance $F_R(\theta_i)$ benchmark data.*

3.2.3 Smooth Conductor

Fresnel reflectance F_R from a conductor with incidence angle θ_i and with index of refraction components η (real) and k (imaginary) is [Born and Wolf 2002]

$$F_R(\theta_i) = \frac{1}{2}(\rho_{||} + \rho_{\perp}) \tag{70}$$

$$\rho_{||} = \frac{(p - \eta_i \sin(\theta_i)\tan(\theta_i))^2 + q^2}{(p + \eta_i \sin(\theta_i)\tan(\theta_i))^2 + q^2}\,\rho_{\perp} \tag{71}$$

$$\rho_{\perp} = \frac{(\eta_i \cos(\theta_i) - p)^2 + q^2}{(\eta_i \cos(\theta_i) + p)^2 + q^2} \tag{72}$$

$$p = \frac{\sqrt{\sqrt{\left(\eta^2 - \eta_i^2 \sin^2(\theta_i) - k^2\right)^2 + 4\eta^2 k^2} + \eta^2 - \eta_i^2 \sin^2(\theta_i) - k^2}}{\sqrt{2}} \tag{73}$$

$$q = \frac{\sqrt{\sqrt{\left(\eta^2 - \eta_i^2 \sin^2(\theta_i) - k^2\right)^2 + 4\eta^2 k^2} - \eta^2 + \eta_i^2 \sin^2(\theta_i) + k^2}}{\sqrt{2}} \tag{74}$$

where θ_i is the angle measured to the surface normal and η_i is the index of refraction of the incident medium. For normal incidence $\theta_i = 0$

$$F_R(0) = 1 - \frac{4\eta\eta_i}{(\eta + \eta_i)^2 + k^2} \tag{75}$$

	$F_R(\theta_i)$					
$\eta + ik$	$\theta_i = 0$	$\theta_i = 0.2$	$\theta_i = 0.5$	$\theta_i = 1$	$\theta_i = 1.2$	$\theta_i = 1.5$
$1.01 + 0.5i$	0.058297	0.0583739	0.0617829	0.143398	0.270677	0.771216
$1.1 + 0.5i$	0.055794	0.0558562	0.0586152	0.127731	0.243942	0.751578
$1.4 + 0.5i$	0.0682196	0.0682653	0.070265	0.121631	0.216441	0.716803
$2 + 0.5i$	0.135135	0.135172	0.136733	0.174903	0.24661	0.694004
$10 + 0.5i$	0.670103	0.67007	0.66871	0.640179	0.594733	0.500498
$1.01 + 5i$	0.860882	0.860862	0.86007	0.845425	0.827007	0.880432
$1.1 + 5i$	0.850391	0.85037	0.849536	0.834112	0.814725	0.871181
$1.4 + 5i$	0.817945	0.817922	0.816973	0.799379	0.777241	0.841838
$2 + 5i$	0.764706	0.764679	0.763584	0.7431	0.716979	0.789545
$10 + 5i$	0.726027	0.725995	0.724679	0.696901	0.651431	0.522924

Table 3: *Fresnel conductor reflectance $F_R(\theta_i)$ benchmark data.*

Several approximate forms of conductive Fresnel reflectance have been reported in the literature, such as Schlick's approximation [1994] and an approximation presented in [Pharr and Humphreys 2010] that is fairly accurate for large k. A common misconception is that the conductive equations can be obtained from substituting a complex index into the dielectric equations and taking the magnitude. None of these forms are accurate for all angles and all refraction index values (Figure 12).

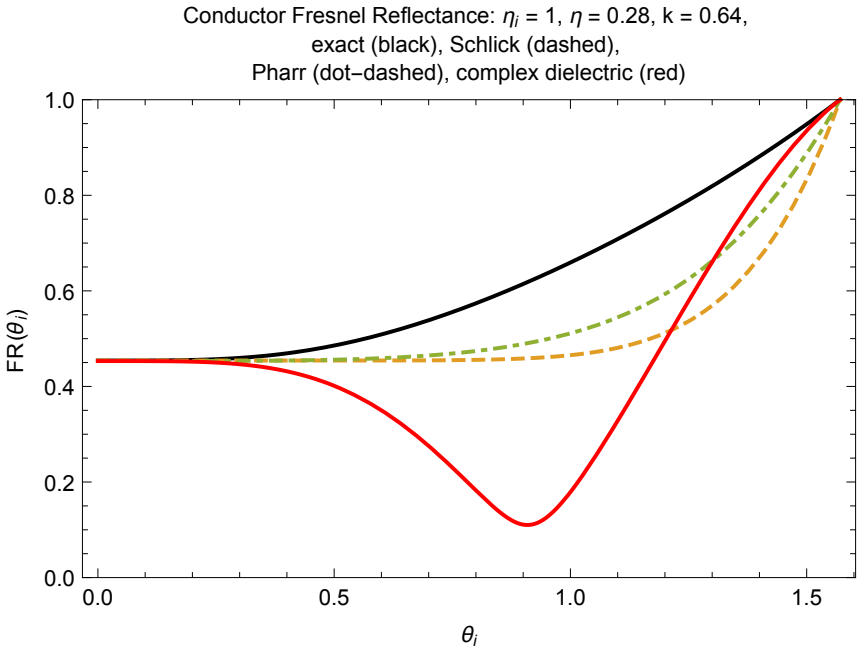

Figure 12: *Comparison of the accuracy of various equations proposed for computing the Fresnel reflectance from a smooth conductive surface.*

3.3 Rough Boundaries

For evaluating and importance sampling Fresnel dielectric, conductive or diffuse reflectance/transmission due to an interface that is rough (with Beckmann or other normal distributions), see [Heitz and d'Eon 2014, Heitz et al. 2015].

4 Rod Model/Two-Stream Approximation: Scattering in a Spatially-1D Universe

In this section we consider transport along the real line where energy can only flow in two discrete directions, right $(+)$ and left $(-)$. The solutions here sometimes are used to approximate transport in a 3D plane-parallel universe (the two-stream approximation and Kubelka-Munk theory). See Section 2.2.3 for further details.

4.1 Rod Model Notation

- Σ_a: absorption coefficient
- Σ_s: scattering coefficient
- $\Sigma_t = \Sigma_a + \Sigma_s$: total interaction coefficient
- F: fraction of energy that scatters forward (same as incoming direction)
- B: fraction of energy that scatters backward (opposite to incoming direction)
- $\alpha = F + B$: single-scattering albedo
- x: position in the rod
- $\tau = \Sigma_t x$: dimensionless position in the rod
- Q_+: source term for rightward-emitted energy
- Q_-: source term for leftward-emitted energy

4.2 Rod Model Transport Equation

The rod model transport equation is a coupled pair of differential equations [Wing 1962]

$$\pm\frac{dL_\pm}{dx} = -\Sigma_t(x)L_\pm(x) + \Sigma_t(x)F(x)L_\pm(x) + \Sigma_t(x)B(x)L_\mp(x) + Q_\pm(x). \tag{76}$$

We now briefly highlight analogies to diffusion theory in higher dimensional spaces, by defining the fluence

$$\phi(x) = L_+(x) + L_-(x) \tag{77}$$

current

$$J_\phi(x) = L_+(x) - L_-(x) \tag{78}$$

and similar source quantities

$$Q(x) = Q_+(x) + Q_-(x) \tag{79}$$

$$J_Q(x) = Q_+(x) - Q_-(x) \tag{80}$$

with mean cosine

$$g = \frac{\Sigma_t F - \Sigma_t B}{\Sigma_s} = \frac{F - B}{\alpha} \tag{81}$$

and reduced transport coefficient

$$\Sigma_t' = \Sigma_t - g\Sigma_s. \tag{82}$$

The angular fluxes can then be found from the total flux

$$L_\pm(x) = \frac{1}{2}\left(\phi(x) \pm J_\phi(x)\right) \tag{83}$$

$$= \frac{1}{2}\left(\phi(x) \mp \frac{1}{\Sigma_t'(x)}\frac{d\phi}{dx} \pm \frac{1}{\Sigma_t'(x)}J_Q(x)\right). \tag{84}$$

Inverse mappings for F and B are

$$F = \frac{1}{2}(1+g)\alpha \tag{85}$$

$$B = \frac{1}{2}(1-g)\alpha. \tag{86}$$

4.3 Infinite Rod, Isotropic Point Source, Isotropic Scattering

4.3.1 Problem Description

This problem considers an infinite, homogeneous rod with isotropic scattering ($F = B = \alpha/2$) with a unit point source $S_{\pm}(x) = \frac{1}{2}\delta(x)$ at the origin (Figure 13). The boundary conditions are that the solution remains bounded at infinity.

Figure 13: *Infinite rod with isotropic point source (energy can only flow left or right with equal emission in both directions from the origin).*

4.3.2 Radiance/Angular-Flux

Exact Solution The angular fluxes at position x in an infinite homogeneous rod with isotropic scattering due to an isotropic unit point source at the origin are

$$L_{+}(x) = \frac{\left(\sqrt{1-\alpha}\,\mathrm{sgn}(x) + 1\right) e^{-\Sigma_t |x| \sqrt{1-\alpha}}}{4\sqrt{1-\alpha}} \tag{87}$$

$$L_{-}(x) = \frac{\left(\sqrt{1-\alpha}\,\mathrm{sgn}(x) - 1\right) e^{-\Sigma_t |x| \sqrt{1-\alpha}}}{4\sqrt{1-\alpha}} \tag{88}$$

where $\mathrm{sgn}(x) = 1$ for $x > 0$, $\mathrm{sgn}(0) = 0$ and $\mathrm{sgn}(x) = -1$ otherwise.

4.3.3 Fluence/Collision-Density

Exact Solution The fluence due to an isotropic unit point source in an infinite homogeneous rod with isotropic scattering is

$$\phi_{\mathrm{pt}}(x) = \frac{1}{2\sqrt{1-\alpha}} \mathrm{e}^{-\Sigma_t |x| \sqrt{1-\alpha}} \tag{89}$$

Exact Solution After Exactly n Scattering Events The radiance due to particles in flight at some position x that have previously suffered exactly n collisions can be found via straightforward Taylor series expansion of the total radiances (demonstrated and validated in the supplementary material), see Figure 16.

The fluence of particles in flight which have suffered exactly n collisions can be written in closed form [Zoia et al. 2011a]:

$$\phi_{\mathrm{pt}}(x|n) = \frac{2^{-n-\frac{1}{2}} \alpha^n \Sigma_t^{n+\frac{1}{2}} |x|^{n+\frac{1}{2}} K_{n+\frac{1}{2}}(\Sigma_t |x|)}{\sqrt{\pi}\Gamma(n+1)} \tag{90}$$

where K is the modified Bessel function of second kind.

4.3.4 Moments

The first form of integer kth moments of the fluence are found via

$$\phi_{pt,k} = \int_{-\infty}^{\infty} \phi(x) x^k dx = \frac{1}{2}\left((-1)^k + 1\right) k! (1-\alpha)^{-\frac{k}{2}-1} \Sigma_t^{-k-1}, \tag{91}$$

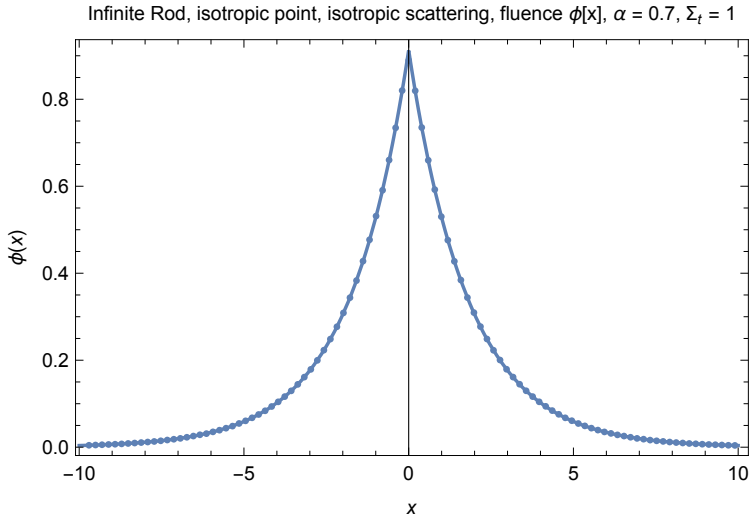

Figure 14: *Fluence due to an isotropic point source inside an infinite rod with isotropic scattering. Validation of analytic (continuous) vs. Monte Carlo (dots).*

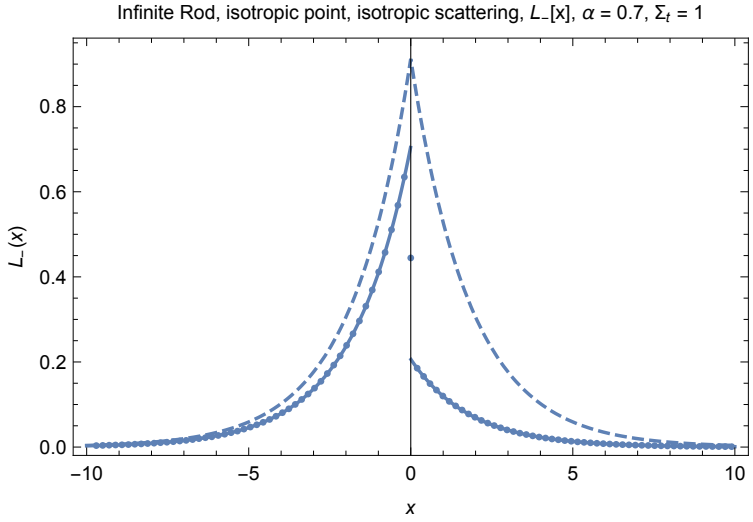

Figure 15: *Left-moving radiance (L_-) due to an isotropic point source inside an infinite rod with isotropic scattering. Validation of analytic (continuous) vs. Monte Carlo (dots). Fluence shown as dashed line for reference.*

which are zero for odd k. These are analagous to the plane-parallel infinite medium problem. Considering, instead, this rod model problem as the limiting case of a spherically-symmetric isotropic point source problem in d dimensions, letting d approach 1, radial moments of real order $k \geq 0$ for the problem are found via

$$\phi_{pt,k} = \int_0^\infty 2\phi(r) r^k dx = (1-\alpha)^{-\frac{k}{2}-1} \Gamma(k+1) \Sigma_t^{-k-1}, \tag{92}$$

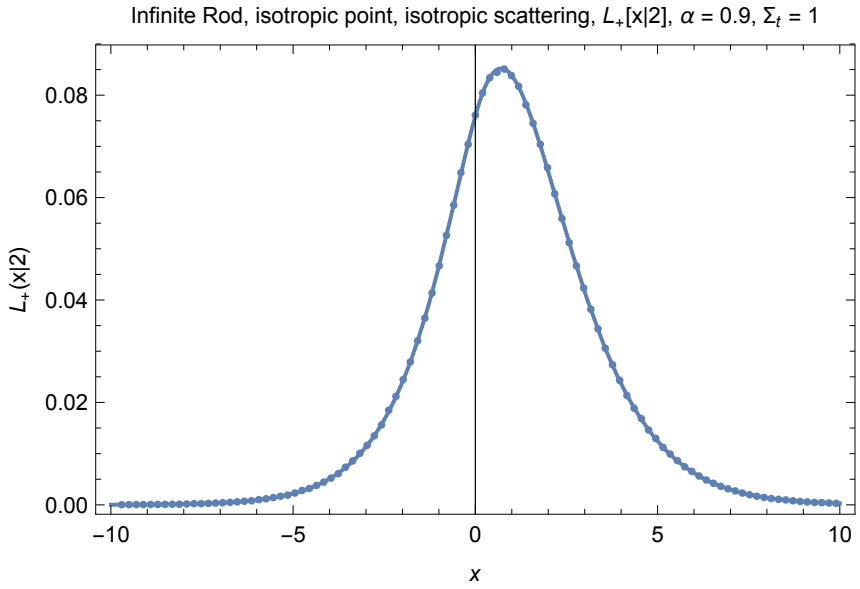

Figure 16: *Doubly-scattered right-moving radiance in a infinite rod with an isotropic point source and isotropic scattering (Monte carlo: dots, analytic: continuous).*

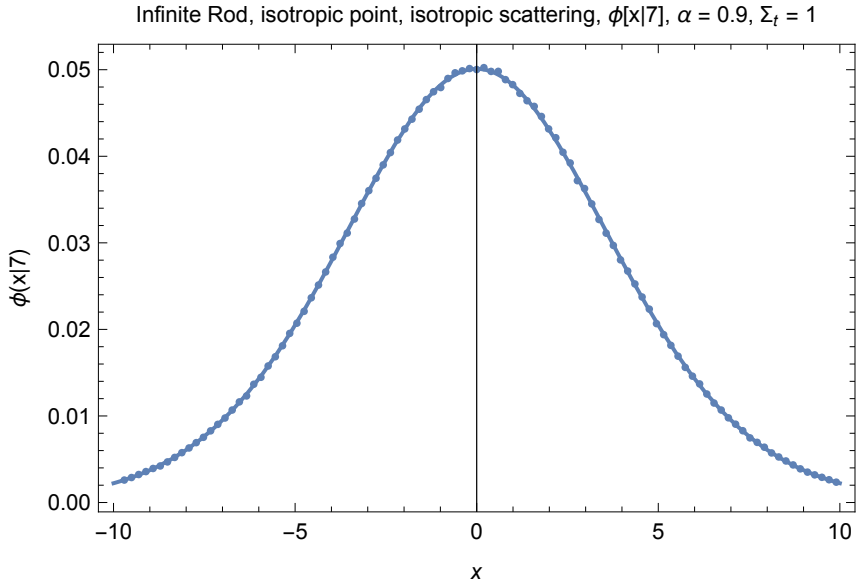

Figure 17: *7th-scattered fluence in a infinite rod with an isotropic point source and isotropic scattering (Monte carlo: dots, analytic: continuous).*

and are not zero for odd k. The first two even moments are independent of dimension [d'Eon 2014], and thus match the corresponding flatland and 3D isotropic point source problems. The

first few even moments are,

$$\phi_{pt,0} = \frac{1}{(1-\alpha)\Sigma_t} \tag{93}$$

$$\phi_{pt,2} = \frac{2}{(1-\alpha)^2\Sigma_t^3} \tag{94}$$

$$\phi_{pt,4} = \frac{24}{(1-\alpha)^3\Sigma_t^5} \tag{95}$$

$$\phi_{pt,6} = \frac{720}{(1-\alpha)^4\Sigma_t^7} \tag{96}$$

MC Code and Mathematica Validation (github):
code/rod/infiniterod/Isotropicpointsource

4.4 Semi-Infinite Rod, Albedo Problem, Isotropic Scattering

4.4.1 Problem Description

This problem considers a semi-infinite ($x \in [0, \infty]$), homogeneous rod with isotropic scattering ($F = B = \alpha/2$) with a unit surface source at $x = 0$ and with interaction coefficient Σ_t and indexed-matched (non-reflecting) boundary conditions (Figure 18).

Figure 18: *Semi-infinite rod with surface source (albedo problem).*

4.4.2 Reflectance/Albedo

Exact Solution The exact solution for the total energy escaping the semi-infinite rod, R, is indepedent of the interaction coefficient and only depends on the single-scattering albedo α,

$$R(\alpha) = \frac{2\left(-\frac{\alpha}{2} - \sqrt{1-\alpha} + 1\right)}{\alpha}. \tag{97}$$

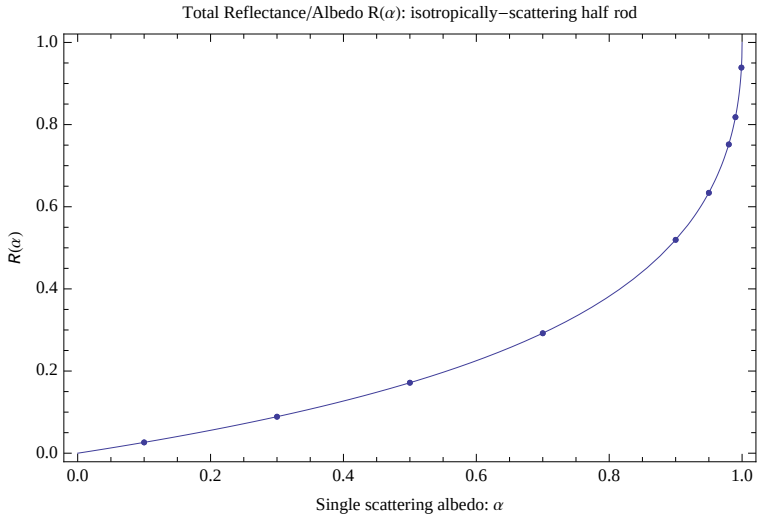

Figure 19: *Rod albedo validation, analytic (continuous) vs. Monte Carlo (dots)*

Exact Solution - Collision Order The exact solution for reflectance due to particles that have scattering exactly n times $R(\alpha|n)$ is found by taking a Taylor expansion of Equation 97 about $\alpha = 0$:

$$R(\alpha) = \frac{\alpha}{4} + \frac{\alpha^2}{8} + \frac{5\alpha^3}{64} + \frac{7\alpha^4}{128} + \frac{21\alpha^5}{512} + \frac{33\alpha^6}{1024} + \frac{429\alpha^7}{16384} + \frac{715\alpha^8}{32768} + \frac{2431\alpha^9}{131072} + \ldots \tag{98}$$

with the general solution

$$R(\alpha|n) = 2(-1)^n \binom{\frac{1}{2}}{n+1} \alpha^n. \tag{99}$$

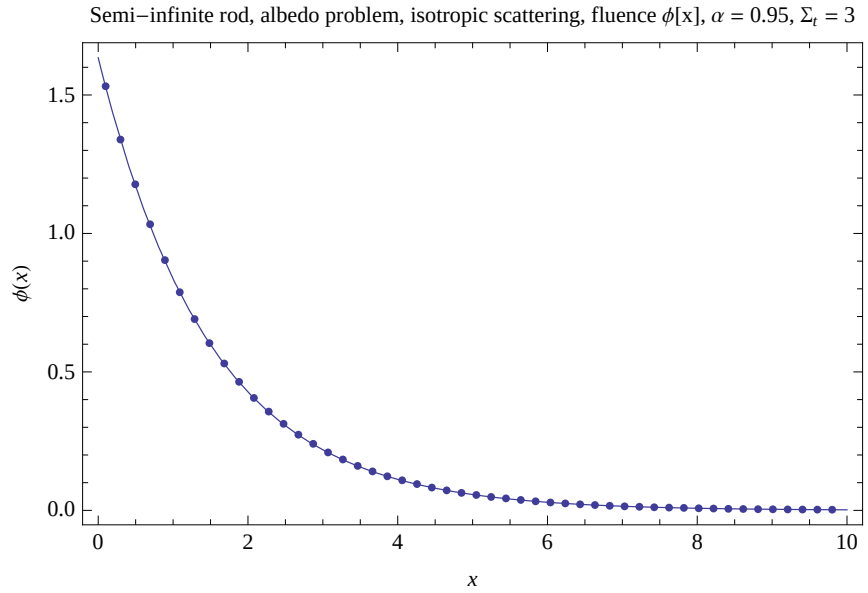

Figure 20: *Fluence in a semi-infinite rod with isotropic scattering due to a surface source. Validation of analytic (continuous) vs. Monte Carlo (dots).*

4.4.3 Internal Distribution

Exact Solution The exact solutions for the right moving radiance L_+ and the left moving radiance L_- are:

$$L_+(x) = \mathrm{e}^{-\Sigma_t x\sqrt{1-\alpha}} \tag{100}$$

$$L_-(x) = \frac{\alpha e^{-\Sigma_t x\sqrt{1-\alpha}}}{-\alpha + 2\sqrt{1-\alpha} + 2} \tag{101}$$

and the fluence / scalar flux / density $\phi(x)$ is:

$$\phi(x) = \frac{2}{\alpha}\left(1 - \sqrt{1-\alpha}\right) e^{-\Sigma_t x\sqrt{1-\alpha}}. \tag{102}$$

The contributions to the density $\phi(x|n)$ due to particles which have scattered exactly $n \geq 0$ times are a product of an exponential $\alpha^n \mathrm{e}^{-\Sigma_t x}$ and a polynomial of degree n in x. These can be found by deriving the Taylor series expansion of Equation 102 about the single-scattering albedo $\alpha = 0$. The first few solutions are

$$\phi(x|0) = e^{-\Sigma_t x} \tag{103}$$

$$\phi(x|1) = \alpha\frac{1}{4}e^{-\Sigma_t x}(2\Sigma_t x + 1) \tag{104}$$

$$\phi(x|2) = \alpha^2\frac{1}{8}e^{-\Sigma_t x}(\Sigma_t x + 1)^2 \tag{105}$$

$$\phi(x|3) = \alpha^3\frac{1}{192}e^{-\Sigma_t x}\left(4\Sigma_t^3 x^3 + 18\Sigma_t^2 x^2 + 30\Sigma_t x + 15\right). \tag{106}$$

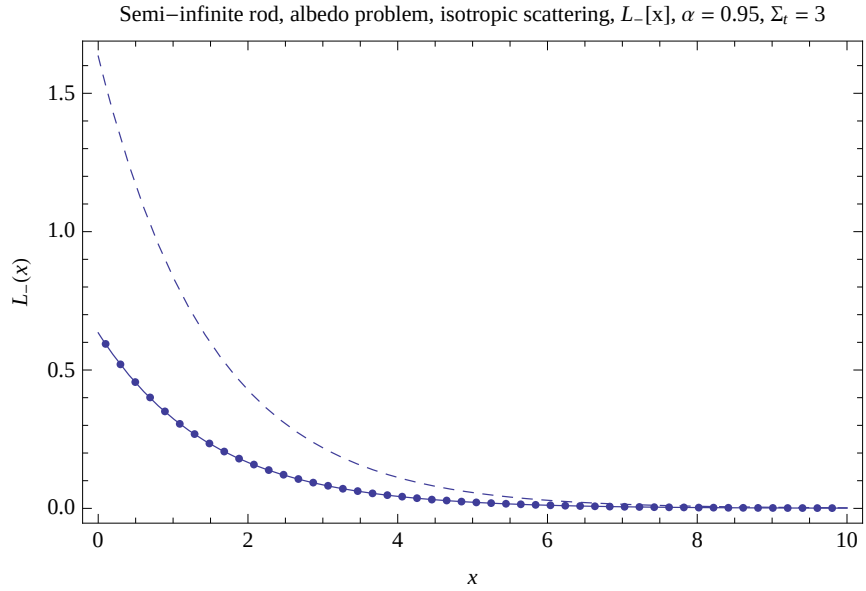

Figure 21: *Left-moving radiance (L_-) in a semi-infinite rod with isotropic scattering due to a surface source. Validation of analytic (continuous) vs. Monte Carlo (dots). Fluence shown as dashed line for reference.*

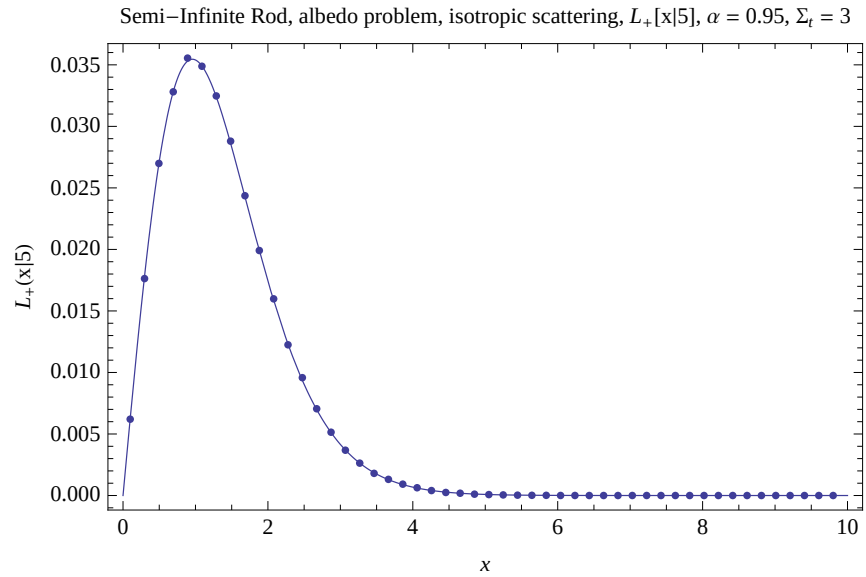

Figure 22: *5th-scattered right-moving radiance ($L_+(x|5)$) in a semi-infinite rod with isotropic scattering due to a surface source. Validation of analytic (continuous) vs. Monte Carlo (dots).*

4.4.4 Moments

Exact Solution The kth moments ϕ_k of the density/fluence/scalar flux are:

$$\phi_k = \int_0^\infty \phi(x)x^k = \frac{2\left(\alpha + \sqrt{1-\alpha} - 1\right) k!\Sigma_t^{-k-1}(1-\alpha)^{-\frac{k}{2}-1}}{\alpha}. \tag{107}$$

The first several collision-order moments $\phi_k(n)$ are:

$$\phi_k(n=0) = \Sigma_t^{-k-1}\Gamma(k+1) \tag{108}$$

$$\phi_k(n=1) = \alpha\frac{1}{4}k(2k+3)\Sigma_t^{-k-1}\Gamma(k) \tag{109}$$

$$\phi_k(n=2) = \alpha^2\frac{1}{8}(k(k+5)+5)\Sigma_t^{-k-1}\Gamma(k+1) \tag{110}$$

$$\phi_k(n=3) = \alpha^3\frac{1}{192}(2k+7)(2k(k+7)+15)\Sigma_t^{-k-1}\Gamma(k+1). \tag{111}$$

MC Code and Mathematica Validation (github):
code/rod/halfrod/albedoProblem

4.5 Semi-Infinite Rod, Albedo Problem, Anisotropic Scattering

4.5.1 Problem Description

This problem considers a semi-infinite ($x \in [0, \infty]$), homogeneous rod with anisotropic scattering ($F + B = \alpha$) with a unit surface source at $x = 0$ and with interaction coefficient Σ_t (see Figure 18). There is no absorption or reflection at the boundary (vacuum/indexed-matched boundary conditions). Section 4.4 is the $g = 0$ special case of this problem.

4.5.2 Reflectance/Albedo

Exact Solution The exact solution is

$$R = \frac{B}{\sqrt{(F-1)^2 - B^2} - F + 1} = \frac{\alpha(1-g)}{2 - \alpha - g\alpha + 2\sqrt{(1-\alpha)(1-\alpha g)}} \tag{112}$$

Exact Solution - Collision Order The exact solution for reflectance due to particles that have scattering exactly n times $R(\alpha|n)$ is found by taking a Taylor expansion of Equation 112 about $\alpha = 0$:

$$R = \frac{1}{4}a(1-g) + \frac{1}{8}a^2\left(1-g^2\right) + \frac{1}{64}a^3\left(-5g^3 - g^2 + g + 5\right) + \ldots \tag{113}$$

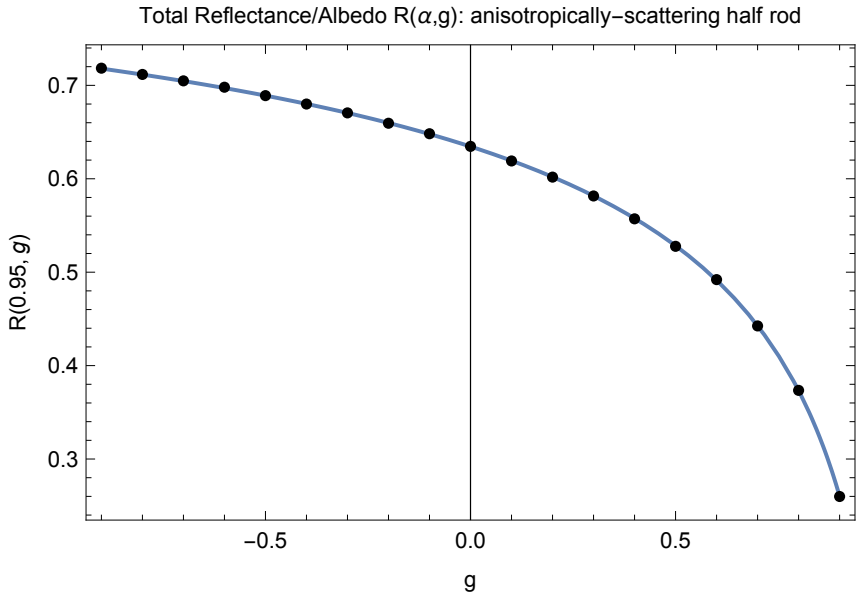

Figure 23: *Variation in albedo of a semi-infinite rod with anisotropic scattering as the mean cosine of scattering g is varied (single-scattering albedo α is fixed at* 0.95*). Monte-Carlo (dots) vs. analytic (continuous).*

4.5.3 Internal Distribution

Exact Solution The exact solutions for the right moving radiance L_+ and the left moving radiance L_- are:

$$L_+(x) = e^{-x\Sigma_t\sqrt{(1-\alpha)(1-\alpha g)}} \tag{114}$$

$$L_-(x) = \frac{\alpha(1-g)e^{-\Sigma_t x\sqrt{(1-\alpha)(1-\alpha g)}}}{2\left(\sqrt{\frac{1-\alpha g}{1-\alpha}}+1\right)-\alpha\left(2\sqrt{\frac{1-\alpha g}{1-\alpha}}+g+1\right)} \tag{115}$$

and the fluence / scalar flux / density $\phi(x)$ is:

$$\phi(x) = L_+(x) + L_-(x) \tag{116}$$

The contributions to the density $\phi(x|n)$ due to particles which have scattered exactly $n \geq 0$ times can be found by deriving the Taylor series expansion of Equation 116 about the single-scattering albedo $\alpha = 0$. The first few solutions are

$$\phi(x|0) = e^{-\Sigma_t x} \tag{117}$$

$$\phi(x|1) = \alpha\frac{1}{4}e^{-\Sigma_t x}(2g\Sigma_t x - g + 2\Sigma_t x + 1). \tag{118}$$

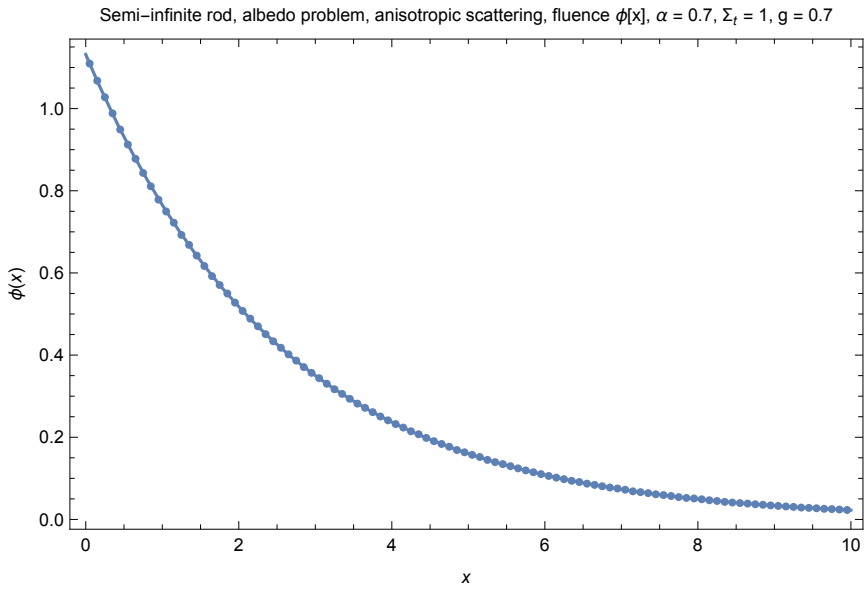

Figure 24: *Fluence in a semi-infinite rod with anisotropic ($g = 0.7$) scattering due to a surface source. Validation of analytic (continuous) vs. Monte Carlo (dots).*

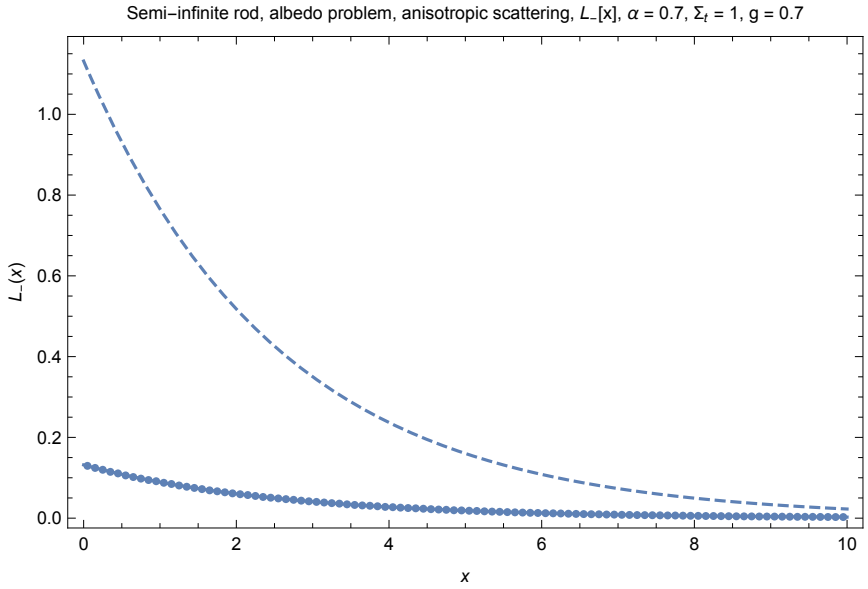

Figure 25: *Left-moving radiance (L_-) in a semi-infinite rod with anisotropic ($g = 0.7$) scattering due to a surface source. Validation of analytic (continuous) vs. Monte Carlo (dots). Fluence shown as dashed line for reference.*

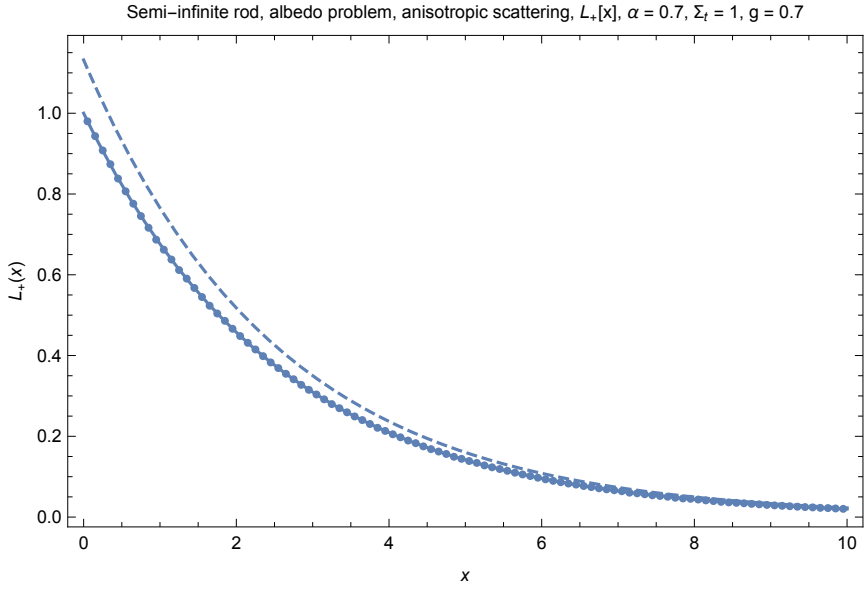

Figure 26: *Right-moving radiance (L_+) in a semi-infinite rod with anisotropic ($g = 0.7$) scattering due to a surface source. Validation of analytic (continuous) vs. Monte Carlo (dots). Fluence shown as dashed line for reference.*

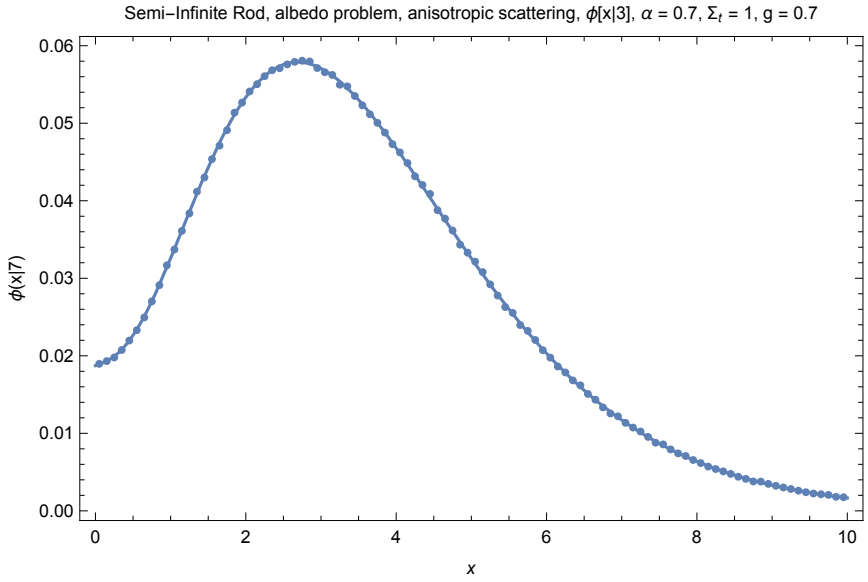

Figure 27: *Third-scattered fluence in a half-rod with anisotropic scattering. Validation of analytic (continuous) vs. Monte Carlo (dots).*

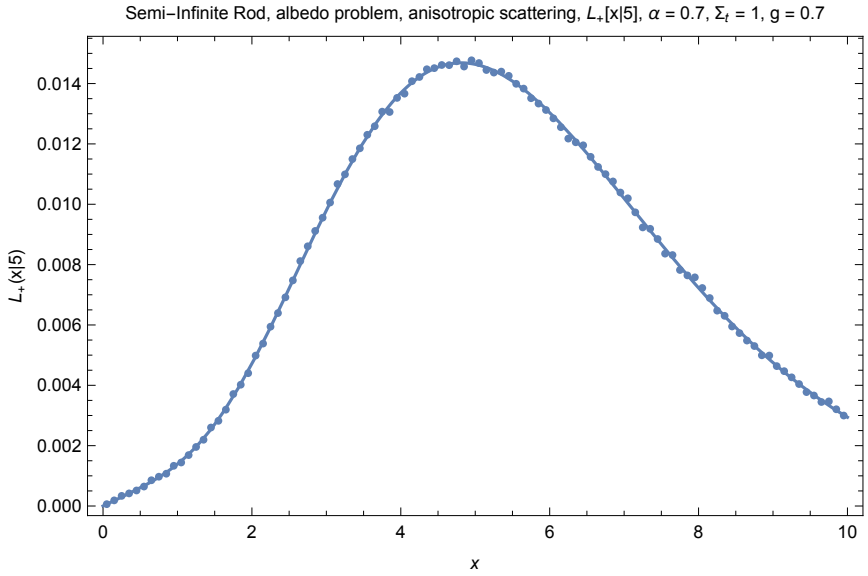

Figure 28: *Third-scattered right-moving radiance in a half-rod with anisotropic scattering. Validation of analytic (continuous) vs. Monte Carlo (dots).*

4.5.4 Moments

Exact Solution The kth moments ϕ_k of the density/fluence/scalar flux are:

$$\phi_k = \int_0^\infty \phi(x)x^k = \left(\frac{(g-1)\alpha}{\alpha\left(2\sqrt{\frac{g\alpha-1}{\alpha-1}}+g+1\right) - 2\left(\sqrt{\frac{g\alpha-1}{\alpha-1}}+1\right)} + 1 \right) \times \Sigma_t^{-k-1}\Gamma(k+1)((\alpha-1)(g\alpha-1))^{\frac{1}{2}(-k-1)}. \quad (119)$$

The first several collision-order moments $\phi_k(n)$ are:

$$\phi_k(n=0) = \Sigma_t^{-k-1}\Gamma(k+1) \quad (120)$$

$$\phi_k(n=1) = \frac{1}{4}\alpha(2gk+g+2k+3)\Sigma_t^{-k-1}\Gamma(k+1). \quad (121)$$

MC Code and Mathematica Validation (github):
code/rod/halfrod/albedoProblem

4.6 Finite Rod, Albedo Problem, Isotropic Scattering

4.6.1 Problem Description

This problem considers a finite ($x \in [0, a]$), homogeneous rod with interaction coefficient Σ_t and isotropic scattering ($F = B = \alpha/2$) with a unit surface source at $x = 0$ (see Figure 29). There is no absorption or reflection at the boundaries (vacuum/indexed-matched boundary conditions).

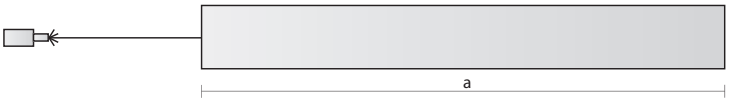

Figure 29: *Rod albedo problem: finite rod of length a with directional (rightward, +) source at the boundary.*

4.6.2 Reflectance and Transmittance

Exact Solution The exact solution for the reflectance $R(\tau_a)$ from a finite rod of thickness a with isotropic scattering and transport coefficient Σ_t with *optical thickness* $\tau_a = a\Sigma_t$:

$$R(\tau_a) = \frac{\alpha}{2\sqrt{1-\alpha}\coth\left(\tau_a\sqrt{1-\alpha}\right) - \alpha + 2} \tag{122}$$

and the exact transmittance $T(\tau_a)$ is

$$T(\tau_a) = \frac{2\sqrt{1-\alpha}}{2\sqrt{1-\alpha}\cosh\left(\tau_a\sqrt{1-\alpha}\right) - (\alpha-2)\sinh\left(\tau_a\sqrt{1-\alpha}\right)}. \tag{123}$$

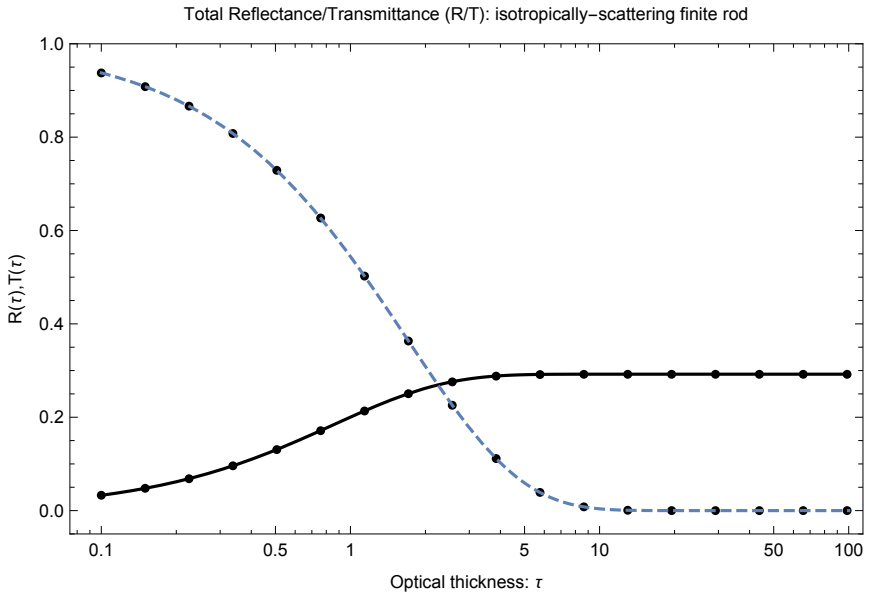

Figure 30: *Reflectance (continuous) and transmittance (dashed) for a finite rod of fixed single-scattering albedo $\alpha = 0.7$ as a function of optical thickness $\tau_a = a\Sigma_t$. Monte Carlo validation shown as dots.*

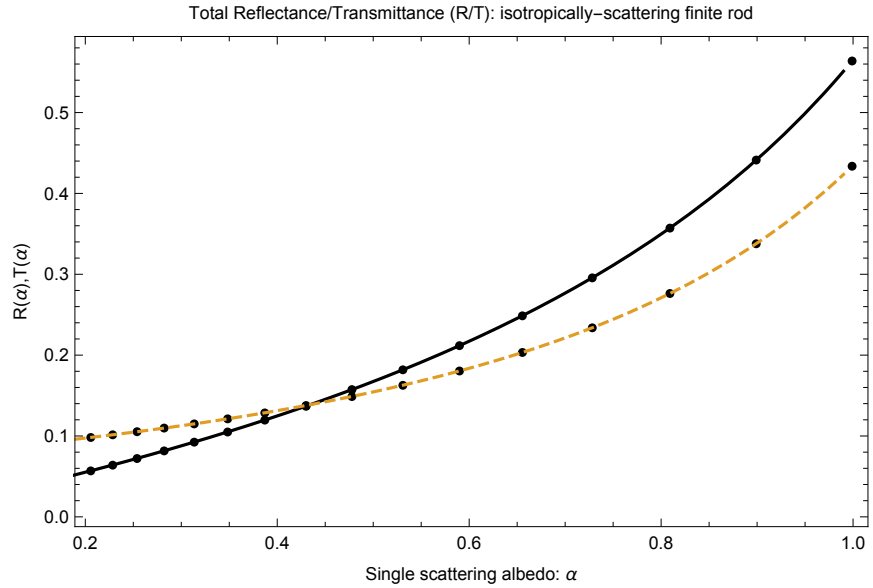

Figure 31: *Reflectance (continuous) and transmittance (dashed) for a finite rod of fixed optical thickness $\tau_a = a\Sigma_t = 2.6$ as a function of single-scattering albedo α. Monte Carlo validation shown as dots.*

Exact Solution - Collision Order The exact solution for reflectance and transmittance due to particles that have scattering exactly n times ($R(\tau_a|n)$ and $T(\tau_a|n)$ are found by taking Taylor series expansions of Equations 133 and 134 about $\alpha = 0$:

$$R(\tau_a|n) = \alpha\frac{1}{2\coth(\tau_a)+2} + \alpha^2\left(\frac{1}{8} - \frac{1}{8}e^{-2\tau_a}(2\tau_a+1)\right) + \ldots \tag{124}$$

$$T(\tau_a|n) = e^{-\tau_a} + \alpha\frac{1}{2}\tau_a e^{-\tau_a} + \alpha^2\frac{1}{8}e^{-2\tau_a}\left(\tau_a e^{\tau_a}(\tau_a+1) - \sinh(\tau_a)\right) + \ldots \tag{125}$$

4.6.3 Internal Distribution

Exact Solution The exact solutions for the right moving radiance L_+ and the left moving radiance L_- are:

$$L_+(x) = \frac{2\sqrt{1-\alpha}\cosh\left(\Sigma_t\sqrt{1-\alpha}(a-x)\right) - (\alpha-2)\sinh\left(\Sigma_t\sqrt{1-\alpha}(a-x)\right)}{2\sqrt{1-\alpha}\cosh\left(\Sigma_t a\sqrt{1-\alpha}\right) - (\alpha-2)\sinh\left(\Sigma_t a\sqrt{1-\alpha}\right)} \tag{126}$$

$$L_-(x) = -\frac{\alpha\sinh\left(\Sigma_t\sqrt{1-\alpha}(a-x)\right)}{(\alpha-2)\sinh\left(\Sigma_t a\sqrt{1-\alpha}\right) - 2\sqrt{1-\alpha}\cosh\left(\Sigma_t a\sqrt{1-\alpha}\right)} \tag{127}$$

and the fluence / scalar flux / density $\phi(x)$ is:

$$\phi(x) = \frac{2\left(\sinh\left(\Sigma_t\sqrt{1-\alpha}(a-x)\right) + \sqrt{1-\alpha}\cosh\left(\Sigma_t\sqrt{1-\alpha}(a-x)\right)\right)}{2\sqrt{1-\alpha}\cosh\left(\Sigma_t a\sqrt{1-\alpha}\right) - (\alpha-2)\sinh\left(\Sigma_t a\sqrt{1-\alpha}\right)} \tag{128}$$

The contributions to the density $\phi(x|n)$ due to particles which have scattered exactly $n \geq 0$ times can be found by deriving the Taylor series expansion of Equation 139 about the single-

scattering albedo $\alpha = 0$. The first few solutions are

$$\phi(x|0) = e^{-\Sigma_t x} \tag{129}$$

$$\phi(x|1) = -\alpha\frac{1}{4}e^{-\Sigma_t x}\left(e^{2\Sigma_t(x-a)} - 2\Sigma_t x - 1\right). \tag{130}$$

MC Code and Mathematica Validation (github):
code/rod/finiterod/albedoProblem

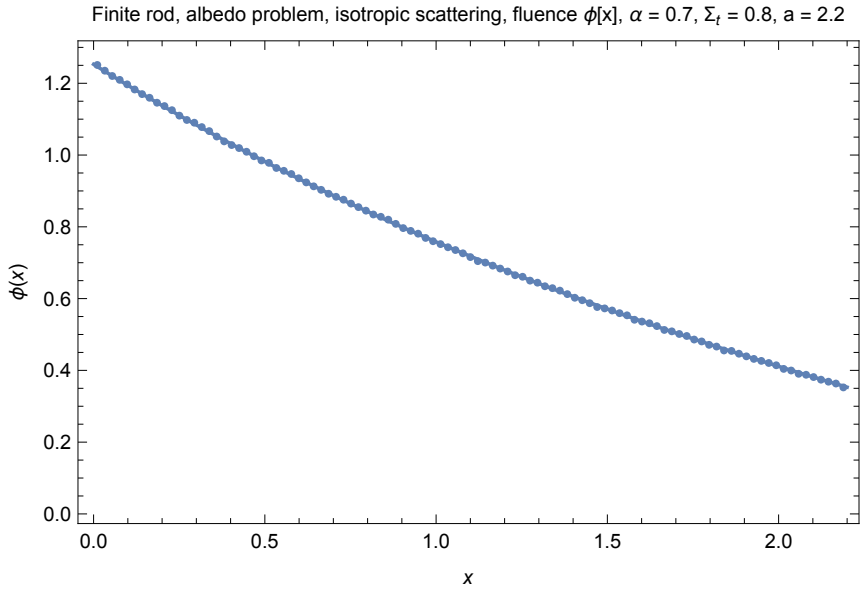

Figure 32: *Fluence in a finite rod with isotropic scattering due to a surface source. Validation of analytic (continuous) vs. Monte Carlo (dots).*

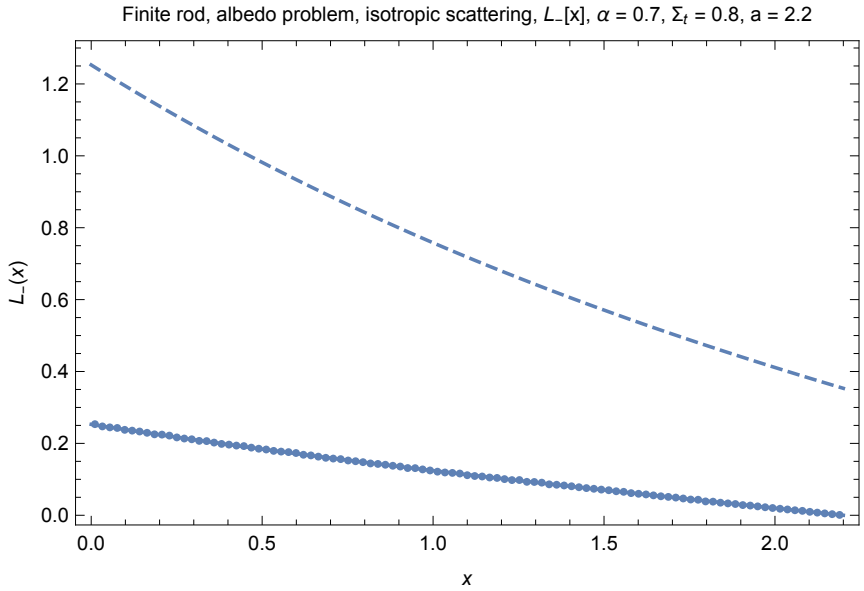

Figure 33: *Left-moving radiance (L_-) in a finite rod with isotropic scattering due to a surface source. Validation of analytic (continuous) vs. Monte Carlo (dots). Fluence shown as dashed line for reference.*

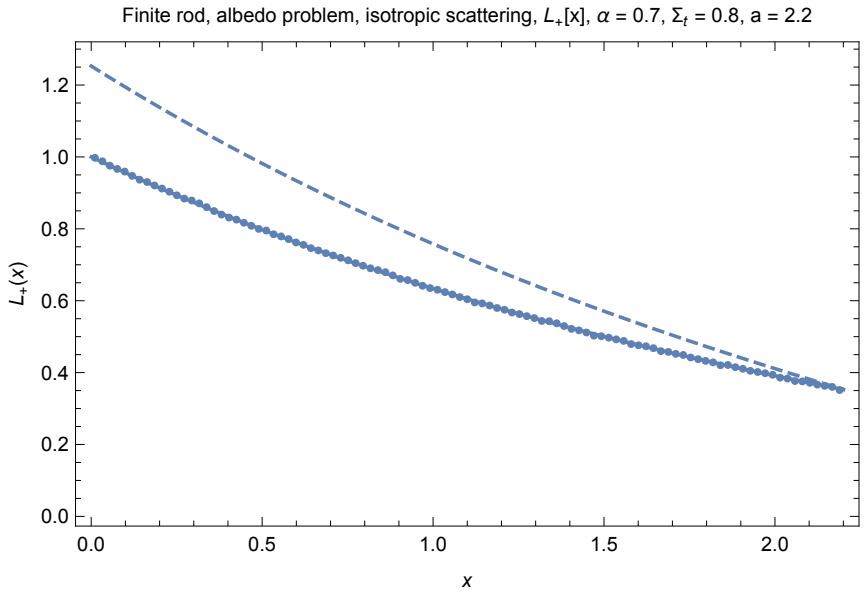

Figure 34: *Right-moving radiance (L_+) in a finite rod with isotropic scattering due to a surface source. Validation of analytic (continuous) vs. Monte Carlo (dots). Fluence shown as dashed line for reference.*

4.7 Finite Rod, Albedo Problem, Anisotropic Scattering

4.7.1 Problem Description

This problem considers a finite ($x \in [0, a]$), homogeneous rod with interaction coefficient Σ_t and anisotropic scattering with a unit surface source at $x = 0$ (see Figure 29). There is no absorption or reflection at the boundaries (vacuum/indexed-matched boundary conditions).

4.7.2 Diffusion Parameters

For the rod model with general anisotropic scattering, the *diffusion coefficient* is

$$D = \frac{1}{\Sigma_t(1-\alpha g)} \tag{131}$$

yielding the effective transport coefficient,

$$\Sigma_{\text{eff}} = \sqrt{\Sigma_a / D} = \Sigma_t \sqrt{(1-\alpha)(1-\alpha g)}. \tag{132}$$

4.7.3 Reflectance and Transmittance

Exact Solution The exact solution for the reflectance $R(\tau_a)$ from a finite rod of thickness a with anisotropic scattering and transport coefficient Σ_t with *optical thickness* $\tau_a = a\Sigma_t$:

$$R(\tau_a) = \frac{\alpha(1-g)}{2\sqrt{(1-\alpha)(1-\alpha g)}\coth\left(\tau_a\sqrt{(1-\alpha)(1-\alpha g)}\right) - \alpha + \alpha(-g) + 2} \tag{133}$$

and the exact transmittance $T(\tau_a)$ is

$$T(\tau_a) = \frac{2}{2\cosh\left(\tau_a\sqrt{(1-\alpha)(1-\alpha g)}\right) - \frac{(\alpha+\alpha g-2)\sinh\left(\tau_a\sqrt{(1-\alpha)(1-\alpha g)}\right)}{\sqrt{(1-\alpha)(1-\alpha g)}}}. \tag{134}$$

Exact Solution - Collision Order The exact solution for reflectance and transmittance due to particles that have scattering exactly n times ($R(\tau_a|n)$ and $T(\tau_a|n)$ are found by taking Taylor series expansions of Equations 133 and 134 about $\alpha = 0$:

$$R(\tau_a|n) = \alpha\frac{(1-g)}{2\coth(\tau_a)+2} + \alpha^2\frac{1}{8}\left(1-g^2\right)e^{-2\tau_a}\left(-2\tau_a + e^{2\tau_a} - 1\right) + \ldots \tag{135}$$

$$T(\tau_a|n) = e^{-\tau_a} + \alpha\frac{1}{2}\tau_a e^{-\tau_a}(1+g) + \ldots \tag{136}$$

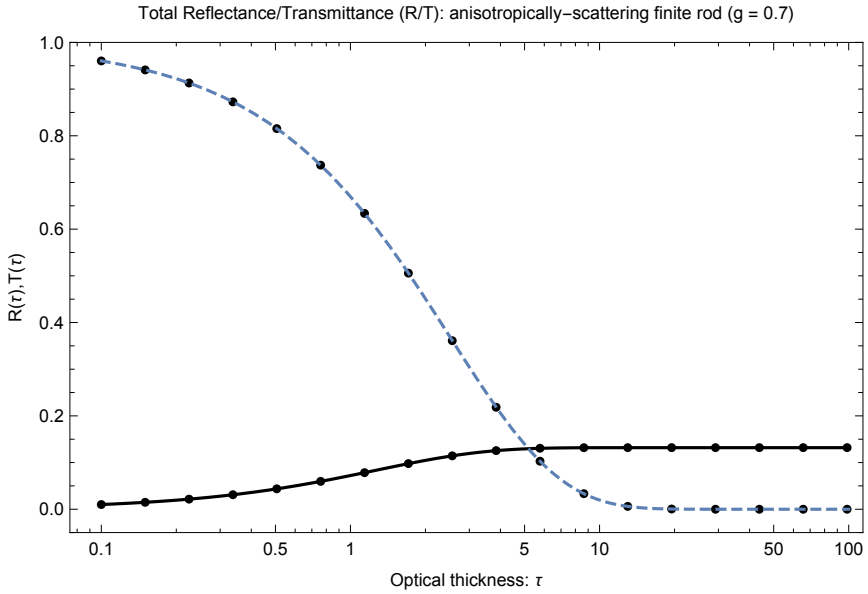

Figure 35: *Reflectance (continuous) and transmittance (dashed) for a finite rod of fixed single-scattering albedo $\alpha = 0.7$ and fixed anisotropic scattering factor $g = 0.7$, as a function of optical thickness $\tau_a = a\Sigma_t$. Monte Carlo validation shown as dots.*

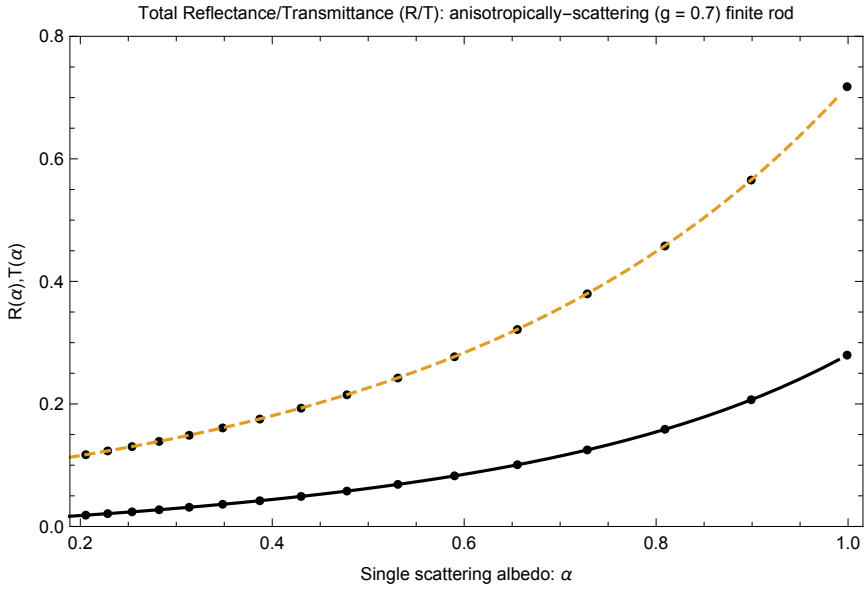

Figure 36: *Reflectance (continuous) and transmittance (dashed) for a finite rod of fixed optical thickness $\tau_a = a\Sigma_t = 2.6$ and fixed anisotropic scattering ($g = 0.7$) as a function of single-scattering albedo α. Monte Carlo validation shown as dots.*

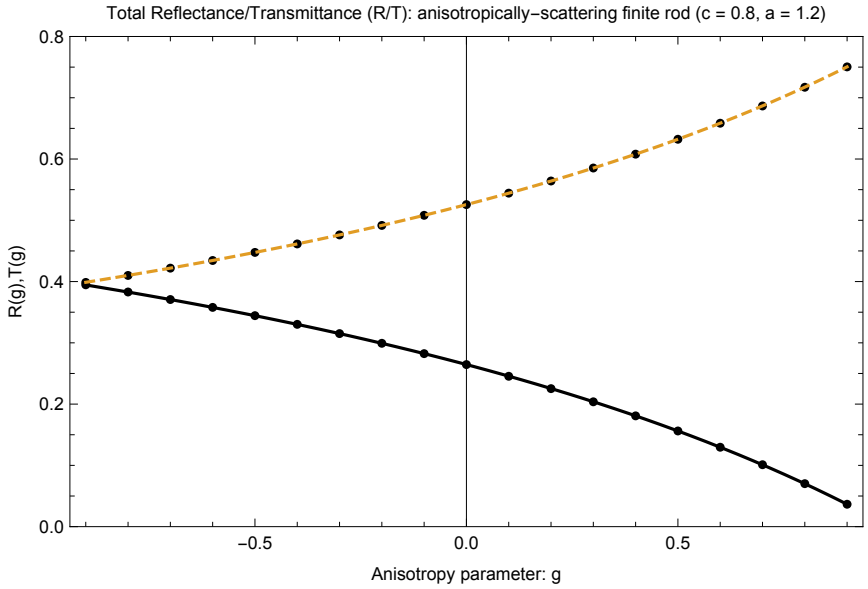

Figure 37: *Reflectance (continuous) and transmittance (dashed) for a finite rod of fixed optical thickness $\tau_a = a\Sigma_t = 1.1$ and fixed single-scattering albedo ($c = 0.8$) as a function of anisotropy parameter g. Monte Carlo validation shown as dots.*

4.7.4 Internal Distribution

Exact Solution The exact solutions for the right moving radiance L_+ and the left moving radiance L_- are [Wing 1962]:

$$L_+(x) = -\frac{D\sqrt{\frac{1-\alpha}{1-\alpha g}}(\Sigma_t(\alpha+\alpha g-2)\sinh(D(a-x)) - 2D\cosh(D(a-x)))}{(\alpha-1)\Sigma_t^2\left((\alpha+\alpha g-2)\sinh(aD) + 2(\alpha-1)\sqrt{\frac{1-\alpha g}{1-\alpha}}\cosh(aD)\right)} \tag{137}$$

$$L_-(x) = \frac{\sqrt{\frac{1-\alpha}{1-\alpha g}}\sinh(D(a-x))\left(D + (\alpha-1)\Sigma_t\left(\frac{1-\alpha g}{1-\alpha}\right)^{3/2}\right)}{\Sigma_t\left((\alpha+\alpha g-2)\sinh(aD) + 2(\alpha-1)\sqrt{\frac{1-\alpha g}{1-\alpha}}\cosh(aD)\right)} \tag{138}$$

and the fluence / scalar flux / density $\phi(x)$ is:

$$\phi(x) = L_+(x) + L_-(x) \tag{139}$$

Exact Solution - Collision Order The contributions to the density $\phi(x|n)$ due to particles which have scattered exactly $n \geq 0$ times can be found by deriving the Taylor series expansion of Equation 139 about the single-scattering albedo $\alpha = 0$. The first few solutions are

$$\phi(x|0) = e^{-\Sigma_t x} \tag{140}$$

$$\phi(x|1) = \alpha\frac{1}{4}e^{\Sigma_t(-(2a+x))}\left(e^{2a\Sigma_t}(2(g+1)\Sigma_t x - g + 1) + (g-1)e^{2\Sigma_t x}\right) \tag{141}$$

MC Code and Mathematica Validation (github):
code/rod/finiterod/albedoProblem

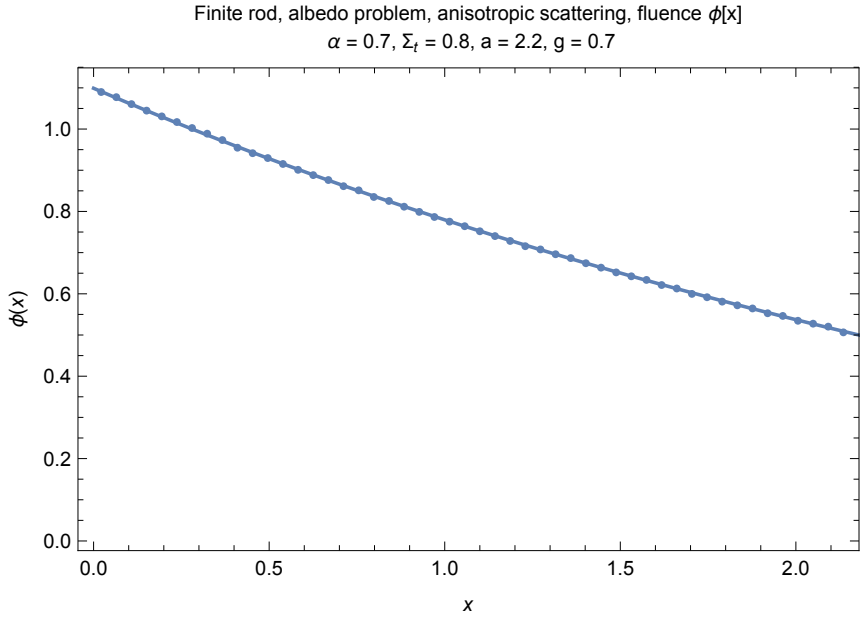

Figure 38: *Fluence in a finite rod with anisotropic scattering due to a surface source. Validation of analytic (continuous) vs. Monte Carlo (dots).*

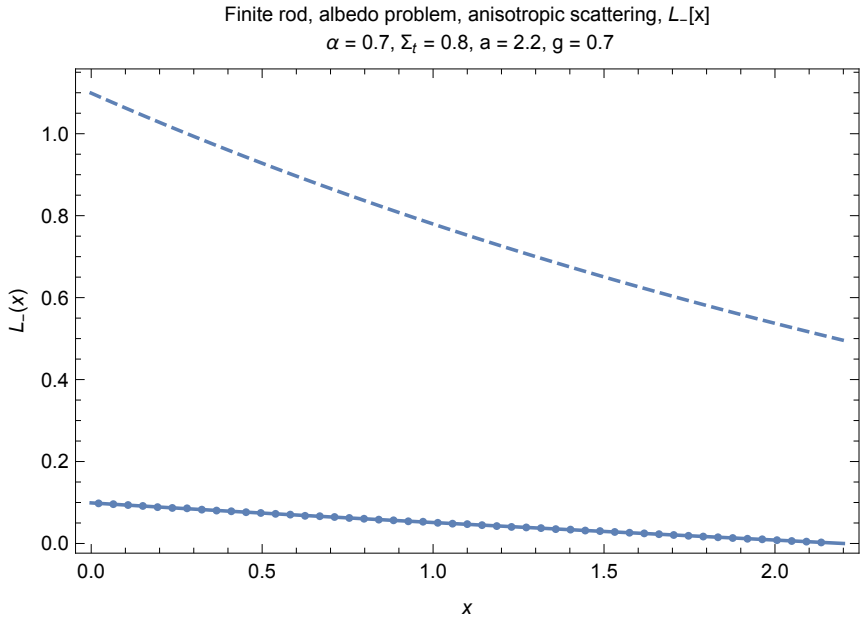

Figure 39: *Left-moving radiance (L_-) in a finite rod with anisotropic scattering due to a surface source. Validation of analytic (continuous) vs. Monte Carlo (dots). Fluence shown as dashed line for reference.*

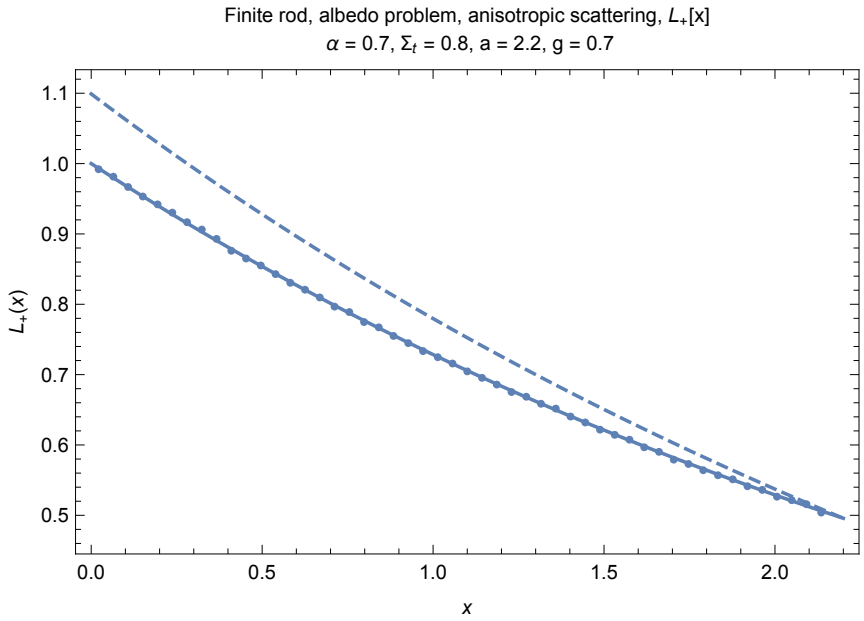

Figure 40: *Right-moving radiance (L_+) in a finite rod with anisotropic scattering due to a surface source. Validation of analytic (continuous) vs. Monte Carlo (dots). Fluence shown as dashed line for reference.*

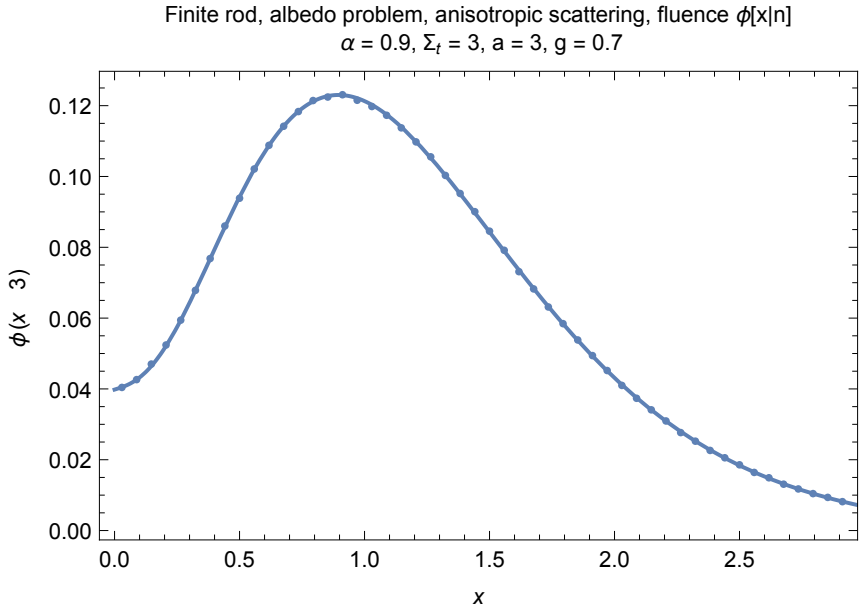

Figure 41: *N-th scattered fluence ($n = 3$) in a finite rod with anisotropic scattering due to a surface source. Validation of analytic (continuous) vs. Monte Carlo (dots)*

5 Flatland - Circular Symmetry

5.1 Isotropic Point Source, Infinite Medium, Isotropic Scattering

5.1.1 Problem Statement

This problem considers a single isotropically-emitting point source at the origin of an infinite homogeneous medium in flatland with isotropic scattering. The scalar spatial coordinate of the solution is the radius r from the point source. The scalar directional parameter is the direction cosine u to the outward direction. Parameter $u \in [-1, 1]$ indexes *pairs* of directions (analogous to cones in 3D). The direction pointing away from the point source is $u = 1$ and the direction pointing towards the point source is $u = -1$. Figure 42 illustrates our notation.

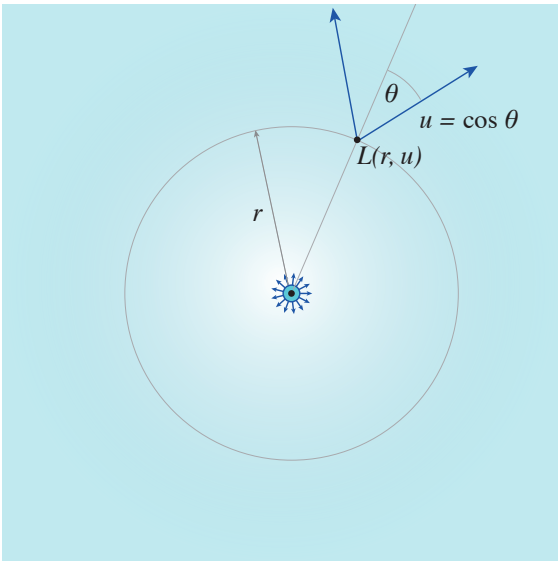

Figure 42: *An isotropic point source in an infinite flatland medium.*

5.1.2 Fluence

The *fluence* ϕ_{pt} due to a point source is proportional to the energy density and is an integral of the radiance L over all directions:

$$\phi_{\text{pt}}(r) = \int_0^{2\pi} L(r, \theta) d\theta. \tag{142}$$

Exact Solution (1) An exact solution derived by Fourier transforms is [d'Eon 2014]

$$\phi_{\text{pt}}(r) = \frac{e^{-\Sigma_t r}}{2\pi r} + \alpha \frac{\Sigma_t}{2\pi} \int_0^{\infty} \frac{z J_0(\Sigma_t\, r\, z)}{1 + z^2 - \alpha\sqrt{1 + z^2}} dz, \tag{143}$$

which separates the uncollided contribution from the collided contribution.

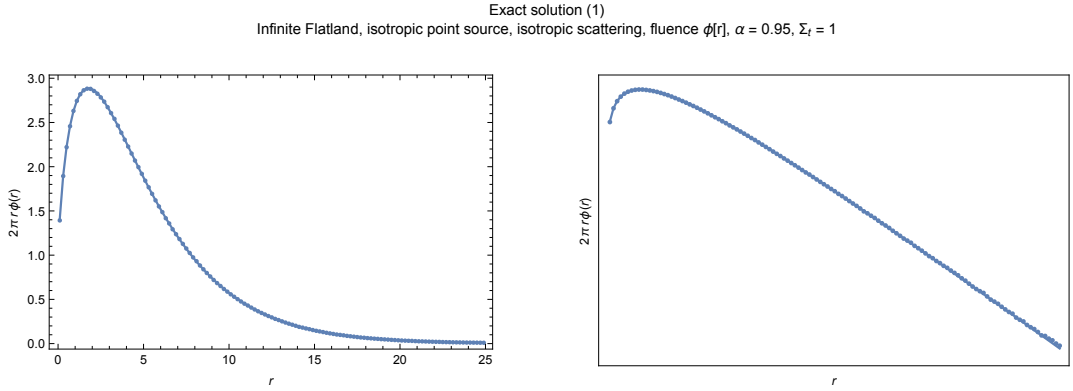

Figure 43: *Fluence $\phi_{pt}(r)$ due to an isotropic point source inside an infinite flatland medium with isotropic scattering. Validation of exact solution (1) (continuous) vs. Monte Carlo (dots).*

Exact Solution (2) An alternative exact solution derived by Fourier transforms is [Zoia et al. 2011a]

$$\phi_{\rm pt}(r) = \Sigma_s \frac{K_0(r\Sigma_t\sqrt{1-\alpha^2})}{\pi} + \frac{\Sigma_t}{2\pi}\int_0^\infty \frac{zJ_0(\Sigma_t rz)}{\sqrt{1+z^2}+c}dz, \tag{144}$$

which is the sum of the rigorous asymptotic diffusion approximation and a transient term.

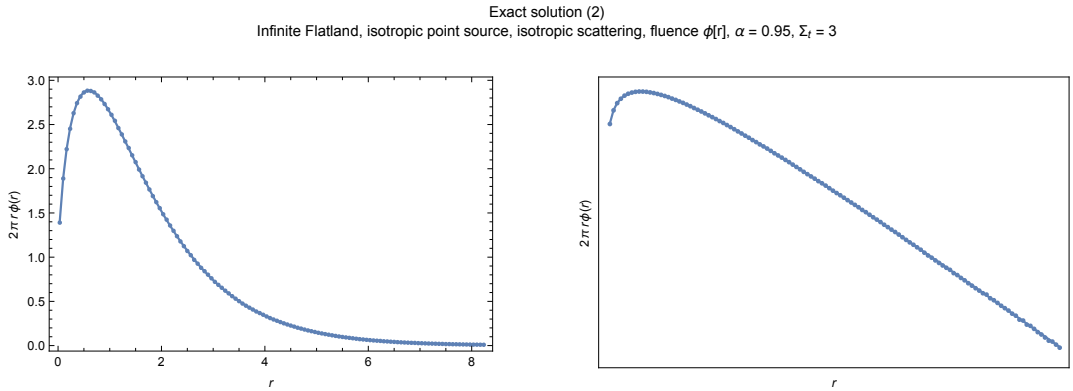

Figure 44: *Fluence $\phi_{pt}(r)$ due to an isotropic point source inside an infinite flatland medium with isotropic scattering. Validation of exact solution (2) (continuous) vs. Monte Carlo (dots).*

Exact Solution (3) An alternative derivation using the method of rotated reference frames is [Liemert and Kienle 2011]

$$\phi_{\rm pt}(r) = \frac{1}{2\pi}\int_0^\infty \frac{zJ_0(rz)}{\sqrt{\Sigma_t^2+z^2}-\Sigma_s}dz \tag{145}$$

which has the expansion

$$\phi_{\rm pt}(r) = \frac{e^{-\Sigma_t r}}{2\pi r} + \Sigma_s \frac{K_0(r\Sigma_t\sqrt{1-\alpha^2})}{2\pi} + \frac{\Sigma_t}{2\pi}\sum_{n=1}^{\infty} \frac{2^{n+\frac{1}{2}} n!\alpha^{2n}(\Sigma_t r)^{n-\frac{1}{2}} K_{n-\frac{1}{2}}(\Sigma_t r)}{\sqrt{\pi}(2n)!}. \tag{146}$$

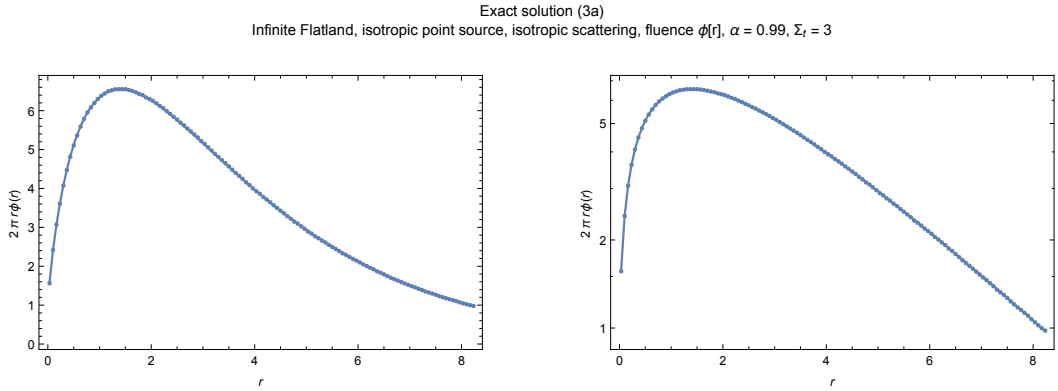

Figure 45: *Fluence $\phi_{pt}(r)$ due to an isotropic point source inside an infinite flatland medium with isotropic scattering. Validation of exact solution (3) (continuous) vs. Monte Carlo (dots).*

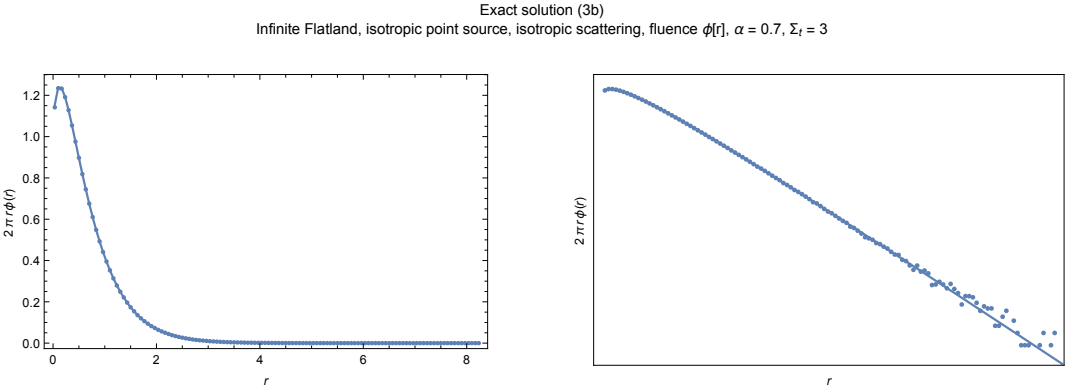

Figure 46: *Fluence $\phi_{pt}(r)$ due to an isotropic point source inside an infinite flatland medium with isotropic scattering. Validation of exact solution (3b) (continuous) vs. Monte Carlo (dots).*

Exact Solution After n Scattering Events The contribution of the fluence due to particles that have scattered exactly n times since leaving the isotropic point source in the infinite flatland isotropically-scattering medium is giving exactly by [Stadje 1987, Zoia et al. 2011a, d'Eon 2014]

$$\phi_{\rm pt}(r|n) = \int_0^{\infty} \frac{zJ_0(rz)\left(\alpha/\sqrt{1+z^2/\Sigma_t^2}\right)^n}{2\pi\sqrt{\Sigma_t^2+z^2}} dz = \frac{2^{\frac{1}{2}(-n-1)}\Sigma_t^{\frac{n+1}{2}} r^{\frac{n-1}{2}}\alpha^n K_{\frac{n-1}{2}}(\Sigma_t r)}{\pi\Gamma\left(\frac{n+1}{2}\right)}. \tag{147}$$

The first few orders of scattered fluence are

$$\phi_{\text{pt}}(r|0) = \frac{e^{-\Sigma_t r}}{2\pi r} \tag{148}$$

$$\phi_{\text{pt}}(r|1) = \frac{\alpha\Sigma_t K_0(\Sigma_t r)}{2\pi} \tag{149}$$

$$\phi_{\text{pt}}(r|2) = \frac{\alpha^2\Sigma_t e^{-\Sigma_t r}}{2\pi} \tag{150}$$

$$\phi_{\text{pt}}(r|3) = \frac{\alpha^3\Sigma_t^2 r K_1(\Sigma_t r)}{4\pi} \tag{151}$$

$$\phi_{\text{pt}}(r|4) = \frac{\alpha^4\Sigma_t e^{-\Sigma_t r}(\Sigma_t r + 1)}{6\pi}. \tag{152}$$

Fluence/Density Moments The fluence moments of order m for the nth scattered fluence are [Zoia et al. 2011a, d'Eon 2014]

$$\int_0^\infty 2\pi r\phi_{\text{pt}}(r|n)dr = \frac{\alpha^n}{\Sigma_t} \tag{153}$$

$$\int_0^\infty 2\pi r r^2\phi_{\text{pt}}(r|n)dr = \frac{2(n+1)\alpha^n}{\Sigma_t^3} \tag{154}$$

$$\int_0^\infty 2\pi r r^m\phi_{\text{pt}}(r|n)dr = \frac{2^m\Sigma_t^{-m-1}\Gamma\left(\frac{m}{2}+1\right)\alpha^n\Gamma\left(\frac{1}{2}(m+n+1)\right)}{\Gamma\left(\frac{n+1}{2}\right)}, \tag{155}$$

which sum to produce the moments for the total fluence,

$$\int_0^\infty 2\pi r\phi_{\text{pt}}(r)dr = \frac{1}{\Sigma_a} \tag{156}$$

$$\int_0^\infty 2\pi r r^2\phi_{\text{pt}}(r)dr = \frac{2}{(\alpha-1)^2\Sigma_t^3} \tag{157}$$

$$\int_0^\infty 2\pi r r^4\phi_{\text{pt}}(r)dr = \frac{8(\alpha-3)}{(\alpha-1)^3\Sigma_t^5} \tag{158}$$

$$\int_0^\infty 2\pi r r^m\phi_{\text{pt}}(r)dr = \left(1-\alpha^2\right)^{-\frac{n}{2}-1}\Sigma_t^{-n-1}\left(\Gamma(n+1)\,{}_2F_1\left(-\frac{1}{2},-\frac{n}{2};\frac{1}{2};\alpha^2\right)+\alpha 2^n\Gamma\left(\frac{n}{2}+1\right)^2\right) \tag{159}$$

where ${}_2F_1$ is a hypergeometric function.

Classical Diffusion Approximation The classical diffusion (P_1) solution for fluence due to an isotropic point source in an infinite, homogeneous 2D flatland medium with isotropic scattering is

$$\phi_{\text{pt}}(r) \approx \frac{1}{2\pi D}K_0(r\sqrt{\Sigma_a/D}). \tag{160}$$

where D is the *classical flatland diffusion coefficient*

$$D = \frac{1}{2\Sigma_t}, \tag{161}$$

where a 2 appears, as opposed to a 3, precisely because of the spatial dimensionality.

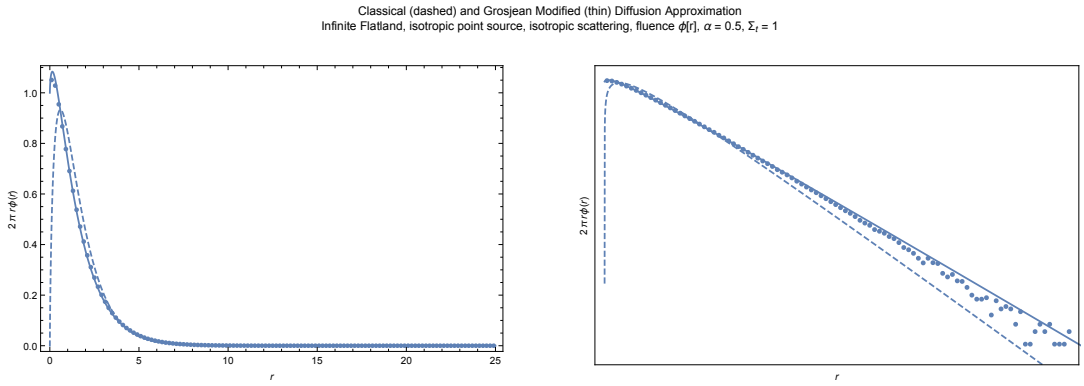

Figure 47: *Fluence $\phi_{pt}(r)$ due to an isotropic point source inside an infinite flatland medium with isotropic scattering. Comparison of classical diffusion (dashed) vs. Grosjean diffusion (continuous) vs. Monte Carlo (dots).*

Modified Diffusion Approximation The Grosjean-style modified diffusion approximation for fluence due to an isotropic point source in an infinite, homogeneous 2D flatland medium with isotropic scattering is [d'Eon 2014]

$$\phi_{\mathrm{pt}}(r) \approx \frac{e^{-\Sigma_t r}}{2\pi r} + \frac{\alpha\Sigma_t}{(2-\alpha)\pi} K_0\left(r\Sigma_t\sqrt{2}\frac{\sqrt{1-\alpha}}{\sqrt{2-\alpha}}\right). \tag{162}$$

Similar to scattering in three dimensions, in flatland Grosjean's modified diffusion approximation is superior to the classical diffusion approximation, especially near sources and for high absorption levels [d'Eon 2014].

Rigorous Diffusion Approximation The rigorous diffusion solution for fluence due to an isotropic point source in an infinite, homogeneous 2D flatland medium with isotropic scattering is [d'Eon 2014]

$$\phi_{\mathrm{pt}}(r) \approx \frac{\Sigma_s K_0\left(r\sqrt{1-\alpha^2}\Sigma_t\right)}{\pi}, \tag{163}$$

which is twice the sum of the odd-order fluences, $\phi_{\mathrm{pt}}(r|n)$. Similar to scattering in three dimensions, in flatland the rigorous diffusion solution is increasingly accurate far from the source [d'Eon 2014].

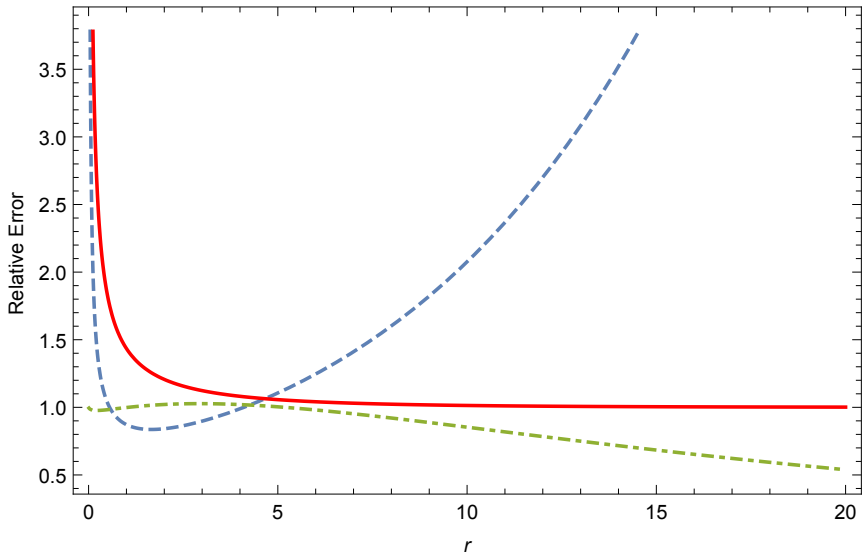

Figure 48: *Relative error $\phi_{exact}(r)/\phi_{diffusion}(r)$ for classical diffusion (dashed), rigorous diffusion (continuous) and Grosjean diffusion (dot-dashed). Properties: $\Sigma_t = 1, \alpha = 0.5$. We see Grosjean diffusion behaving best near the source and performing better than classical diffusion overall for very small densities (high r), with the rigorous diffusion approximation becoming increasingly accurate for very low densities.*

5.1.3 Radiance (Angularly-Resolved Solutions)

Exact solution (1) An exact solution can be readily formed by back integrating the known fluence [Liemert and Kienle 2011]

$$L(r,u) = \frac{e^{-\Sigma_t r}}{2\pi r}\delta(u) + \frac{\Sigma_s}{2\pi}\int_0^\infty \phi_{\text{pt}}(\sqrt{r^2+t^2-2rtu})e^{-\Sigma_t t}dt. \tag{164}$$

Classical Diffusion Approximation The classical diffusion solution is [Liemert and Kienle 2011]

$$L(r,u) \approx \frac{\Sigma_t\left(K_0\left(r\sqrt{2-2\alpha}\Sigma_t\right) + \sqrt{2-2\alpha}uK_1\left(r\sqrt{2-2\alpha}\Sigma_t\right)\right)}{2\pi^2} \tag{165}$$

MC Code and Mathematica Validation (github):
code/flatland/infiniteFlatland/Isotropicpointsource

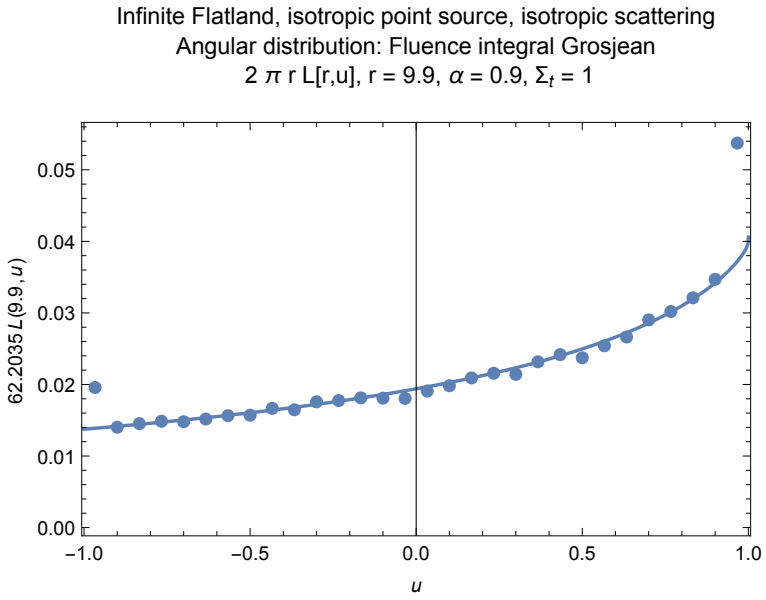

Figure 49: *Angular flux $L(r,u)$ due to an isotropic point source inside an infinite flatland medium with isotropic scattering. Comparison of exact solution (continuous) vs. Monte Carlo (dots).*

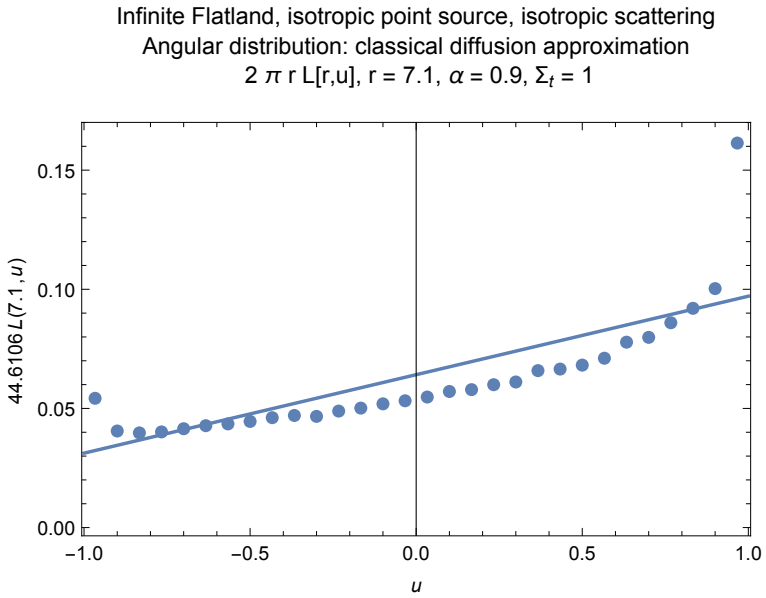

Figure 50: *Angular flux $L(r,u)$ due to an isotropic point source inside an infinite flatland medium with isotropic scattering. Comparison of classical diffusion (continuous) vs. Monte Carlo (dots).*

6 3D Volume - Spherical Symmetry

If scattering in a 3D volume satisfies:

- The distribution of particle sources is spherically symmetric: particles are emitted either from the point at the origin or from shells centered about the origin (i.e. the source function can be expressed as $Q(r, \vec{\omega})$ where r is the distance from the origin in *some* coordinate system)
- The boundaries between differing media are spheres centered about the origin
- The medium properties Σ_a, Σ_s and p depend only upon r.
- The angular distribution of emission is spherically symmetric (i.e. depends only upon a directional cosine u measured to the normalized radius vector)

then the radiance in the volume L will depend only on a scalar positional variable r (and a scalar directional variable) and so we refer to this as a $1D$ problem.

6.1 Isotropic Point Source, Infinite Medium, Isotropic Scattering

6.1.1 Problem Statement

This problem considers a single isotropically-emitting point source at the origin of an infinite homogeneous medium with isotropic scattering. The scalar spatial coordinate of the solution is the radius r from the point source. The scalar directional parameter is the direction cosine u to the outward direction. Parameter $u \in [-1, 1]$ indexes *cones* of directions. The direction pointing away from the point source is $u = 1$ and the direction pointing towards the point source is $u = -1$. Figure 51 illustrates our notation.

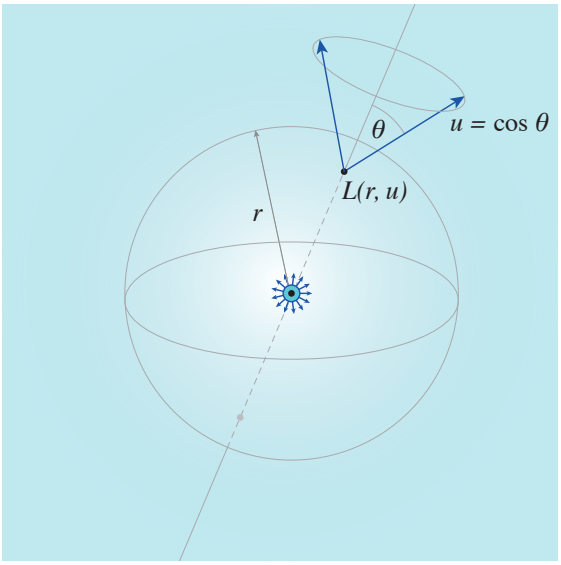

Figure 51: *An isotropic point source in an infinite 3D medium.*

6.1.2 Transport Equation

The transport equation for a homogeneous 3D volume with spherical symmetry and isotropic scattering is:

$$u\frac{\partial\psi(r,u)}{\partial r} + \frac{1-u^2}{r}\frac{\partial\psi(r,u)}{\partial u} + \Sigma_t\psi(r,u) = \Sigma_t\frac{\alpha}{2}\phi_{\text{pt}}(r) + Q(r). \tag{166}$$

The source function $Q(r) = \delta(r)/2$ is a dirac delta describing the unit emission of an isotropic point source. The in-scattering term is based on ϕ_{pt}, the fluence at a point and $\psi(r,u)$ is 2π times the radiance $L(r,\vec{\omega})$.

Further Reading

The classic work on this problem is Davisons's 1943 paper [2000]. Also, see [Williams 1971] Section 6.2, [Sen and Wilson 1990] pp.24-26, [Ganapol 2003], and [Prinja and Larsen 2010] Section 3.4.

6.1.3 Fluence

The *fluence* ϕ_{pt} due to a point source is proportional to the energy density and is a uniform integral of the radiance L over all directions:

$$\phi_{\text{pt}}(r) = \int_{4\pi} L(r,\vec{\omega})d\vec{\omega} = \frac{1}{2}\int_{-1}^{1} \psi(r,u)du \tag{167}$$

The fluence satisfies the integral equation:

$$\phi_{\text{pt}}(\vec{x}) = \alpha \int \Sigma_t \phi_{\text{pt}}(\vec{x}') \frac{\mathrm{e}^{-\Sigma_t|\vec{x}-\vec{x}'|}}{4\pi|\vec{x}-\vec{x}'|^2} d\vec{x}' \tag{168}$$

which is equivalent to:

$$r\phi_{\text{pt}}(r) = r\delta(r) + \frac{\alpha}{2}\int_0^\infty r'\phi_{\text{pt}}(r')\left[E_1(|r-r'|) - E_1(r+r')\right]dr', \tag{169}$$

where E_1 is the exponential integral function.

Exact Solution (1a) The first known exact solution (found using spherically-symmetric Fourier transforms) for the fluence due to a point source is [Bothe 1942, Placzek and Volkoft 1943, Nuyens and Grosjean 1949, Grosjean 1951, Case et al. 1953]

$$\phi_{\text{pt}}(r) = \frac{1}{2\pi^2 r}\int_0^\infty \frac{z\arctan(z/\Sigma_t)}{z - \alpha\,\Sigma_t \arctan(z/\Sigma_t)}\,\sin(r\,z)\,dz. \tag{170}$$

This involves a problematic oscillatory integral and is not absolutely convergent (and so is only exact in the sense of Cesaro summability).

Exact Solution (1b) An alternative convergent form of this exact solution explicitly separates the uncollided fluence (and is sometimes referred to as “Case’s solution")

$$\phi_{\text{pt}}(r) = \frac{\mathrm{e}^{-\Sigma_t r}}{4\pi r^2} + \frac{\Sigma_s}{2\pi^2 r}\int_0^\infty \frac{\arctan^2 \nu}{\nu - \alpha\arctan\nu}\,\sin(r\,\Sigma_t\,\nu)\,d\nu. \tag{171}$$

The exact solution for the point source is related to the isotropic plane source problem (Section 7.1) by the plane-to-point transform (Section 8.4).

Further Reading

A survey article on random flights [Dutka 1985] notes very similar Fourier solutions that were discovered in 1906 by Von Smoluchowski and later identified as applying to random flights [Smoluchowski 1916].

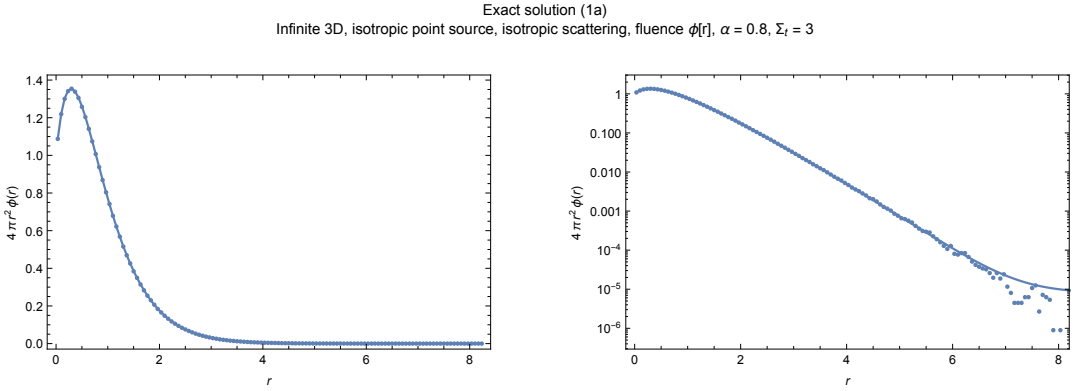

Figure 52: *Fluence $\phi_{pt}(r)$ due to an isotropic point source in an infinite 3D medium with isotropic scattering. Validation of exact solution (1a) (continuous) vs. Monte Carlo (dots).*

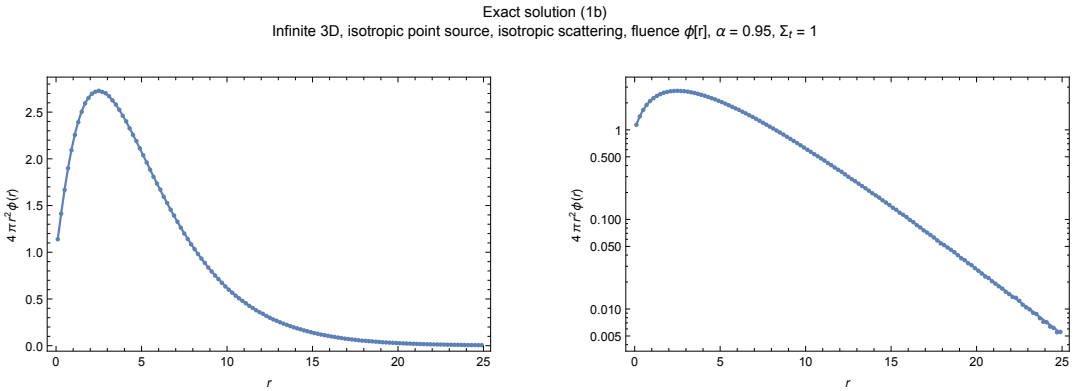

Figure 53: *Fluence $\phi_{pt}(r)$ due to an isotropic point source in an infinite 3D medium with isotropic scattering. Validation of exact solution (1b) (continuous) vs. Monte Carlo (dots).*

Exact Solution (2a) Two equivalent exact solutions are given here, which decompose the solution into diffusion and transient components related to the eigenstructure of the transport operator. The first is due to Davison in 1945 [Davison 2000]. For the case of non-zero absorption ($\alpha < 1$) the solution is

$$\phi_{\rm pt}(r) = \frac{\Sigma_t}{4\pi r}\left[\frac{\mathrm{e}^{-r\Sigma_t/\nu_0}}{\nu_0 N_0^+} + \int_1^\infty \frac{\mathrm{e}^{-r\Sigma_t y}}{\frac{\pi^2\alpha^2}{4y^2} + \left(1 - \frac{\alpha}{2y}\log\frac{y+1}{y-1}\right)^2} dy\right] \tag{172}$$

where ν_0 is the *asymptotic relaxation length* (a constant that depends only on α). This quantity and the quantity N_0^+ are defined in Section 8.6 .

Exact Solution (2b) An alternative form arising from a singular-eigenfunction derivation [Case and Zweifel 1967, McCormick and Kuščer 1973] in plane-parallel infinite media

(after applying the plane-to-point transformation (Section 8.4)) is:

$$\phi_{\text{pt}}(r) = \frac{\Sigma_t}{4\pi r}\left[\frac{\mathrm{e}^{-r\Sigma_t/\nu_0}}{\nu_0 N_0^+} + \int_0^1 \frac{\mathrm{e}^{-r\Sigma_t/\nu}}{\nu N_\nu} d\nu\right] \tag{173}$$

where the quantities ν_0, N_0^+ and N_ν are defined in Section 8.6.

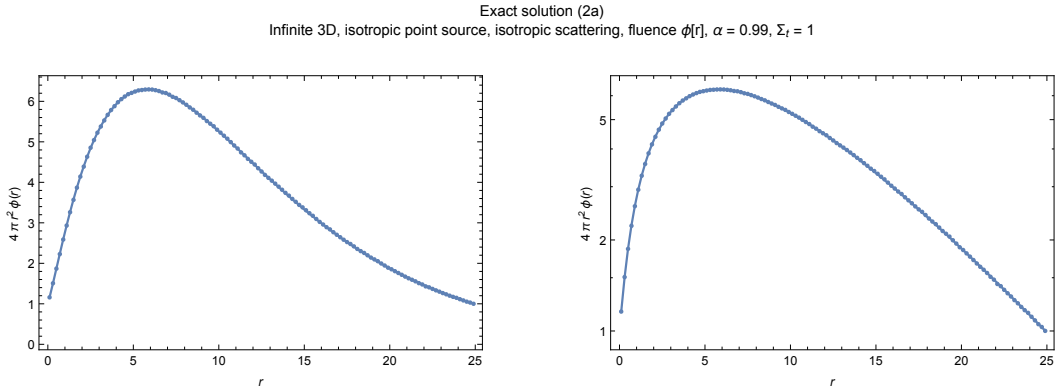

Figure 54: *Fluence $\phi_{pt}(r)$ due to an isotropic point source in an infinite 3D medium with isotropic scattering. Validation of exact solution (2a) (continuous) vs. Monte Carlo (dots).*

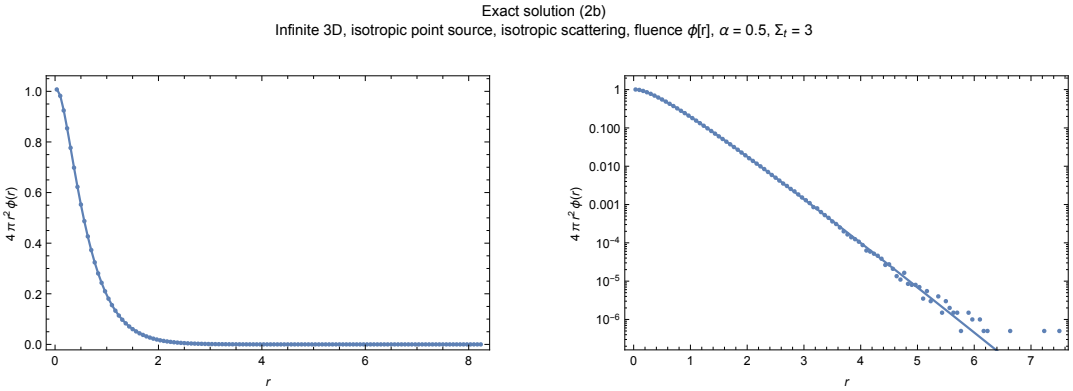

Figure 55: *Fluence $\phi_{pt}(r)$ due to an isotropic point source in an infinite 3D medium with isotropic scattering. Validation of exact solution (2b) (continuous) vs. Monte Carlo (dots).*

Rigourous Diffusion Approximation Equation 172 and 173 are related by a change of variable $y = 1/\nu$ for the continuous eigenvalues. The solution is a sum of a diffusion-like term

$$\phi_{\text{pt-rigorous-diffusion}}(r) = \frac{\Sigma_t}{4\pi r}\frac{\mathrm{e}^{-r\Sigma_t/\nu_0}}{\nu_0 N_0^+} \tag{174}$$

that is dominant far from the source and a transient term

$$\phi_{\text{pt-transient}}(r) = \frac{\Sigma_t}{4\pi r}\int_0^1 \frac{\mathrm{e}^{-r\Sigma_t/v}}{v\,N_v}dv \tag{175}$$

that is dominant near the source or for very high absorption levels.

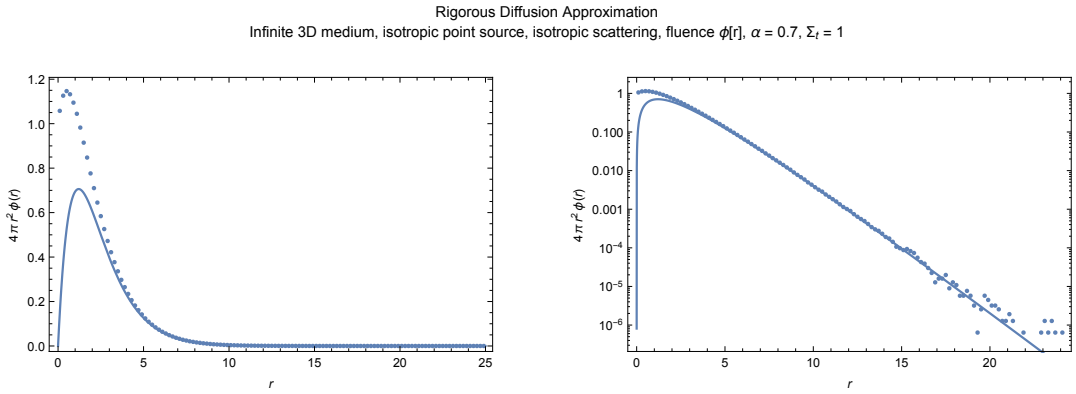

Figure 56: *Fluence $\phi_{pt}(r)$ due to an isotropic point source in an infinite 3D medium with isotropic scattering. Comparison of rigorous diffusion component (continuous) to Monte Carlo (dots).*

Exact Solution After n Scattering Events The total fluence ϕ_{pt} can be decomposed into a sum of terms that correspond to fluence (energy density) of particles that have collided (scattered) exactly n times, which we denote $\phi_{\text{pt}}(r|n)$. These quantities are related to the total fluence by the Neumann series:

$$\phi_{\text{pt}}(r) = \sum_{n=0}^{\infty}\phi_{\text{pt}}(r|n) \tag{176}$$

The case of $n = 0$ corresponds to the *uncollided (ballistic) fluence* and is given exactly as

$$\phi_{\text{pt}}(r|0) = \frac{\mathrm{e}^{-\Sigma_t r}}{4\pi r^2}. \tag{177}$$

Starting with the Fourier transform solution for the total fluence (Equation 171) and expanding the integrand as a series of powers of the single-scattering albedo α gives [Placzek and Volkoft 1943]:

$$\phi_{\text{pt}}(r|n>0) = \frac{(\alpha\,\Sigma_t)^n}{2\pi^2 r}\int_0^{\infty}\frac{(\arctan\,(z/\Sigma_t))^{n+1}}{z^n}\sin(r\,z)dz. \tag{178}$$

An alternative exact solution derived by Grosjean [1951] is:

$$\phi_{\text{pt}}(r|n>0) = \frac{\alpha^n\,\Sigma_t}{2^{n+3}\,\pi^2\,i\,r}\int_1^{\infty}\frac{e^{-kr\Sigma_t}}{k^n}\left(\left(\log\left(\frac{k+1}{k-1}\right)+i\pi\right)^{n+1}-\left(\log\left(\frac{k+1}{k-1}\right)-i\pi\right)^{n+1}\right)dk. \tag{179}$$

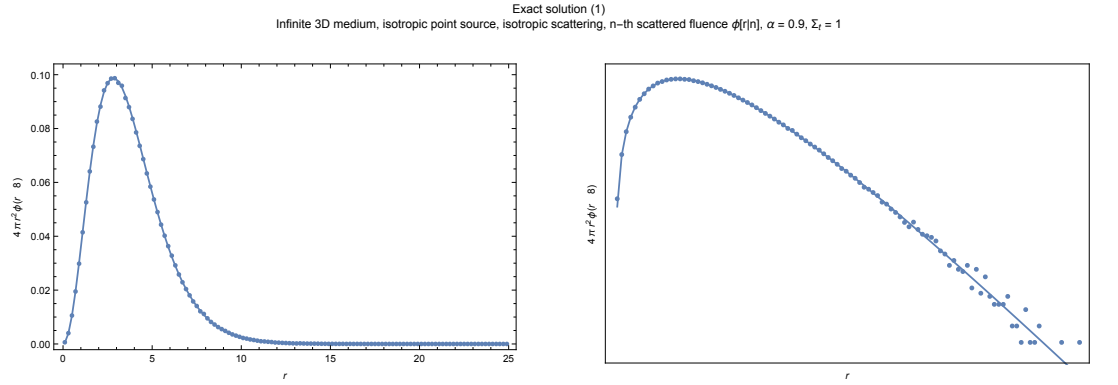

Figure 57: *Nth-collided fluence $\phi_{pt}(r|n)$ due to an isotropic point source in an infinite 3D medium with isotropic scattering. Validation of exact solution (continuous) vs. Monte Carlo (dots).*

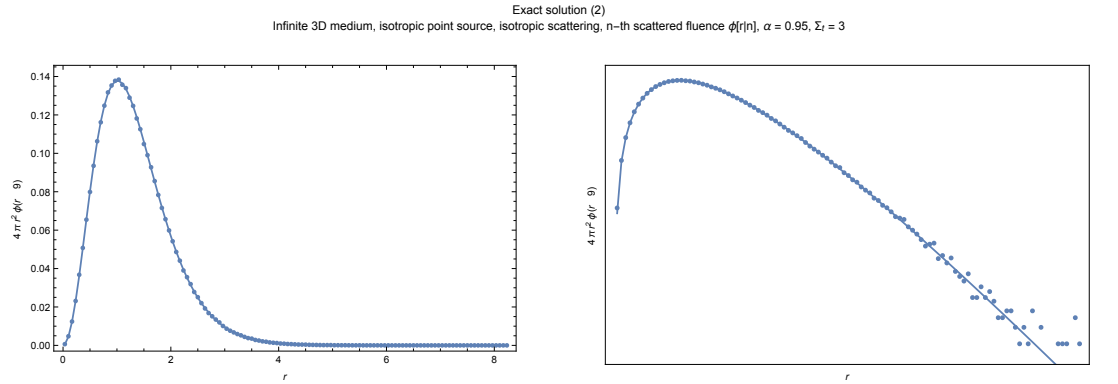

Figure 58: *Nth-collided fluence $\phi_{pt}(r|n)$ due to an isotropic point source in an infinite 3D medium with isotropic scattering. Validation of Grosjean's exact solution (continuous) vs. Monte Carlo (dots).*

Fluence/Density Moments Known [Grosjean 1963, Case and Zweifel 1967] moments for the exact solution:

$$\int_0^\infty 4\pi r^2 \phi_{\text{pt}}(r) dr = \int d^3 r \phi_{\text{pt}}(r) = \frac{1}{(1-\alpha)\Sigma_t} \tag{180}$$

$$\int r^2 d^3 r \phi_{\text{pt}}(r) = \frac{2}{(1-\alpha)^2 \Sigma_t^3} \tag{181}$$

$$\int r^4 d^3 r \phi_{\text{pt}}(r) = \frac{8(4\alpha - 9)}{3(\alpha-1)^3 \Sigma_t^5} \tag{182}$$

$$\int r^6 d^3 r \phi_{\text{pt}}(r) = \frac{16(4\alpha(11\alpha - 36) + 135)}{3(\alpha-1)^4 \Sigma_t^7} \tag{183}$$

the general case for even $m \geq 0$ found via [Zoia et al. 2011a]

$$\int_0^\infty 4\pi r^2 r^m \phi_{\text{pt}}(r) dr = 2 i^m \frac{\Gamma\left(\frac{m+3}{2}\right)}{\Gamma\left(\frac{m+1}{2}\right)} \left[\frac{\partial^m}{\partial z^m} \frac{\arctan\left(\frac{z}{\Sigma_t}\right)}{z - c\Sigma_t \arctan\left(\frac{z}{\Sigma_t}\right)} \bigg|_{z=0} \right]. \tag{184}$$

Moments of the fluence after n scattering events (Equation 178) can be found by expanding the moments equations above into a Taylors series about $\alpha = 0$:

$$\int_0^\infty 4\pi r^2 \phi_{\text{pt}}(r|n) dr = \frac{\alpha^n}{\Sigma_t} \tag{185}$$

$$\int_0^\infty 4\pi r^4 \phi_{\text{pt}}(r|n) dr = \frac{2(n+1)\alpha^n}{\Sigma_t^3} \tag{186}$$

$$\int_0^\infty 4\pi r^6 \phi_{\text{pt}}(r|n) dr = \frac{4(n+1)(5n+18)\alpha^n}{3\Sigma_t^5} \tag{187}$$

$$\int_0^\infty 4\pi r^8 \phi_{\text{pt}}(r|n) dr = \frac{8(n+1)\left(35n^2 + 343n + 810\right)\alpha^n}{9\Sigma_t^7} \tag{188}$$

Classical Diffusion Approximation The classical diffusion (P_1) solution for fluence due to an isotropic point source is

$$\phi_{\text{pt}}(r) \approx \frac{1}{4\pi D} \frac{\mathrm{e}^{-\sqrt{\frac{\Sigma_a}{D}} r}}{r} \tag{189}$$

where D is the diffusion coefficient (which may be defined/derived in several ways). Typically, $D = 1/(3\Sigma_t)$. A derivation of this result using Fourier transforms can be found in [Placzek and Volkoft 1943].

Grosjean's Modified Diffusion Approximation A compact and moderately accurate diffusion-like approximation for the fluence due to an isotropic point source is [Grosjean 1956]

$$\phi_{\text{pt}}(r) \approx \frac{\mathrm{e}^{-\Sigma_t r}}{4\pi r^2} + \frac{1}{4\pi} \frac{3\Sigma_s \Sigma_t}{2\Sigma_a + \Sigma_s} \frac{\mathrm{e}^{-\sqrt{\frac{\Sigma_a}{D_{\text{G}}}} r}}{r} \tag{190}$$

where D_{G} is Grosjean's modified diffusion coefficient

$$D_{\text{G}} = \frac{2\Sigma_a + \Sigma_s}{3(\Sigma_a + \Sigma_s)^2}. \tag{191}$$

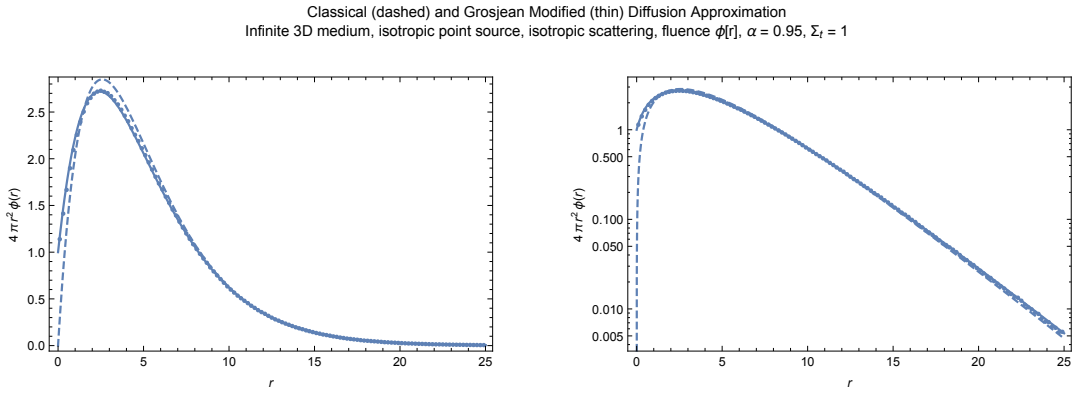

Figure 59: *Fluence $\phi_{pt}(r)$ due to an isotropic point source in an infinite 3D medium with isotropic scattering. Comparison of Classical diffusion (dashed) vs. Grosjean's modified diffusion (thin) vs. Monte Carlo (dots).*

Approximate Solution After n Scattering Events A Gaussian approximation for the nth scattered fluence that preserves the first two event moments of the exact solution is [Grosjean 1951, Zoia et al. 2011a]

$$\phi_{\text{pt}}(r|n) \approx= \frac{3\sqrt{3}\Sigma_t^2\alpha^n e^{-\frac{3r^2\Sigma_t^2}{4(n+1)}}}{8\pi^{3/2}\sqrt{(n+1)^3}}. \tag{192}$$

More accurate low order approximations are derivable as the Taylor series terms of order α^n of the classical diffusion and Grosjean diffusion fluence approximations [d'Eon 2014]. The first few terms are:

$$\begin{pmatrix} \text{n} & \text{Classical} & \text{Grosjean} \\ 0 & \frac{3e^{-\sqrt{3}r\Sigma_t}\Sigma_t}{4\pi r} & \frac{e^{-r\Sigma_t}}{4\pi r^2} \\ 1 & \frac{3\sqrt{3}e^{-\sqrt{3}r\Sigma_t}\alpha\Sigma_t^2}{8\pi} & \frac{3e^{-\sqrt{\frac{3}{2}}r\Sigma_t}\alpha\Sigma_t}{8\pi r} \\ 2 & \frac{3e^{-\sqrt{3}r\Sigma_t}\alpha^2\Sigma_t^2\left(3r\Sigma_t+\sqrt{3}\right)}{32\pi} & \frac{3e^{-\sqrt{\frac{3}{2}}r\Sigma_t}\alpha^2\Sigma_t\left(\sqrt{6}r\Sigma_t+4\right)}{64\pi r} \\ 3 & \frac{3e^{-\sqrt{3}r\Sigma_t}\alpha^3\Sigma_t^2\left(r\Sigma_t\left(\sqrt{3}r\Sigma_t+3\right)+\sqrt{3}\right)}{64\pi} & \frac{3e^{-\sqrt{\frac{3}{2}}r\Sigma_t}\alpha^3\Sigma_t\left(3r\Sigma_t\left(r\Sigma_t+3\sqrt{6}\right)+16\right)}{512\pi r} \end{pmatrix} \tag{193}$$

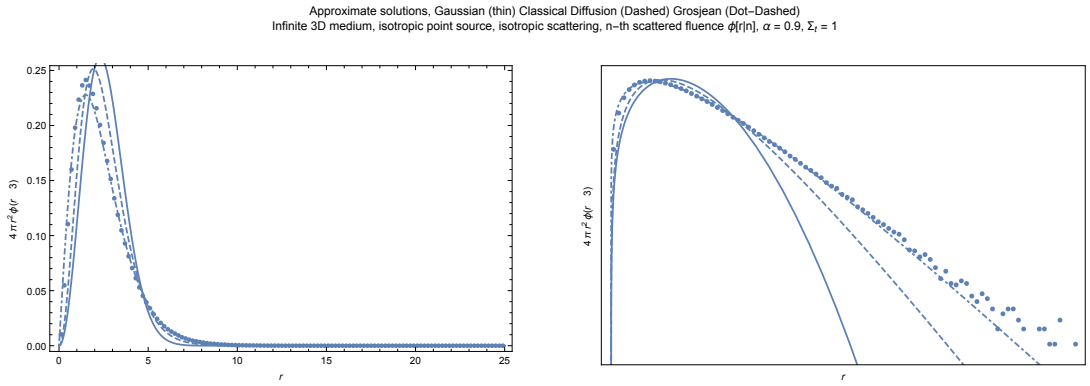

Figure 60: *Nth-scattered fluence $\phi_{pt}(r|3)$ due to an isotropic point source in an infinite 3D medium with isotropic scattering. Comparison of various approximations.*

6.1.4 Radiance (Angularly-resolved solutions)

Exact Solution A Legendre polynomial expansion for the exact angular distribution was given by Davison [2000]. As Davison notes, a more efficient way to compute the angular solution is to back integrate the fluence:

$$L(r,u) = \frac{1}{4\pi r^2}\mathrm{e}^{-r\Sigma_t}\delta(u-1) + \frac{\alpha\Sigma_t}{4\pi}\int_0^\infty \phi_{\mathrm{pt}}(\sqrt{r^2+t^2-2rtu})\mathrm{e}^{-t\Sigma_t}dt, \tag{194}$$

which is particularly effective using Grosjean's approximate fluence.

Classical diffusion approximation The angular distribution predicted by the classical diffusion approximation is

$$L(r,u) \approx \frac{1}{4\pi}\left(\phi_{\mathrm{pt}}(r) + u\,\frac{3e^{-r\sqrt{3-3\alpha}\,\Sigma_t}\left(r\sqrt{3-3\alpha}\,\Sigma_t+1\right)}{4\pi r^2}\right), \tag{195}$$

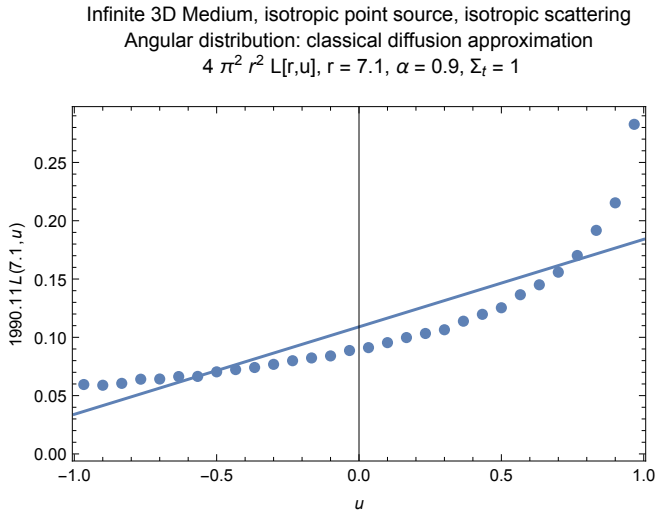

Figure 61: *Radiance $L(r,u)$ due to an isotropic point source in an infinite 3D medium with isotropic scattering. Comparison of classical diffusion approximation (thin) vs. Monte Carlo (dots).*

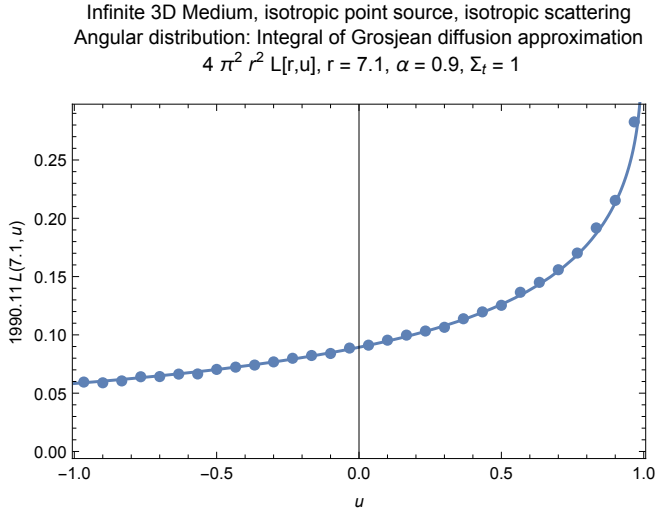

Figure 62: *Radiance $L(r,u)$ due to an isotropic point source in an infinite 3D medium with isotropic scattering. Comparison of Grosjean diffusion integral form (thin) vs. Monte Carlo (dots).*

Further Reading

For the case of purely absorbing media with spherical symmetry [Case et al. 1953] present exact analytical solutions. For an extension of this to both spherical and clyindrical media with off-centre point sources, see [Mikata 2014].

6.2 Isotropic Point Source, Infinite Medium, Linearly-Anisotropic Scattering

6.2.1 Problem Statement

This problem considers a single isotropically-emitting point source at the origin of an infinite homogeneous medium with a linearly-anisotropic scattering law (described in Section 2.3.2) with free parameter b. The scalar spatial coordinate of the solution is the radius r from the point source. The scalar directional parameter is the direction cosine u to the outward direction. Parameter $u \in [-1,1]$ indexes *cones* of directions. The direction pointing away from the point source is $u = 1$ and the direction pointing towards the point source is $u = -1$. Figure 51 illustrates our notation.

6.2.2 Fluence/Density

Exact Solution The exact fluence is given by [Williams 1977] where $g = b/3$ is the mean cosine,

$$\phi_{\text{pt}}(r) = \frac{\nu_0 \Sigma_t}{2\pi r} W \mathrm{e}^{-\nu_0 r \Sigma_t} + \frac{\Sigma_t}{4\pi r} \int_0^1 \frac{1}{u^2} \gamma(\alpha, g, u) \mathrm{e}^{-\Sigma_t \frac{r}{u}} du \tag{196}$$

$$\gamma(\alpha, g, u) = \frac{1}{\frac{1}{4}\pi^2 \alpha^2 u^2 (X+1)^2 + \left(-\frac{1}{2}\alpha u (X+1) \log\left(\frac{u+1}{1-u}\right) + \alpha X + 1\right)^2} \tag{197}$$

$$X = 3u^2((1-\alpha)g) \tag{198}$$

$$W = \frac{\nu_0 \left(1 - \nu_0^2\right)}{\alpha \left(3(1-\alpha)g \left(-\frac{3(1-\alpha)(1-\alpha g)}{\nu_0^2} - \alpha + 3\right) + \alpha + \nu_0^2 - 1\right)} \tag{199}$$

where $\nu_0 > 0$ is the solution of

$$0 = \frac{3(1-\alpha)\alpha g}{\nu_0^2} - \frac{\alpha \log\left(\frac{\nu_0+1}{1-\nu_0}\right)\left(\frac{3(1-\alpha)g}{\nu_0^2} + 1\right)}{2\nu_0} + 1. \tag{200}$$

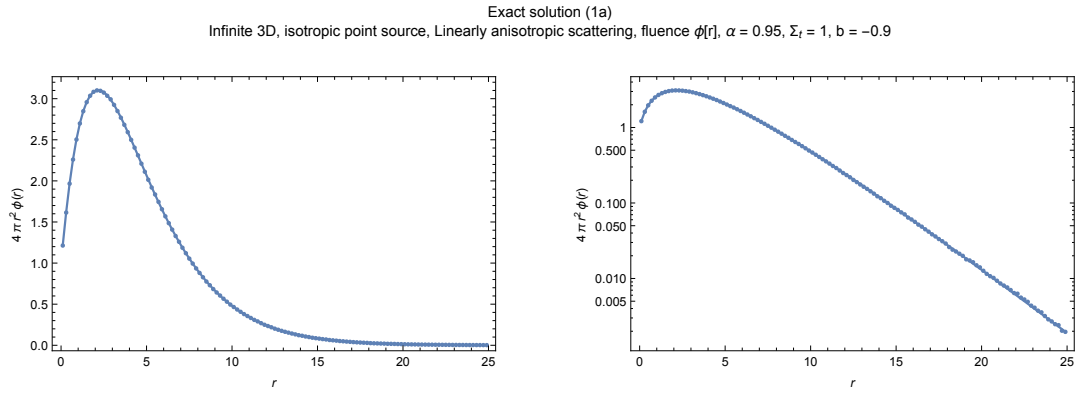

Figure 63: *Fluence $\phi_{pt}(r)$ due to an isotropic point source in an infinite 3D medium with linearly anisotropic scattering.*

Fluence/Density moments Known [Grosjean 1963] moments for the exact solution:

$$\int_0^\infty 4\pi r^2 \phi_{\rm pt}(r) dr = \int d^3 r \phi_{\rm pt}(r) = \frac{1}{1-\alpha}\frac{1}{\Sigma_t} \tag{201}$$

$$\int r^2 d^3 r \phi_{\rm pt}(r) = -\frac{6}{(\alpha-1)^2(\alpha b-3)}\frac{1}{\Sigma_t^3} \tag{202}$$

$$\int r^4 d^3 r \phi_{\rm pt}(r) = \frac{24(4\alpha-9)}{(\alpha-1)^3(\alpha b-3)^2}\frac{1}{\Sigma_t^5} \tag{203}$$

$$\int r^6 d^3 r \phi_{\rm pt}(r) = \frac{144\left(4\alpha\left(-55\alpha+9(\alpha-1)^2 b+180\right)-675\right)}{5(\alpha-1)^4(\alpha b-3)^3}\frac{1}{\Sigma_t^7} \tag{204}$$

Moments of the fluence after n scattering events (Equation 178) can be found by expanding the moments equations above into a Taylors series about $\alpha = 0$:

$$\phi_{0,n} = \int_0^\infty 4\pi r^2 \phi_{\rm pt}(r|n) dr = \frac{\alpha^n}{\Sigma_t} \tag{205}$$

$$\phi_{2,n} = \int_0^\infty 4\pi r^4 \phi_{\rm pt}(r|n) dr = \frac{2\,3^{-n}\left(b^{n+2} - b3^{n+1}(n+2) + 3^{n+2}(n+1)\right)\alpha^n}{(b-3)^2\Sigma_t^3} \tag{206}$$

Classical Diffusion Approximation The classical diffusion (P_1) solution for fluence due to an isotropic point source is

$$\phi_{\rm pt}(r) \approx \frac{\Sigma_t(3-\alpha\, b)e^{-r\Sigma_t\sqrt{(1-\alpha)(3-\alpha\, b)}}}{4\pi r} \tag{207}$$

Grosjean's Modified Diffusion Approximation A compact and moderately accurate diffusion-like approximation for the fluence due to an isotropic point source is [Grosjean 1956]

$$\phi_{\rm pt}(r) \approx \frac{e^{-r\Sigma_t} - \frac{3\alpha r\Sigma_t(\alpha b-3)\exp\left(-\sqrt{3}r\Sigma_t\sqrt{\frac{(\alpha-1)(\alpha b-3)}{-3\alpha+(\alpha-1)^2 b+6}}\right)}{-3\alpha+(\alpha-1)^2 b+6}}{4\pi r^2} \tag{208}$$

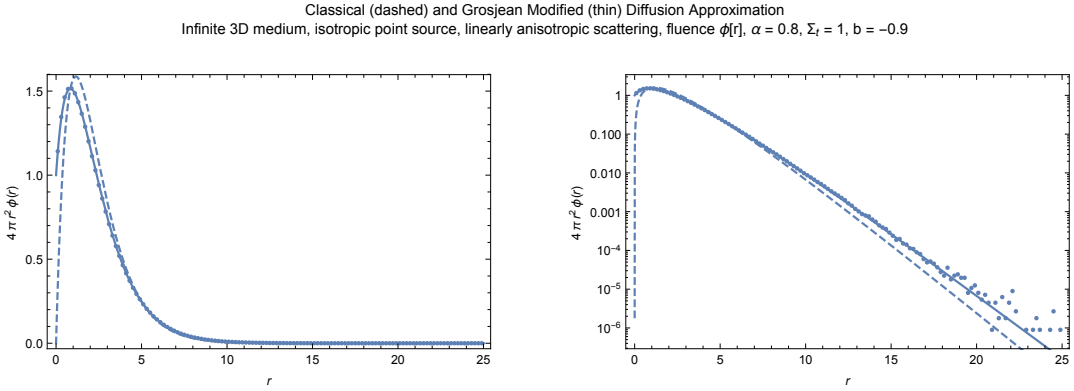

Figure 64: *Fluence $\phi_{pt}(r)$ due to an isotropic point source in an infinite 3D medium with linearly anisotropic scattering. Comparison of Classical diffusion (dashed) vs. Grosjean's modified diffusion (thin) vs. Monte Carlo (dots).*

Approximate Solution After n Scattering Events A Gaussian approximation for the nth scattered fluence that preserves the first two event moments of the exact solution is

$$\phi_{\rm pt}(r|n) \approx= \frac{3\sqrt{\frac{3}{2}}\phi_{0,n}^{5/2} e^{-\frac{3r^2\phi_{0,n}}{2\phi_{2,n}}}}{2\pi^{3/2}\phi_{2,n}^{3/2}}, \tag{209}$$

where $\phi_{0,n}$, $\phi_{2,n}$ are moments defined above.

More accurate low order approximations are derivable as the Taylor series terms of order α^n of the classical diffusion and Grosjean diffusion fluence approximations.

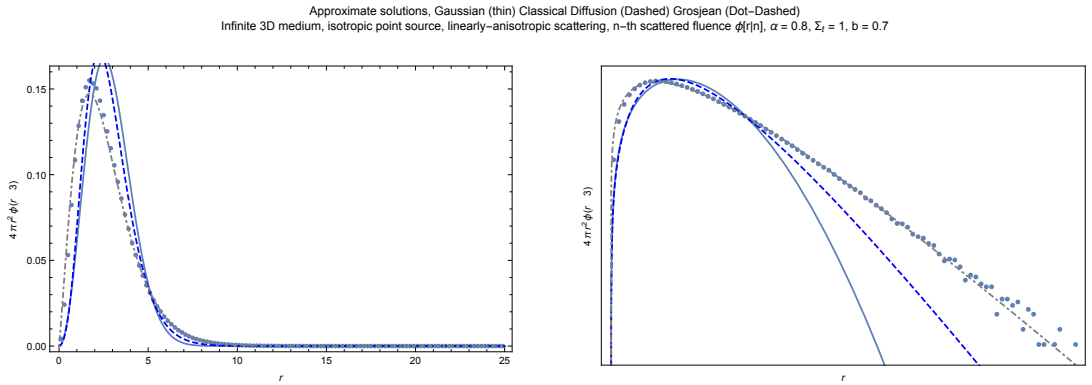

Figure 65: *Nth-scattered fluence $\phi_{pt}(r|3)$ due to an isotropic point source in an infinite 3D medium with linearly anisotropic scattering. Comparison of various approximations.*

7 3D Volume - Plane Symmetry

7.1 Isotropic Plane Source, Infinite Medium, Isotropic Scattering

7.1.1 Problem Statement

This problem considers a unit-power, isotropically-emitting plane source at the origin ($z = 0$) of an infinite homogeneous medium with isotropic scattering. The scalar spatial coordinate of the solution is the distance z from the plane source (which is a plane at the origin orthogonal to the z axis). The scalar directional parameter is the direction cosine u to the z axis. Parameter $u \in [-1, 1]$ indexes cones of directions. Figure 66 illustrates our notation.

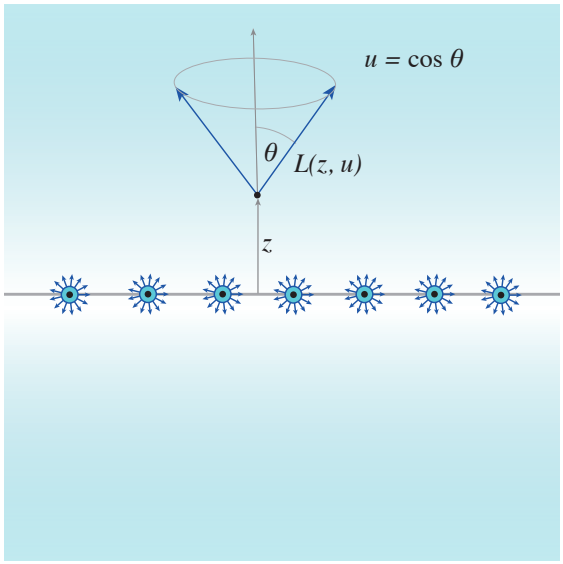

Figure 66: *An isotropically-emitting plane source in an infinite 3D medium: every position on the 2D plane acts like an isotropic point source emitter. We consider the radiance and fluence/density at each point in the volume, indexed by its distance z from the plane source and by direction u, the cosine of the angle between a given direction and the z-axis.*

7.1.2 Transport Equation

The transport equation for a homogeneous 3D volume with plane symmetry and isotropic scattering is [Case and Zweifel 1967]:

$$u\frac{\partial L(z,u)}{\partial z} + L(z,u) = \frac{\alpha}{2}\int_{-1}^{1} L(z,u')du' + Q(z,u). \tag{210}$$

For an isotropic plane source the source function Q is

$$Q(z,u) = \frac{\delta(z)}{4\pi}. \tag{211}$$

7.1.3 Fluence

The *fluence* ϕ_{pl} due to a plane source is proportional to the energy density and is an average of the radiance L over all directions:

$$\phi_{\text{pl}}(z) = \int_{4\pi} L(z, \vec{\omega}) d\vec{\omega} \tag{212}$$

Exact Solution The fluence due to an isotropic plane source at depth $z = 0$ is [Case and Zweifel 1967]

$$\phi_{\text{pl}}(z) = \frac{1}{2}\left[\frac{\mathrm{e}^{-|z|\Sigma_t/\nu_0}}{N_0^+} + \int_0^1 \frac{\mathrm{e}^{-|z|\Sigma_t/\nu}}{N_\nu} d\nu\right]. \tag{213}$$

where N_0^+ and N_ν are given in Section 8.6. An additional assumption leading to this solution was that the flux vanish as $z \to \infty$. The case for $c = 1$ and $c < 1$ are derived in slightly different ways. The exact solution for the plane source is related to the isotropic point source problem (Section 6.1) by the plane-to-point transform (Section 8.4).

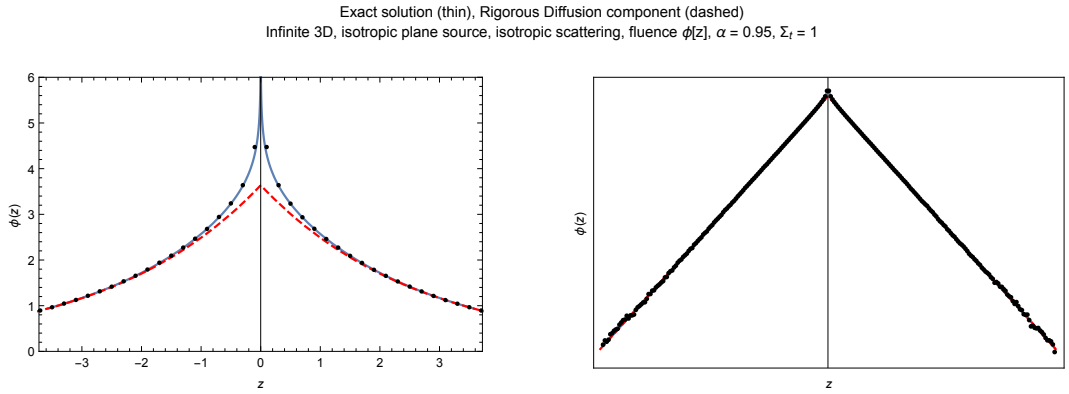

Figure 67: *Fluence $\phi_{pl}(z)$ due to an isotropic plane source in an infinite 3D medium with isotropic scattering. Validation of exact solution (continuous) vs. Rigorous diffusion (dashed) vs. Monte Carlo (dots).*

Rigourous Diffusion Approximation The rigorous diffusion approximation arises from discarding the transient term in the exact Caseology solution [Case and Zweifel 1967], leaving

$$\phi_{\text{pl}}(z) \approx \frac{1}{2}\frac{\mathrm{e}^{-|z|\Sigma_t/\nu_0}}{N_0^+}, \tag{214}$$

which is especially accurate far from the source and for low absorption.

Exact Solution After n Scattering Events The total fluence ϕ_{pl} can be decomposed into a sum of terms that correspond to fluence (energy density) of particles that have collided (scattered) exactly n times, which we denote $\phi_{\text{pl}}(z|n)$. These quantities are related to the total fluence by the Neumann series:

$$\phi_{\text{pl}}(z) = \sum_{n=0}^{\infty} \phi_{\text{pl}}(z|n) \tag{215}$$

The case of $n = 0$ corresponds to the *uncollided (ballistic) fluence* and is given exactly as

$$\phi_{\text{pl}}(z|0) = -\frac{\text{Ei}(-\Sigma_t\,|z|)}{2} \tag{216}$$

where $\text{Ei}(z)$ is the exponential integral function.

An exact form of the nth-scattered fluence is [Grosjean 1951]

$$\phi_{\text{pl}}(z|n>0) = \frac{(\alpha\,\Sigma_t)^n}{\pi}\int_0^\infty \frac{(\arctan\,(k/\Sigma_t))^{n+1}}{k^{n+1}}\cos(k\,z)dk. \tag{217}$$

An alternative exact solution is [Grosjean 1951]

$$\phi_{\text{pl}}(z|n>0) = \frac{i\,\alpha^n}{2^{n+2}\,\pi}\int_1^\infty \frac{e^{-k|z|\Sigma_t}}{k^{n+1}}\left(\left(\log\left(\frac{k+1}{k-1}\right)-i\pi\right)^{n+1}-\left(\log\left(\frac{k+1}{k-1}\right)+i\pi\right)^{n+1}\right)dk. \tag{218}$$

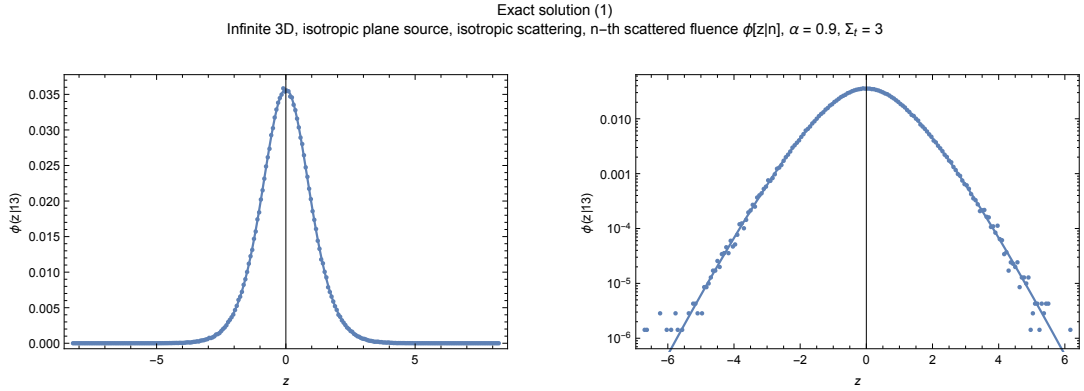

Figure 68: *Nth-collided fluence $\phi_{pt}(r|n)$ due to an isotropic plane source in an infinite 3D medium with isotropic scattering. Validation of exact solution (1) (continuous) vs. Monte Carlo (dots).*

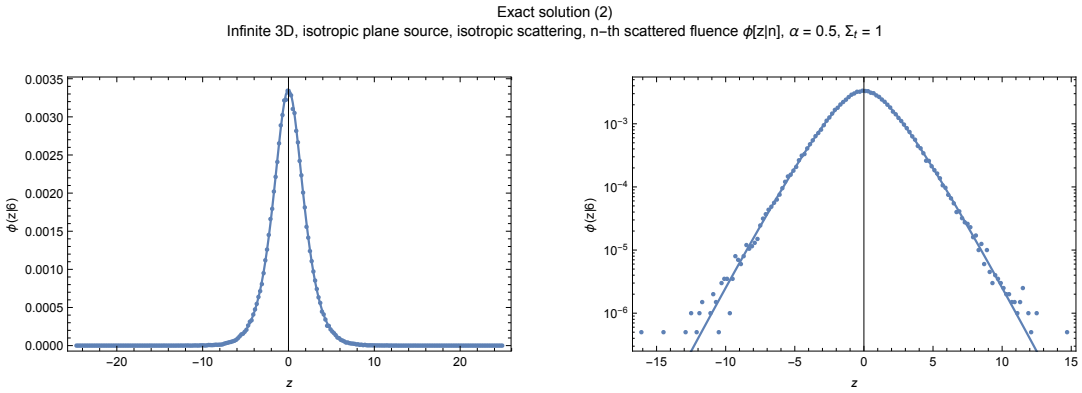

Figure 69: *Nth-collided fluence $\phi_{pt}(r|n)$ due to an isotropic plane source in an infinite 3D medium with isotropic scattering. Validation of exact solution (2) (continuous) vs. Monte Carlo (dots).*

Fluence/Density Moments Known even moments for the exact solution:

$$\int_{-\infty}^{\infty} \phi_{\text{pl}}(z)dz = \frac{1}{(1-\alpha)\Sigma_t} \tag{219}$$

$$\int_{-\infty}^{\infty} \phi_{\text{pl}}(z)z^2dz = \frac{2}{3(1-\alpha)^2\Sigma_t^3}. \tag{220}$$

Moments of the fluence after n scattering events can be found by expanding the moments equations above into a Taylors series about $\alpha = 0$:

$$\int_{-\infty}^{\infty} \phi_{\text{pl}}(z|n)dz = \frac{\alpha^n}{\Sigma_t} \tag{221}$$

$$\int_{-\infty}^{\infty} \phi_{\text{pl}}(z|n)z^2dz = \frac{2(n+1)\alpha^n}{3\Sigma_t^3} \tag{222}$$

Classical Diffusion Approximation The classical diffusion (P_1) solution for fluence due to an isotropic plane source [Weinberg and Wigner 1958] can be found by applying the point-to-plane transform (Section 8.4) to the isotropic point source solution (Equation 189)

$$\phi_{\text{pl}}(z) \approx \frac{3e^{-\sqrt{3-3\alpha}\Sigma_t|x|}}{2\sqrt{3-3\alpha}}. \tag{223}$$

Grosjean's Modified Diffusion Approximation Applying the point-to-plane transform (Section 8.4) to Grosjean's point source approximation (Equation 208) yields a modified diffusion approximation for the plane source

$$\phi_{\text{pt}}(z) \approx \frac{\sqrt{\frac{3}{\alpha-2}+3}\alpha e^{-\sqrt{\frac{3}{\alpha-2}+3}\Sigma_t|x|}}{2(1-\alpha)} - \frac{\text{Ei}(-\Sigma_t|x|)}{2} \tag{224}$$

which has the same advantages over the classical diffusion approximation.

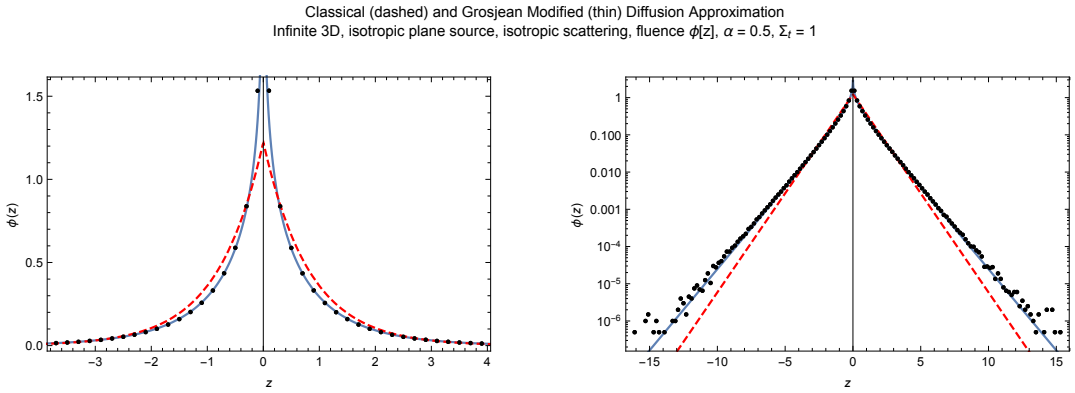

Figure 70: *Fluence $\phi_{pt}(z)$ due to an isotropic plane source in an infinite 3D medium with isotropic scattering. Comparison of Classical diffusion (dashed) vs. Grosjean's modified diffusion (thin) vs. Monte Carlo (dots).*

Approximate Solution After n Scattering Events A Gaussian approximation for the nth scattered fluence that preserves the first two event moments of the exact solution is [Grosjean 1951]

$$\phi_{\text{pl}}(z|n) \approx= \frac{\sqrt{\frac{3}{\pi}}\alpha^n e^{-\frac{3\Sigma_t^2 x^2}{4(n+1)}}}{2\sqrt{n+1}} \tag{225}$$

More accurate low order approximations are derivable as the Taylor series terms of order α^n of the classical diffusion and Grosjean diffusion fluence approximations [d'Eon 2014]. The first few terms are:

$$\begin{pmatrix} \text{n} & \text{Classical} & \text{Grosjean} \\ 0 & \frac{1}{2}\sqrt{3}e^{-\sqrt{3}\Sigma_t|z|} & -\frac{\text{Ei}(-\Sigma_t|z|)}{2} \\ 1 & \frac{1}{4}e^{-\sqrt{3}\Sigma_t|z|}\alpha\left(3\Sigma_t|z|+\sqrt{3}\right) & \frac{1}{2}\sqrt{\frac{3}{2}}e^{-\sqrt{\frac{3}{2}}\Sigma_t|z|}\alpha \\ 2 & \frac{3}{16}e^{-\sqrt{3}\Sigma_t|z|}\alpha^2\left(\sqrt{3}\Sigma_t^2|z|^2+3\Sigma_t|z|+\sqrt{3}\right) & \frac{3}{16}e^{-\sqrt{\frac{3}{2}}\Sigma_t|z|}\alpha^2\left(\Sigma_t|z|+\sqrt{6}\right) \\ 3 & \frac{1}{32}e^{-\sqrt{3}\Sigma_t|z|}\alpha^3\left(3\Sigma_t^3|z|^3+6\sqrt{3}\Sigma_t^2|z|^2+15\Sigma_t|z|+5\sqrt{3}\right) & \frac{1}{256}e^{-\sqrt{\frac{3}{2}}\Sigma_t|z|}\alpha^3\left(3\sqrt{6}\Sigma_t^2|z|^2+66\Sigma_t|z|+38\sqrt{6}\right) \end{pmatrix} \tag{226}$$

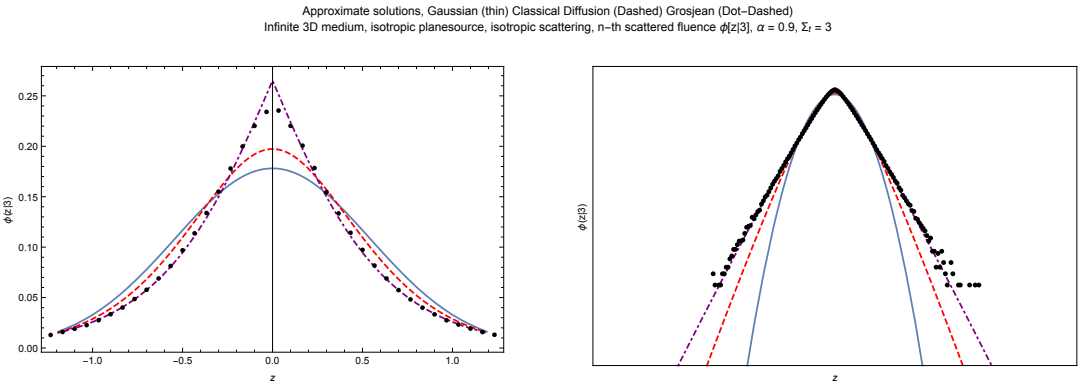

Figure 71: *Nth-scattered fluence $\phi_{pl}(z|n)$ due to an isotropic plane source in an infinite 3D medium with isotropic scattering. Comparison of various approximations.*

7.1.4 Radiance / Vector-flux

Exact solution The singular eigenfunction expansion for the exact radiance is given by [Case and Zweifel 1967]

$$L(z>0,u) = \frac{1}{4\pi}\left[\frac{\psi_0^+(u)\mathrm{e}^{-|z|\Sigma_t/\nu_0}}{N_0^+} + \int_0^1 \frac{\psi_\nu(u)\mathrm{e}^{-|z|\Sigma_t/\nu}}{N_\nu}\right] \tag{227}$$

using the Caseology quantities defined in Section 8.6.

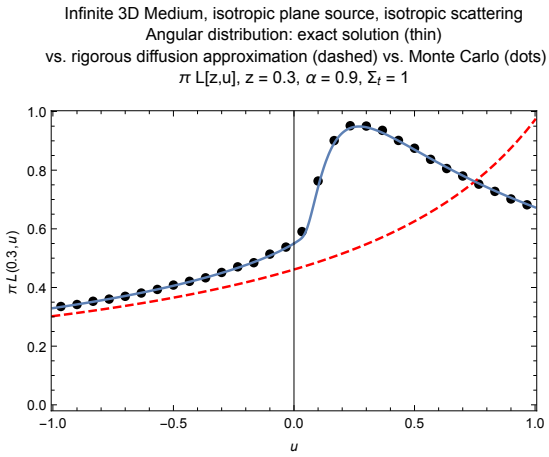

Figure 72: *Radiance $L(z,u)$ due to an isotropic plane source in an infinite 3D medium with isotropic scattering.*

7.2 Delta-Plane Source, Infinite Medium, Isotropic Scattering

Problem Statement This problem considers a unit plane source in an infinite homogeneous medium with isotropic scattering where emission is constrained to a single direction cosine u_0, thereby emitting from the plane in cones of directions. The scalar spatial coordinate of the solution is the distance z from the plane source (which is a plane at the origin orthogonal to the z axis). The scalar directional parameter is the direction cosine u to the z axis. Parameter $u \in [-1, 1]$ indexes cones of directions.

Transport Equation The transport equation for a homogeneous 3D volume with plane symmetry and isotropic scattering is [Case and Zweifel 1967]:

$$u\frac{\partial L(z,u)}{\partial z} + L(z,u) = \frac{\alpha}{2}\int_{-1}^{1} L(z,u')du' + Q(z,u). \tag{228}$$

With a delta plane source at depth z_0 emitting along directions with cosine u_0:

$$Q(z,u) = \frac{\delta(z-z_0)\delta(u-u_0)}{2\pi}. \tag{229}$$

The solution for the radiance is the Green's function for the half-space. The Green's function $G(z_0, u_0 \to z, u)$ satisfies

$$u\frac{\partial G}{\partial z} + G = \frac{c}{2}\int_{-1}^{1} G(z_0, u_0 \to z, u')du' + Q(z,u). \tag{230}$$

The angular flux at z, u can be written as

$$L(z,u) = \frac{1}{2\pi}\left[\pm\frac{\psi_0^{\pm}(u_0)\psi_0^{\pm}(u)\mathrm{e}^{-|z-z_0|/v_0}}{N_0^{\pm}}\int_0^1 \frac{\psi_{\pm v}(u_0)\psi_{\pm v}(u)\mathrm{e}^{-|z-z_0|/v}}{N_v}dv\right] \tag{231}$$

where the plus signs apply to $z > z_0$ and the minus signs to $z < z_0$.

The Green's function in terms as a Fourier inversion [Benoist and Kavenoky 1968]

$$G(z,u,u') = \frac{\alpha}{4\pi}\int_{-\infty}^{\infty} \frac{\mathrm{e}^{-ikz}}{(1-iku)(1-iku')(1-\frac{\alpha \arctan k}{k})}dk \tag{232}$$

7.3 Albedo Problem, Half-Space, Isotropic Scattering

7.3.1 Problem Statement

This problem considers plane-parallel surface illumination of a half-space with isotropic scattering and vacuum boundary conditions.

7.3.2 Albedo (Delta Illumination)

Exact Solution The escape probability (total diffuse albedo) for a photon arriving along direction cosine u_i to a semi-infinite, indexed-matched, isotropically-scattering half-space with single-scattering albedo α is [Chandrasekhar 1960]

$$R(\alpha, u_i) = 1 - H(u_i)\sqrt{1-\alpha} \tag{233}$$

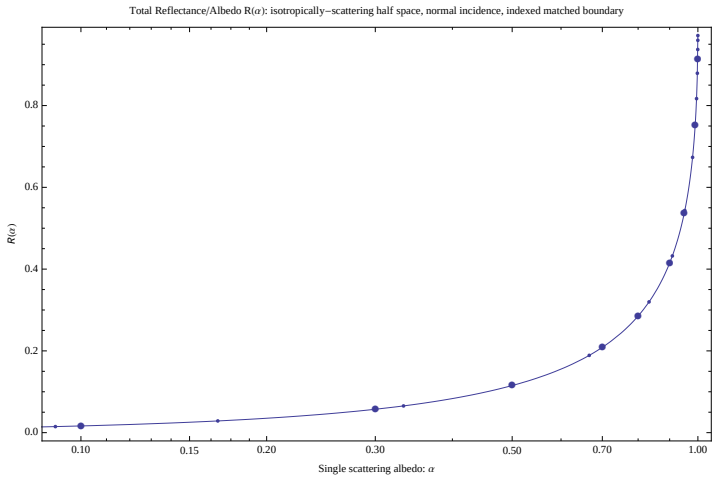

(a)

α	Diffuse Albedo
0.001	0.000153524
0.01	0.00154406
0.05	0.0079235
0.1	0.0163903
0.2	0.0352305
0.3	0.0572144
0.5	0.115226
0.7	0.20868
0.8	0.285255
0.85	0.33966
0.9	0.414947
0.95	0.535541
0.98	0.671084
0.99	0.752721
0.995	0.817047
0.999	0.912845
0.9999	0.971418
0.99999	0.990855
0.999999	0.997097

(b)

Figure 73: *Benchmark solutions for an isotropically-scattering half space with index matched boundary conditions: Total reflectance (escape probability) for illumination normal to the surface. (a) Continuous curve: exact solution numerically integration of Stibbs-Weir H-function in Mathematica. Small dots: MCML Monte Carlo solution. Large dots: Analog Monte Carlo Estimator used in this paper. (b) Exact benchmark values.*

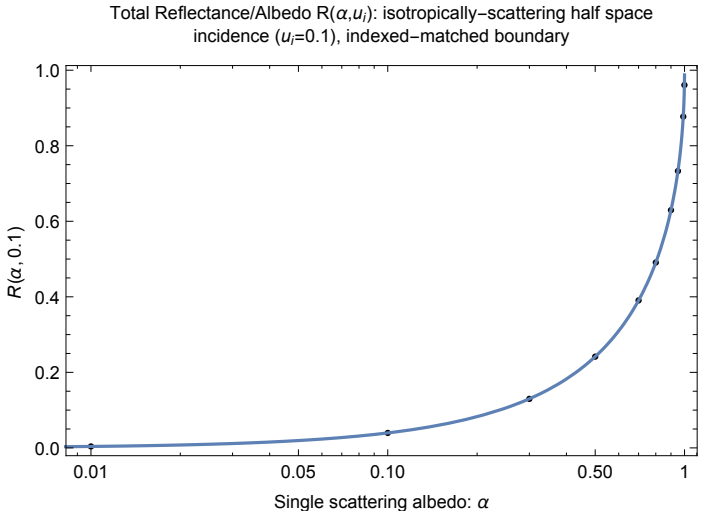

Figure 74: *Total reflectances (albedos) from an index-matched isotropically-scattering half space under uniform illumination along direction cosine* $u_i = 0.1$. *Exact solution (thin) vs. Monte Carlo (dots).*

Singly-Scattered Albedo The once-scattered energy emerging from a half space with vacuum boundary conditions and isotropic scattering is having arrived along direction cosine u_i is

$$R_1(\alpha, u_i) = \frac{1}{2}\alpha\left(1 + u_i \log\left(\frac{u_i}{1+u_i}\right)\right). \tag{234}$$

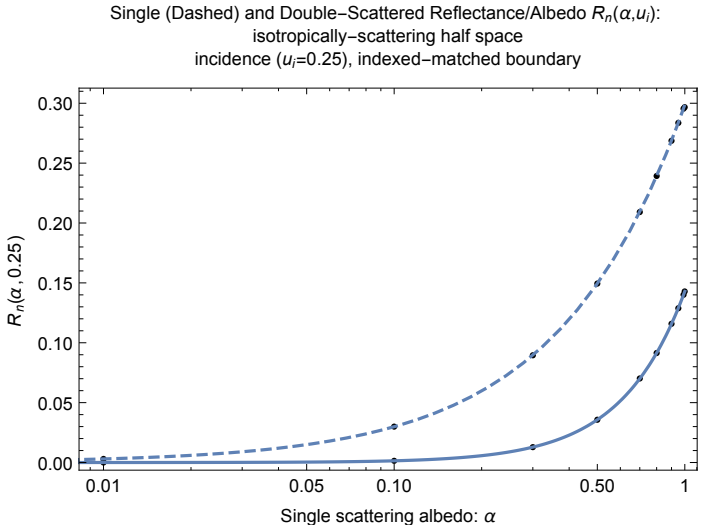

Figure 75: *Total Single- and Double-Scattered reflectances (albedos) from an index-matched isotropically-scattering half space under uniform illumination along direction cosine* $u_i = 0.25$. *Exact solution (thin) vs. Monte Carlo (dots).*

Classical Diffusion Approximation The classical diffusion approximations for the indexed-matched half space with plane-parallel illumination along direction cosine u_i predicts the albedo [Grosjean 1958]

$$R(\alpha, u_i) \approx \frac{\alpha}{\left(\frac{2\sqrt{1-\alpha}}{\sqrt{3}} + 1\right)\left(\sqrt{3}\sqrt{1-\alpha}u_i + 1\right)}. \tag{235}$$

Rigorous Diffusion Approximation The rigorous diffusion approximations for the indexed-matched half space with plane-parallel illumination along direction cosine u_i predicts the albedo [Grosjean 1958]

$$R(\alpha, u_i) \approx \frac{\alpha}{(2(1-\alpha)\nu_0 + 1)\left(\frac{u_i}{\nu_0} + 1\right)} \tag{236}$$

where the rigorous diffusion length ν_0 is defined in Section 8.6.

Grosjean's Modified Diffusion Approximation Grosjean [1958] gave two albedo approximations based on his modified diffusion theory for the indexed-matched half space with plane-parallel illumination along direction cosine u_i, form 1:

$$\begin{aligned} R(\alpha, u_i) \approx & \frac{(13-5\alpha)\alpha^2}{\left(\frac{16\sqrt{\frac{1-\alpha}{2-\alpha}}(2-\alpha)}{\sqrt{3}} - 5\alpha + 13\right)\left(\sqrt{3}\sqrt{\frac{1-\alpha}{2-\alpha}}u_i + 1\right)} \\ & - \frac{5\sqrt{3}\sqrt{\frac{1-\alpha}{2-\alpha}}(2-\alpha)\alpha^2\left(-2u_i + 2u_i^2 \log\left(\frac{u_i+1}{u_i}\right) + 1\right)}{4\left(\frac{16\sqrt{\frac{1-\alpha}{2-\alpha}}(2-\alpha)}{\sqrt{3}} - 5\alpha + 13\right)} \\ & + \frac{1}{2}\left(1 - \frac{(13-5\alpha)\alpha}{\frac{16\sqrt{\frac{1-\alpha}{2-\alpha}}(2-\alpha)}{\sqrt{3}} - 5\alpha + 13}\right)\alpha\left(1 - u_i \log\left(\frac{u_i+1}{u_i}\right)\right) \end{aligned} \tag{237}$$

and a simpler, less accurate form 2,

$$\begin{aligned} R(\alpha, u_i) \approx & \frac{\alpha^2}{\left(\frac{2\sqrt{\frac{1-\alpha}{2-\alpha}}(2-\alpha)}{\sqrt{3}} + 1\right)\left(\sqrt{3}\sqrt{\frac{1-\alpha}{2-\alpha}}u_i + 1\right)} \\ & + \frac{1}{2}\left(1 - \frac{\alpha}{\frac{2\sqrt{\frac{1-\alpha}{2-\alpha}}(2-\alpha)}{\sqrt{3}} + 1}\right)\alpha\left(1 - u_i \log\left(\frac{u_i+1}{u_i}\right)\right) \end{aligned} \tag{238}$$

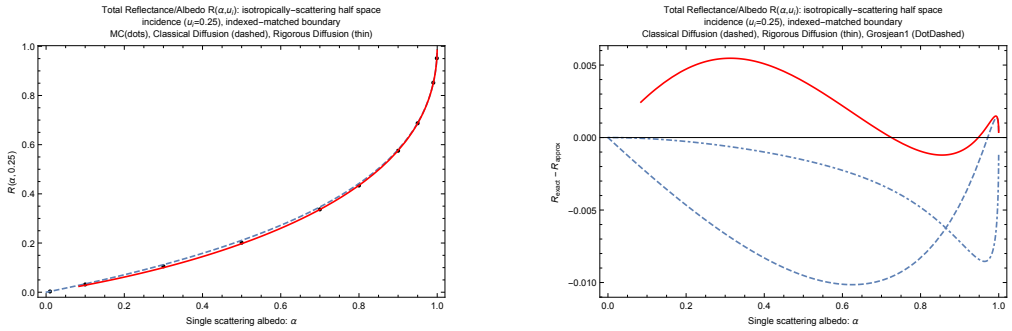

Figure 76: *Comparison and error plots for various approximation.*

Pomraning's Approximation for Normal Incidence A variational approximation for the albedo under normally-incident illumination is [Pomraning 1965]

$$R(\alpha,1) \approx \frac{2\left(\log\left(\frac{1}{\nu_0}+1\right)-\frac{1}{\nu_0}\right)}{\left(\frac{1}{\nu_0}+1\right)\log\left(1-\frac{1}{\nu_0^2}\right)} \tag{239}$$

where the rigorous diffusion length ν_0 is defined in Section 8.6.

Empirical Approximation for Normal Incidence An approximate albedo for normally-incident illuimation by Prahl [2002] is

$$R(\alpha,1) \approx \frac{\left(1-\sqrt{1-\alpha}\right)\left(1-0.128\sqrt{1-\alpha}\right)}{1.83\sqrt{1-\alpha}+1}. \tag{240}$$

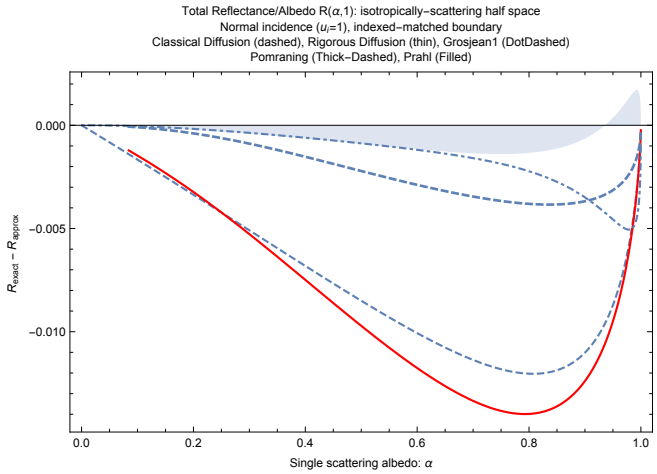

Figure 77: *Normal incidence: error plots for various approximations.*

7.3.3 Albedo (Uniform/White-Sky Illumination) / Escape probability

This subproblem considers illumination of the Half space by external white-sky illumination: uniform unit radiance in all directions arriving at the surface. By reciprocity, the internal distri-

butions will corresponding exactly to the escape probabilities for a particle starting at any given depth and direction.

Exact Solution An exact total albedo for an isotropic half space under diffuse illumination can be found as an integral of the H function (using the solution in Equation 233)

$$R(\alpha) = \int_0^1 2uR(\alpha, u)du. \tag{241}$$

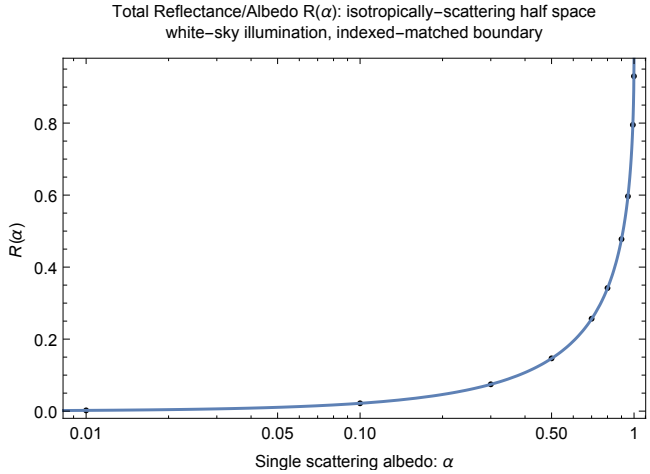

Figure 78: *Total reflectances (albedos) from an index-matched isotropically-scattering half space under uniform diffuse (white-sky) illumination. Exact solution (thin) vs. Monte Carlo (dots).*

Singly-Scattered Albedo The once-scattered energy emerging from a half space with vacuum boundary conditions and isotropic scattering under white-sky illumination is

$$R_1(\alpha) = \frac{2}{3}(\alpha - \alpha\log(2)). \tag{242}$$

Doubly-Scattered Albedo The twice-scattered energy emerging from a half space with vacuum boundary conditions and isotropic scattering under white-sky illumination is

$$R_1(\alpha) = \frac{1}{24}\alpha^2\left(4 + \pi^2 - 16\log(2)\right). \tag{243}$$

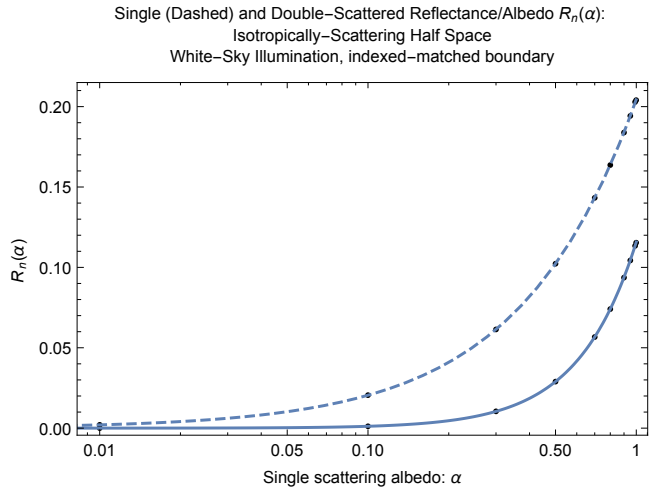

Figure 79: *Total Single- and Double-Scattered reflectances (albedos) from an index-matched isotropically-scattering half space under uniform diffuse (white-sky) illuminatoin. Exact solution (thin) vs. Monte Carlo (dots).*

Probability of Uncollided Escape Escape probability for leaving a half-space starting in an isotropically random direction at depth z (in mfps) and escaping without scatter is:

$$e^{-z} - z\Gamma(0, z). \tag{244}$$

Pomraning's Approximation for White-sky Illumination A variational approximation for the albedo under white-sky illumination is [Pomraning 1965]

$$R(\alpha) \approx -\frac{4\nu_0^2 \left(\log\left(\frac{1}{\nu_0}+1\right) - \frac{1}{\nu_0}\right)^2}{\log\left(1-\frac{1}{\nu_0^2}\right)} \tag{245}$$

where the rigorous diffusion length ν_0 is defined in Section 8.6.

Van De Hulst's Approximation for White-sky Illumination An accurate and compact approximation for the albedo under white-sky illumination [van de Hulst 1980]

$$R(\alpha) \approx \frac{\left(1-\sqrt{1-\alpha}\right)\left(1-0.139\sqrt{1-\alpha}\right)}{1.17\sqrt{1-\alpha}+1}. \tag{246}$$

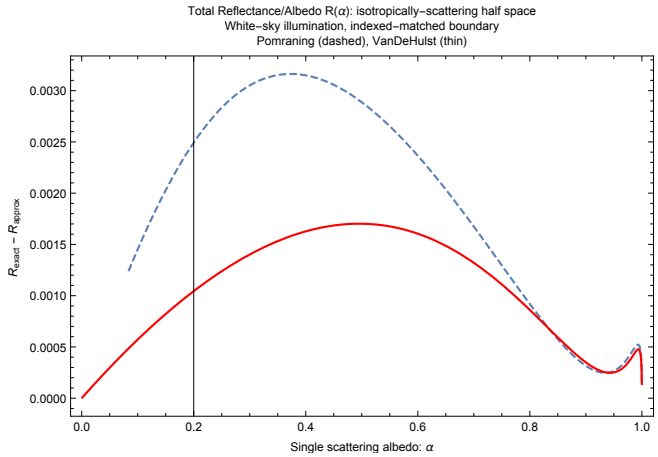

Figure 80: *White-sky illumination: error plots for various approximations.*

7.3.4 Emerging Distribution (BRDF)

Exact Solution The exact emerging distribution from an isotropic half space under delta illumination along direction cosine u_i is (expressed in BRDF form) [Chandrasekhar 1960]

$$f_r(u_i, u_o) = \frac{\alpha}{4\pi} \frac{H(u_i)H(u_o)}{u_i + u_o}. \tag{247}$$

The exact single-scattering from the half space is [Chandrasekhar 1960]

$$f_1(u_i, u_o) = \frac{\alpha}{4\pi} \frac{1}{u_i + u_o}. \tag{248}$$

The exact double-scattering from the half space is [Sears 1975]

$$f_2(u_i, u_o) = \frac{\alpha^2 \left(u_i \coth^{-1}(2u_i + 1) + u_o \coth^{-1}(2u_o + 1)\right)}{4\pi (u_i + u_o)}. \tag{249}$$

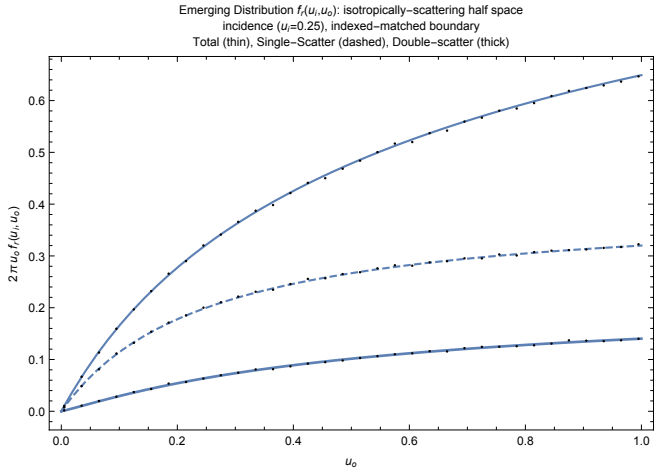

Figure 81: *Total-, Single-scattering- and Double-Scattering- BRDFs for the index-matched isotropically-scattering half space. Analytic exact solutions vs MC (Dots).*

7.4 Albedo Problem, Half-Space, Isotropic Scattering, Smooth Fresnel Boundary

7.4.1 Problem Statement

This problem considers plane-parallel surface illumination of a half-space with isotropic scattering and smooth Fresnel boundary conditions.

Exact Solutions

Further Reading

Exact solutions are given by Williams [2006].

7.5 Albedo Problem, Half-Space, Anisotropic Scattering

7.5.1 Problem Statement

This problem considers plane-parallel surface illumination of a half-space with anisotropic scattering and vacuum boundary conditions.

7.5.2 Escape probability / White-sky Illumination

This subproblem considers illumination of the Half space by external white-sky illumination: unit radiance in all directions arriving at the surface. By reciprocity, the internal distributions will corresponding exactly to the escape probabilities for a particle starting at any given depth and direction.

7.5.3 Albedo (white-sky illumination)

Approximate Albedo of van de Hulst Approximate total reflectance from a semi-infinte medium with no Fresnel and diffuse illumination is [van de Hulst 1980]:

$$R = \frac{(1-s)(1-0.139s)}{1+1.17s} \tag{250}$$

where

$$s = \sqrt{\frac{1-c}{1-cg}}. \tag{251}$$

"which has an error of less than 0.003 for any albedo and anisotropy"[Prahl 2002]. The inverse mapping is

$$s = 4.20863R - 0.00359712\sqrt{R(1.3689\times 10^6 R + 3.22126\times 10^6) + 741321} + 4.09712. \tag{252}$$

7.5.4 Similarity Relations

Similarity Relation of Irvine Irvine [1975] provides a similarity relation for half spaces with general anisotropic scattering (mean cosine g) proposing approximating a general half space with an isotropic half space using the modified single-scattering albedo $\alpha^\star$

$$\alpha^\star = (1-g)\alpha/(1-g\alpha). \tag{253}$$

8 Common Quantities, Functions and Relations

This section contains an assorted collection of quantities and functions that repeatedly appear in various transport solutions.

8.1 Surface Area of Unit Sphere in d Dimensions

We occasionally require the surface area of the unit "sphere" in d dimensions

$$\Omega_d(r) = \frac{d\pi^{d/2} r^{d-1}}{\Gamma\left(\frac{d}{2}+1\right)}. \tag{254}$$

8.2 Spherically-Symmetric Fourier Transforms in d Dimensions

Random flight problems with spherical symmetry and isotropic scattering are often easily expressed using spherically-symmetric Fourier transforms [Grosjean 1953, Dutka 1985]. The forward and inverse spherical Fourier transforms of a radially-symmetric function $f(r)$ (with radius $r \geq 0$) in the general d-dimensional case are

$$\mathcal{F}_d\{f(r)\} = z^{1-d/2}(2\pi)^{d/2} \int_0^\infty r^{d/2} J_{d/2-1}(rz) f(r) dr \tag{255}$$

$$\mathcal{F}_d^{-1}\{f(z)\} = r^{1-d/2}(2\pi)^{-d/2} \int_0^\infty z^{d/2} J_{d/2-1}(rz) f(z) dz \tag{256}$$

where z is the transformed coordinate relating to r and J_k is the modified Bessel function of the first kind. Note that these transforms are well defined for arbitrary (even non-integer) dimensions $d \geq 1$.

8.3 Spherical Diffusion Mode in d Dimensions

The radial diffusion mode about a point source in an infinite medium of dimension d with diffusion length $\nu > 0$ is the inverse spherical Fourier transform

$$m_d(\nu, r) = \mathcal{F}_d^{-1}\left\{\frac{1}{1+(z\nu)^2}\right\} = (2\pi)^{-d/2} r^{1-\frac{d}{2}} \nu^{-\frac{d}{2}-1} K_{\frac{d-2}{2}}\left(\frac{r}{\nu}\right) \tag{257}$$

where $K_n(x)$ is the modified Bessel function of the second kind. This form is chosen for its unit normalization,

$$\int_0^\infty \Omega_d(r) m_d(\nu, r) = 1, \tag{258}$$

yielding a second spatial moment of

$$\int_0^\infty r^2\, \Omega_d(r) m_d(\nu, r) = 2d\nu^2. \tag{259}$$

The radial diffusion mode for the one-dimensional rod ($d = 1$) is

$$m_1(\nu, r) = \frac{e^{-\frac{r}{\nu}}}{2\nu}, \tag{260}$$

for flatland ($d = 2$) is

$$m_2(\nu, r) = \frac{K_0\left(\frac{r}{\nu}\right)}{2\pi\nu^2}, \tag{261}$$

and for three dimensions is

$$m_3(\nu, r) = \frac{e^{-\frac{r}{\nu}}}{4\pi r\nu^2}. \tag{262}$$

MC Code and Mathematica Validation (github):
code/common

8.4 Plane-to-Point Transformation

The fluence due to an isotropic *plane* source ϕ_{pl} is related to the fluence due to an isotropic *point* source ϕ_{pt} by [Bell and Glasstone 1970]

$$\phi_{\text{pl}}(x) = 2\pi \int_0^\infty \phi_{\text{pt}}(r)\, y\, dy = 2\pi \int_{|x|}^\infty \phi_{\text{pt}}(r)\, r\, dr, \tag{263}$$

where $r^2 = y^2 + x^2$. Upon differentiation with respect to x, the result is

$$\phi_{\text{pt}}(r) = -\frac{1}{2\pi r} \frac{d\phi_{\text{pl}}(x)}{dx}|_{x=r} \tag{264}$$

8.5 The H-function

The H-function appears in the solution to 1D steady-state half-space problems. It is the solution of the integral equation:

$$\frac{1}{H(u)} = 1 - \frac{\alpha u}{2} \int_0^1 \frac{H(u')}{u + u'} du' \tag{265}$$

where α is the single-scattering albedo. Additionally,

$$\frac{1}{H(u)} = \sqrt{1-\alpha} + \frac{1}{2}\alpha \int_0^1 \frac{u' H(u')}{u + u'} du' \tag{266}$$

8.5.1 H-function numerical evaluation (Stibbs-Weir)

A stable numerical integral for computing the H-function is [Stibbs and Weir 1959]

$$H(u) = \exp\left(-\frac{u}{\pi} \int_0^{\frac{\pi}{2}} \frac{\log(1 - t\alpha\cot(t))}{u^2 \sin^2(t) + \cos^2(t)}\, dt \right) \tag{267}$$

8.5.2 H-function Benchmark Values

Benchmark values for $H(u)$ are given in Table 4. This implementation has been validated again data given by [Chandrasekhar 1960].

8.5.3 H-function Approximations

Approximation 1 The H-function can be evaluated approximately to within 6% by [Hapke 1981] (getting worse for α near 1)

$$H(u) \approx \frac{1 + 2u}{1 + 2\,u\,\sqrt{1-\alpha}}. \tag{268}$$

Approximation 2 The H-function can be evaluated approximately to within 1% by [Hapke 2012]

$$H(u) \approx \frac{1}{1 - u(1-y)\left(\left(n(-u) - \frac{n}{2} + 1\right)\log\left(\frac{u+1}{u}\right) + n\right)} \tag{269}$$

where

$$n = \frac{1-y}{1+y},$$

			u		
α	0.01	0.1	0.2	0.5	1.0
0.001	1.00002	1.00012	1.00018	1.00027	1.00035
0.01	1.00023	1.0012	1.0018	1.00276	1.00349
0.05	1.00116	1.00609	1.00914	1.01409	1.01785
0.1	1.00235	1.01238	1.01864	1.02892	1.03682
0.2	1.00478	1.02562	1.03892	1.06118	1.07865
0.3	1.0073	1.03987	1.06115	1.09756	1.12684
0.5	1.01272	1.07237	1.11346	1.18774	1.25126
0.7	1.01887	1.11303	1.18252	1.31795	1.44475
0.8	1.02242	1.13881	1.22864	1.41326	1.59822
0.9	1.0266	1.17214	1.29143	1.55603	1.8501
0.95	1.02923	1.19523	1.33734	1.67179	2.07712
0.98	1.03131	1.21513	1.37876	1.78629	2.32579
0.99	1.03226	1.22488	1.39977	1.8486	2.47279
0.995	1.03289	1.23162	1.41463	1.89463	2.58735
0.999	1.03367	1.24042	1.43442	1.95869	2.75607
0.9999	1.03408	1.24518	1.44532	1.99545	2.85822
0.99999	1.03421	1.24667	1.44876	2.00728	2.89196
0.999999	1.03424	1.24713	1.44985	2.01104	2.90278

Table 4: *H-function benchmark solutions: $H(u)$ for various single-scattering albedos α*

$$y = \sqrt{1-\alpha}.$$

8.5.4 H-function Moments

The average value of the H-function is [Chandrasekhar 1960] (Section 38, Theorem 1)

$$\frac{\alpha}{2}\int_0^1 H(u)du = 1 - \sqrt{1-\alpha} \tag{270}$$

An approximation for general moments of order j is

$$\int_0^1 H(u)u^j du \approx \frac{1}{j+1}\frac{2}{1+y}\left(1 + \frac{j}{2(j+2)}\frac{1-y}{1+y}\right) \tag{271}$$

8.5.5 Further Reading

See [Chandrasekhar 1960, Stibbs and Weir 1959, Case and Zweifel 1967, McCormick and Kuščer 1973] for more on the properties of exact H functions. Three additional H-function approximations are given in [Abu-Shumays 1967].

MC Code and Mathematica Validation (github):
code/common

8.6 Singular Eigenfunctions (Caseology)

The singular eigenfunction anaylsis of Case [1960, 1967] (see also [McCormick and Kuščer 1973]) leads to functions and singular distributions that appear repeatedly in many simple isotropic scattering problem solutions. These are listed here.

8.6.1 Asymptotic Relaxation Length (The Discrete Eigenvalue for Isotropic Scattering)

For non-zero absorption levels, $0 < \alpha < 1$, ν_0 is the *asymptotic relaxation length* (sometimes called the rigorous or asymptotic diffusion length)—the positive solution of:

$$1 = \alpha\nu_0 \tanh^{-1}\frac{1}{\nu_0} = \frac{\alpha\nu_0}{2}\log\frac{\nu_0+1}{\nu_0-1}. \tag{272}$$

Note that ν_0 is real only when $\alpha < 1$. Closed-form expressions for ν_0 include [Siewert et al. 1999]:

$$\nu_0 = (1-\alpha)^{-1/2}\exp\left[-\frac{1}{\pi}\int_0^1 \Theta(\alpha,x)\frac{dx}{x}\right] \tag{273}$$

$$\nu_0 = \left[\frac{3-2\alpha}{3-3\alpha} - \frac{2}{\pi}\int_0^1 \Theta(\alpha,x)x\,dx\right]^{1/2} \tag{274}$$

$$\Theta(\alpha,x) = \arctan\left[\frac{\alpha\pi x}{2[1-\alpha x\,\mathrm{arctanh}(x)]}\right] \tag{275}$$

Further Reading

For more closed form expressions also see [McInerney 1964].

Approximations An approximation for ν_o due to Case et al. [1953] accurate to within 0.05% is:

$$\nu_0(\alpha) \approx \begin{cases} 1/\kappa_0 & \text{if } \alpha \le 0.56 \\ 1/\kappa_1 & \text{if } \alpha > 0.56 \end{cases} \tag{276}$$

where

$$\kappa_0 = 1 - 2e^{-2/\alpha}\left(1 + \frac{e^{-2/\alpha}(4-\alpha)}{\alpha} + \frac{e^{-4/\alpha}\left(\alpha^2-12\alpha+24\right)}{\alpha^2} + \frac{e^{-6/\alpha}\left(-3\alpha^3+72\alpha^2-384\alpha+512\right)}{3\alpha^3}\right) \tag{277}$$

and

$$\kappa_1 = \sqrt{3}\left(\frac{166(1-\alpha)^4}{67375} - \frac{2}{125}(1-\alpha)^3 - \frac{12}{175}(1-\alpha)^2 - \frac{2(1-\alpha)}{5} + 1\right)\sqrt{1-\alpha} \tag{278}$$

Benchmark data Benchmark values for ν_0 are given in Figure 82. For $\alpha = 0.999$ this implementation using MATHEMATICA's FindRoot function with a working precision of 40 digits matches the value presented in [Siewert et al. 1999] (and the author's response). For very high absorption levels the value is very near 1 and may cause issues in floating point precision.

α	ν_0
0.01	1.000000000000000000000000000000093600630
0.05	1.000000000000000000849670851058318091 4518
0.1	1.000000004122307593242207339133885345957
0.2	1.000090886544380710821109192160326963735
0.3	1.002592888793223199142982501642964092168
0.5	1.044382033760833484984013906344747760869
0.7	1.206804253985286033572144537105448397639
0.8	1.407634309062772015890071825808163836056
0.85	1.588558625363179696428421317704501663412
0.9	1.903204856044847718980561237457780816825
0.95	2.635148834268739177311679967586549522622
0.98	4.115520476316445421271431792682995753410
0.99	5.796729451302002309775836365597598793316
0.995	8.181342535857420321730013033380917475302
0.999	18.264725726526673733563504629269480435 53
0.9999	57.737336452012897174190884598051472613 47
0.99999	182.574916135971860243033628341329873 7341
0.999999	577.350500129865406213129205961077343272 2

(a)

Figure 82: *Benchmark values for the asymptotic relaxation length (the discrete eigenvalue)* ν_0 *for a medium with isotropic scattering.*

MC Code and Mathematica Validation (github):
code/common

8.6.2 Normalization Integrals

The normalization integrals are given by

$$N_0^{\pm} = \pm\frac{\alpha}{2}\nu_0^3\left[\frac{\alpha}{\nu_0^2-1} - \frac{1}{\nu_0^2}\right], \tag{279}$$

$$N_\nu = \nu\left[\lambda^2(\nu) + \frac{\pi^2\alpha^2}{4}\nu^2\right], \tag{280}$$

$$\lambda(\nu) = 1 - \alpha\nu\tanh^{-1}\nu. \tag{281}$$

8.6.3 The Singular Eigenfunctions

The singular eigenfunctions for plane symmetry with isotropic scattering are given by

$$\psi_\nu(u) = \frac{\alpha}{2}P\frac{\nu}{\nu-u} + \lambda(\nu)\delta(u-\nu) \tag{282}$$

$$\psi_0^{\pm}(u) = \frac{\alpha}{2}\frac{\nu_0}{\nu_0 \mp u} \tag{283}$$

and satisfy

$$\int_{-1}^{1}\psi_\nu(u)du = 1 \tag{284}$$

$$N_0^{\pm} = \int_{-1}^{1} u\psi_0^{\pm}(u)\psi_0^{\pm}(u)du \tag{285}$$

The "P" indicates the need for Cauchy principal value when the singular eigenfuctions appear inside of integrals.

References

ABU-SHUMAYS, I. 1967. The Albedo Problem and Chandrasekhar's H-Function II. *Nucl. Sci. Eng. 27*, 607–608.

ANLI, F., YASA, F., AND GUENGOER, S. 2005. General eigenvalue spectrum in a one-dimensional slab geometry transport equation. *Nucl. Sci. Eng. 150*, 1, 72–77.

ASADZADEH, M., AND LARSEN, E. 2008. Linear transport equations in flatland with small angular diffusion and their finite element approximations. *Mathematical and Computer Modelling 47*, 3-4, 495–514.

BALLINGER, C., RATHKOPF, J., AND MARTIN, W. 1992. The response history monte carlo method for electron transport. *Nucl. Sci. Eng. 112*, 4, 283–295.

BARO, J., SEMPAU, J., FERNÁNDEZ-VAREA, J., AND SALVAT, F. 1995. PENELOPE: an algorithm for Monte Carlo simulation of the penetration and energy loss of electrons and positrons in matter. *Nuclear Instruments and Methods in Physics Research Section B: Beam Interactions with Materials and Atoms 100*, 1, 31–46.

BAXTER, R. 1967. Method of solution of the percus-yevick, hypernetted-chain, or similar equations. *Physical Review 154*, 1, 170.

BELL, G. I., AND GLASSTONE, S. 1970. *Nuclear reactor theory*. Van Nostrand Reinhold.

BENOIST, P., AND KAVENOKY, A. 1968. A new method of approximation of the Boltzmann equation. *Nucl. Sci. Eng. 32*, 225–232.

BERGER, M. J. 1963. Monte carlo calculation of the penetration and diffusion of fast charged particles. *Methods in computational physics 1*, 135–215.

BHAN, K., AND SPANIER, J. 2007. Condensed history monte carlo methods for photon transport problems. *Journal of computational physics 225*, 2, 1673–1694.

BOLTZMANN, L. 1878. Zur theorie der elastischen nachwirkung. *Annalen der Physik 241*, 11, 430–432.

BORN, M., AND WOLF, E. 2002. *Principles of optics: electromagnetic theory of propagation, interference and diffraction of light*. Cambridge University Press.

BOROVOI, A. 2002. On the extinction of radiation by a homogeneous but spatially correlated random medium: comment. *JOSA A 19*, 12, 2517–2520.

BOTHE, W. 1942. Die diffusion von einer punktquelle aus (nachtrag zu der arbeit einige diffusionsprobleme). *Zeitschrift für Physik A Hadrons and Nuclei 119*, 7, 493–497.

CASE, K., AND ZWEIFEL, P. 1963. Existence and uniqueness theorems for the neutron transport equation. *Journal of Mathematical Physics 4*, 11, 1376–1385.

CASE, K. M., AND ZWEIFEL, P. F. 1967. *Linear Transport Theory*. Addison-Wesley.

CASE, K. M., DE HOFFMAN, F., AND PLACZEK, G. 1953. *Introduction to the Theory of Neutron Diffusion*, vol. 1. US Government Printing Office.

CASE, K. 1960. Elementary solutions of the transport equation and their applications* 1. *Annals of Physics 9*, 1, 1–23.

CASSELL, J., AND WILLIAMS, M. 1992. Discrete eigenvalues of the one-speed transport equation for asymmetric scattering. *Annals of Nuclear Energy 19*, 7, 403–407.

CHANDRASEKHAR, S. 1960. *Radiative Transfer*. Dover.

CHU, C.-M., AND CHURCHILL, S. W. 1955. Representation of the angular distribution of radiation scattered by a spherical particle. *J. Opt. Soc. Am. 45*, 11 (Nov), 958–961.

CHWOLSON, O. 1890. Grundzuge einer mathematischen theorie der inneren diffusion des lichtes. *Bull. St. Petersburg Acad. Sci 33*, 2, 221–256.

COOPER, M. 2000. *Angular Distribution of Particles Emerging from a Diffusive Region and its Implications for the Fleck-Canfield Random Walk Algorithm for Implicit Monte Carlo Radiation Transport*. Jul.

COVEYOU, R. 1965. A monte carlo technique for selecting neutron scattering angles from anisotropic distributions. *Nucl. Sci. Eng. 21*, 260–262.

DAVIS, A., AND MARSHAK, A., 1997. Levy kinetics in slab geometry: Scaling of transmission probability.

DAVIS, A. B., AND MARSHAK, A. 2004. Photon propagation in heterogeneous optical media with spatial correlations: enhanced mean-free-paths and wider-than-exponential free-path distributions. *Journal of Quantitative Spectroscopy and Radiative Transfer 84*, 1, 3–34.

DAVIS, A. B., AND XU, F. 2014. A generalized linear transport model for spatially correlated stochastic media. *Journal of Computational and Theoretical Transport 43*, 1-7, 474–514.

DAVIS, A., LOVEJOY, S., AND SCHERTZER, D. 1993. Supercomputer simulation of radiative transfer inside multifractal cloud models. In *International Radiation Symposium*, vol. 92, 112–115.

DAVIS, A. B. 2006. Effective propagation kernels in structured media with broad spatial correlations, illustration with large-scale transport of solar photons through cloudy atmospheres. In *Computational Methods in Transport*. Springer, 85–140.

DAVISON, B. 1957. *Neutron Transport Theory*. Oxford University Press.

DAVISON, B. 2000. Angular distribution due to an isotropic point source and spherically symmetrical eigensolutions of the transport equation (mt-112). *Progress in Nuclear Energy 36*, 3, 323 – 365. Nuclear Reactor Theory in Canada 1943-1946.

DENSMORE, J. D., EVANS, T. M., AND BUKSAS, M. W. 2008. A hybrid transport-diffusion algorithm for monte carlo radiation-transport simulations on adaptive-refinement meshes in xy geometry. *Nucl. Sci. Eng. 159*, 1, 1–22.

D'EON, E. 2014. Rigorous asymptotic and moment-preserving diffusion approximations for generalized linear boltzmann transport in arbitrary dimension. *Transport Theory and Statistical Physics 42*, 6-7, 237–297.

D'EON, E. 2016. Diffusion approximations for nonclassical boltzmann transport in arbitrary dimension. Tech. rep.

DUDERSTADT, J., AND MARTIN, W. 1979. *Transport theory.* Wiley-Interscience.

DUTKA, J. 1985. On the problem of random flights. *Archive for history of exact sciences 32*, 3, 351–375.

FLECK, J., AND CANFIELD, E. 1984. A random walk procedure for improving the computational efficiency of the implicit monte carlo method for nonlinear radiation transport. *Journal of Computational Physics 54*, 3, 508–523.

FLOCK, S., WILSON, B., AND PATTERSON, M. 1987. Total attenuation coefficients and scattering phase functions of tissues and phantom materials at 633 nm. *Medical physics 14*, 835.

FOMENKO, V. N., SHVARTS, F. M., AND SHVARTS, M. A. 2000. Exact description of photon migration in anisotropically scattering media. *Phys. Rev. E 61*, 2 (Feb), 1990–1995.

FRANK, M., GOUDON, T., ET AL. 2010. On a generalized boltzmann equation for non-classical particle transport. *Kinetic and Related Models 3*, 395–407.

FRANK, M., KRYCKI, K., LARSEN, E. W., AND VASQUES, R. 2015. The nonclassical boltzmann equation and diffusion-based approximations to the boltzmann equation. *SIAM Journal on Applied Mathematics 75*, 3, 1329–1345.

FRANKE, B. C., AND PRINJA, A. K. 2005. Monte carlo electron dose calculations using discrete scattering angles and discrete energy losses. *Nucl. Sci. Eng. 149*, 1, 1–22.

FURFARO, R., AND GANAPOL, B. 2007. Spectral Theory for Photon Transport in Dense Vegetation Media: Caseology for the Canopy Equation. *Transport Theory and Statistical Physics 36*, 1, 107–135.

GANAPOL, B., AND MYNENI, R. 1992. The application of the principles of invariance to the radiative transfer equation in plant canopies. *Journal of Quantitative Spectroscopy and Radiative Transfer 48*, 3, 321–339.

GANAPOL, B., AND MYNENI, R. 1992. The fn method for the one-angle radiative transfer equation applied to plant canopies. *Remote sensing of environment 39*, 3, 213–231.

GANAPOL, B. D. 2003. Fourier transform transport solutions in spherical geometry. *Transport Theory and Statistical Physics 32*, 5, 587 – 605.

GIUSTO, A., SAIJA, R., IATÌ, M. A., DENTI, P., BORGHESE, F., AND SINDONI, O. I. 2003. Optical properties of high-density dispersions of particles: application to intralipid solutions. *Applied optics 42*, 21, 4375–4380.

GKIOULEKAS, I., XIAO, B., ZHAO, S., ADELSON, E. H., ZICKLER, T., AND BALA, K. 2013. Understanding the role of phase function in translucent appearance. *ACM Transactions on Graphics (TOG) 32*, 5, 147.

GOLSE, F. 2012. Recent results on the periodic lorentz gas. *Nonlinear Partial Differential Equations*, 39–99.

GOUDSMIT, S., AND SAUNDERSON, J. 1940. Multiple scattering of electrons. *Physical Review 57*, 1, 24.

GRIESHEIMER, D. P., MILLMAN, D. L., AND WILLIS, C. R. 2011. Analysis of distances between inclusions in finite binary stochastic materials. *Journal of Quantitative Spectroscopy and Radiative Transfer 112*, 4, 577–598.

GROSJEAN, C. 1951. The Exact Mathematical Theory of Multiple Scattering of Particles in an Infinite Medium. *Memoirs Kon. Vl. Ac. Wetensch. 13*, 36.

GROSJEAN, C. C. 1953. Solution of the non-isotropic random flight problem in the k-dimensional space. *Physica 19*, 1-12, 29–45.

GROSJEAN, C. C. 1956. A high accuracy approximation for solving multiple scattering problems in infinite homogeneous media. *Il Nuovo Cimento 3*, 6 (Jun), 1262–1275.

GROSJEAN, C. C. 1958. Multiple Isotropic Scattering in Convex Homogeneous Media Bounded by Vacuum. *Proceedings of the Second International Conference on the Peaceful Uses of Atomic Energy 16*, 431.

GROSJEAN, C. C. 1963. A new approximate one-velocity theory for treating both isotropic and anisotropic multiple scattering problems. Part I. Infinite homogeneous scattering media. Tech. rep., Universiteit, Ghent.

GUÉRIN, C.-A., MALLET, P., AND SENTENAC, A. 2006. Effective-medium theory for finite-size aggregates. *JOSA A 23*, 2, 349–358.

GUÉRON, D., AND MAZZOLO, A. 2003. Properties of chord length distributions across ordered and disordered packing of hard disks. *Phys. Rev. E 68* (Dec), 066117.

GUTH, E., AND INÖNÜ, E. 1960. Random-walk interpretation and generalization of linear boltzmann equations, particularly for neutron transport. *Phys. Rev. 118*, 4 (May), 899–900.

HAPKE, B. 1981. Bidirectional reflectance spectroscopy: 1. theory. *Journal of Geophysical Research: Solid Earth (1978–2012) 86*, B4, 3039–3054.

HAPKE, B. 2012. *Theory of reflectance and emittance spectroscopy*. Cambridge University Press.

HEINO, J., ARRIDGE, S., SIKORA, J., AND SOMERSALO, E. 2003. Anisotropic effects in highly scattering media. *Phys. Rev. E 68*, 3 (Sep), 031908.

HEITZ, E., AND D'EON, E. 2014. Importance sampling microfacet-based BSDFs using the distribution of visible normals. *Computer Graphics Forum*.

HEITZ, E., HANIKA, J., D'EON, E., AND DACHSBACHER, C. 2015. Multiple-scattering microfacet bsdfs with the smith model. Technical report.

HENYEY, L. G., AND GREENSTEIN, H. L. 1941. Diffuse radiation in the galaxy. *Astrophys. J. 43*, 70–83.

HOOGENBOOM, J. 2008. The two-direction neutral-particle transport model: A useful tool for research and education. *Transport Theory and Statistical Physics 37*, 1, 65–108.

IRVINE, W. M. 1975. Multiple scattering in planetary atmospheres. *Icarus 25*, 2, 175–204.

ISHIMARU, A., AND KUGA, Y. 1982. Attenuation constant of a coherent field in a dense distribution of particles. *JOSA 72*, 10, 1317–1320.

JAKEMAN, E., AND TOUGH, R. 1987. Generalized k distribution: a statistical model for weak scattering. *JOSA A 4*, 9, 1764–1772.

JAKOB, W., ARBREE, A., MOON, J., BALA, K., AND MARSCHNER, S. 2010. A radiative transfer framework for rendering materials with anisotropic structure. *ACM Transactions on Graphics (TOG) 29*, 4, 1–13.

JENSEN, H. W., MARSCHNER, S. R., LEVOY, M., AND HANRAHAN, P. 2001. A practical model for subsurface light transport. In *Proceedings of ACM SIGGRAPH 2001*, 511–518.

JI, W., AND MARTIN, W. R. 2007. Determination of chord length distributions in stochastic media composed of dispersed microspheres. *TRANSACTIONS-AMERICAN NUCLEAR SOCIETY 96*, 467.

KAGIWADA, H., AND KALABA, R. 1967. Multiple anisotropic scattering in slabs with axially symmetric fields. Tech. rep., DTIC Document.

KAPER, H. G., SHULTIS, J. K., AND VENINGA, J. G. 1970. Numerical evaluation of the slab albedo problem solution in one-speed anisotropic transport theory. *Journal of Computational Physics 6*, 2, 288–313.

KAWRAKOW, I., AND BIELAJEW, A. F. 1998. On the condensed history technique for electron transport. *Nuclear Instruments and Methods in Physics Research Section B: Beam Interactions with Materials and Atoms 142*, 3, 253–280.

KELLOGG, R. 1974. First derivatives of solution of the plane neutron transport equation. *Technical Note BN-783, Institute for Fluid Dynamics and Applied Mathematics, Univ. Maryland*.

KIENLE, A., AND PATTERSON, M. 1996. Determination of the optical properties of turbid media from a single monte carlo simulation. *Physics in medicine and biology 41*, 2221.

KLUYVER, J. 1906. A local probability problem. *Nederl. Acad. Wetensch. Proc 8*, 341–350.

KOSTINSKI, A. B. 2001. On the extinction of radiation by a homogeneous but spatially correlated random medium. *JOSA A 18*, 8, 1929–1933.

KOSTINSKI, A. B. 2002. On the extinction of radiation by a homogeneous but spatially correlated random medium: reply to comment. *JOSA A 19*, 12, 2521–2525.

KUGA, Y., AND ISHIMARU, A. 1984. Retroreflectance from a dense distribution of spherical particles. *JOSA A 1*, 8, 831–835.

KUŠČER, I., AND SUMMERFIELD, G. C. 1969. Symmetries in scattering of slow neutrons. *Phys. Rev. 188*, 3 (Dec), 1445–1449.

LARSEN, M. L., AND CLARK, A. S. 2013. On the link between particle size and deviations from the beer-lambert-bouguer law for direct transmission. *Journal of Quantitative Spectroscopy and Radiative Transfer*.

LARSEN, E. W., AND VASQUES, R. 2011. A generalized linear boltzmann equation for non-classical particle transport. *Journal of Quantitative Spectroscopy and Radiative Transfer 112*, 4, 619–631.

LARSEN, E. W. 1992. A theoretical derivation of the condensed history algorithm. *Annals of Nuclear Energy 19*, 10-12, 701–714.

LEWIS, H. 1950. Multiple scattering in an infinite medium. *Physical review 78*, 5, 526.

LIEMERT, A., AND KIENLE, A. 2011. Radiative transfer in two-dimensional infinitely extended scattering media. *Journal of Physics A: Mathematical and Theoretical 44*, 505206.

LIEMERT, A., AND KIENLE, A. 2012. Analytical approach for solving the radiative transfer equation in two-dimensional layered media. *Journal of Quantitative Spectroscopy and Radiative Transfer 113*, 7, 559–564.

LIEMERT, A., AND KIENLE, A. 2012. Green's functions for the two-dimensional radiative transfer equation in bounded media. *Journal of Physics A: Mathematical and Theoretical 45*, 17, 175201–175209.

LIU, P. 1994. A new phase function approximating to mie scattering for radiative transport equations. *Physics in Medicine and Biology 39*, 1025.

LOMMEL, E. 1889. Subjective Interferenzstreifen im objectiven Spectrum. *Annalen der Physik 272*, 729–730.

MACHIDA, M. 2015. The radiative transport equation in flatland with separation of variables. *arXiv preprint arXiv:1511.05723*.

MARCHESINI, R., BERTONI, A., ANDREOLA, S., MELLONI, E., AND SICHIROLLO, A. 1989. Extinction and absorption coefficients and scattering phase functions of human tissues in vitro. *Appl. Opt 28*, 12, 2318–2324.

MCCORMICK, N., AND KUŠČER, I. 1973. Singular eigenfunction expansions in neutron transport theory. *Advan. Nucl. Sci. Technol., v. 7, pp. 181-282 7*.

MCINERNEY, J. 1964. Some exact expressions for the monoenergetic neutron diffusion length. *Nucl. Sci. Eng. 19*, 458–460.

METROPOLIS, N., ROSENBLUTH, A. W., ROSENBLUTH, M. N., TELLER, A. H., AND TELLER, E. 1953. Equation of state calculations by fast computing machines. *The journal of chemical physics 21*, 1087.

METZLER, R., AND KLAFTER, J. 2000. The random walk's guide to anomalous diffusion: a fractional dynamics approach. *Physics reports 339*, 1, 1–77.

MIKATA, Y. 2014. Exact analytical solution of time-independent neutron transport equation, and its applications to systems with a point source. *Annals of Nuclear Energy 64*, 152–155.

MISHCHENKO, M. I. 2013. 125 years of radiative transfer: Enduring triumphs and persisting misconceptions. In *AIP Conference Proceedings*, vol. 1531, 11.

MISHCHENKO, M. I. 2014. Directional radiometry and radiative transfer: The convoluted path from centuries-old phenomenology to physical optics. *Journal of Quantitative Spectroscopy and Radiative Transfer*.

MOON, J., WALTER, B., AND MARSCHNER, S. 2007. Rendering discrete random media using precomputed scattering solutions. *Rendering Techniques 2007*, 231–242.

MOURANT, J., FREYER, J., HIELSCHER, A., EICK, A., SHEN, D., AND JOHNSON, T. 1998. Mechanisms of light scattering from biological cells relevant to noninvasive optical-tissue diagnostics. *Applied Optics 37*, 16, 3586–3593.

MYNENI, R. B., MARSHAK, A. L., AND KNYAZIKHIN, Y. V. 1991. Transport theory for a leaf canopy of finite-dimensional scattering centers. *Journal of Quantitative Spectroscopy and Radiative Transfer 46*, 4, 259–280.

NICKELL, S., HERMANN, M., ESSENPREIS, M., FARRELL, T. J., KRAMER, U., AND PATTERSON, M. S. 2000. Anisotropy of light propagation in human skin. *Physics in Medicine and Biology 45*, 10, 2873.

NIGMATULLIN, R. 1986. The realization of the generalized transfer equation in a medium with fractal geometry. *physica status solidi (b) 133*, 1, 425–430.

NUYENS, M., AND GROSJEAN, C. 1949. Sur la diffusion des neutrons thermiques. *C.R. Acad. Sci. Paris 228*, 245–246.

OLSON, G. L., MILLER, D. S., LARSEN, E. W., AND MOREL, J. E. 2006. Chord length distributions in binary stochastic media in two and three dimensions. *Journal of Quantitative Spectroscopy and Radiative Transfer 101*, 2, 269–283.

OLSON, G. L. 2008. Chord length distributions between hard disks and spheres in regular, semi-regular, and quasi-random structures. *Annals of Nuclear Energy 35*, 11, 2150–2155.

PAASSCHENS, J. C. J. 1997. Solution of the time-dependent boltzmann equation. *Phys. Rev. E 56*, 1 (Jul), 1135–1141.

PEARSON, K. 1905. The problem of the random walk. *Nature 72*, 1865, 294.

PERCUS, J. K., AND YEVICK, G. J. 1958. Analysis of classical statistical mechanics by means of collective coordinates. *Physical Review 110*, 1, 1.

PERRAM, J. 1975. Hard sphere correlation functions in the percus-yevick approximation. *Molecular Physics 30*, 5, 1505–1509.

PETERSON, M. A. 1983. Angular distributions in multiple scattering. *Physical Review A 28*, 1, 135.

PHARR, M., AND HUMPHREYS, G. 2010. *Physically Based Rendering, Second Edition: From Theory To Implementation*, 2 ed. Morgan Kaufmann, July.

PICCA, P., AND FURFARO, R. 2013. Analytical discrete ordinate method for radiative transfer in dense vegetation canopies. *Journal of Quantitative Spectroscopy and Radiative Transfer 118*, 60–69.

PICCA, P., FURFARO, R., AND GANAPOL, B. D. 2012. An efficient multiproblem strategy for accurate solutions of linear particle transport problems in spherical geometry. *Nucl. Sci. Eng. 170*, 2, 103–124.

PLACZEK, G., AND VOLKOFT, G. 1943. Notes on diffusion of neutrons without change in energy. *National Research Council of Canada, Montreal Laboratories Document MT-4*.

PLACZEK, G. 1941. Manhattan report, a-25.

POMRANING, G. 1965. The albedo problem. *Nucl. Sci. Eng. 21*, 265–268.

POMRANING, G. 1992. The Fokker-Planck operator as an asymptotic limit. *Math. Models Methods Appl. Sci 2*, 1, 21–36.

POMRANING, G. 1997. Transport theory in discrete stochastic mixtures. *Advances in Nuclear Science and Technology*, 47–93.

PRAHL, S. 2002. Simple and accurate approximations fo reflectance from a semi-infinite turbid medium. In *Biomedical Topical Meeting*, Optical Society of America.

PRINJA, A., AND LARSEN, E. 2010. General principles of neutron transport. Springer, 427–542.

RAYLEIGH, L. 1919. Xxxi. on the problem of random vibrations, and of random flights in one, two, or three dimensions. *The London, Edinburgh, and Dublin Philosophical Magazine and Journal of Science 37*, 220, 321–347.

REINERT, D., SCHNEIDER, E., AND BIEGALSKI, S. 2010. Investigation of stochastic radiation transport methods in binary random heterogeneous mixtures. *Nucl. Sci. Eng. 166*, 2, 167–174.

REYNOLDS, L., AND MCCORMICK, N. 1980. Approximate two-parameter phase function for light scattering. *JOSA 70*, 10, 1206–1212.

SAVO, R., BURRESI, M., SVENSSON, T., VYNCK, K., AND WIERSMA, D. S. 2014. Walk dimension for light in complex disordered media. *Phys. Rev. A 90* (Aug), 023839.

SCHLICK, C. 1994. An inexpensive brdf model for physically-based rendering. *Computer Graphics Forum 13*, 3, 223–246.

SCHUSTER, A. 1905. Radiation through a foggy atmosphere. *Astrophys. J. 21*, 1–22.

SEARS, V. F. 1975. Slow-neutron multiple scattering. *Advances in Physics 24*, 1, 1–45.

SEN, K., AND WILSON, S. J. 1990. *Radiative Transfer in Curved Media: Basic and Mathematical Methods for Radiative Transfer and Transport Problems in Participating Media of Spherical and Cylindrical Geometry*. World Scientific.

SHARMA, S. K. 2015. A review of approximate analytic light-scattering phase functions. In *Light Scattering Reviews 9*. Springer, 53–100.

SIEWERT, C., PEROVICH, S., DJUROVIC, I., AND TOSIC, D. 1999. Some comments concerning the discrete eigenvalue (and author's reply). *Nucl. Sci. Eng. 131*, 3, 439–441.

SMITH, W., AND HENDERSON, D. 1970. Analytical representation of the percus-yevick hard-sphere radial distribution function. *Molecular Physics 19*, 3, 411–415.

SMOLUCHOWSKI, M. V. 1916. Drei vortrage uber diffusion, brownsche bewegung und koagulation von kolloidteilchen. *Zeitschrift fur Physik 17*, 557–585.

SOBOLEV, V. 1975. *Light scattering in planetary atmospheres*. Pergamon Press (Oxford and New York).

STADJE, W. 1987. The exact probability distribution of a two-dimensional random walk. *Journal of statistical physics 46*, 1-2, 207–216.

STIBBS, D., AND WEIR, R. 1959. On the H-functions for isotropic scattering. *Monthly Notices of the Royal Astronomical Society 119*, 512.

SVENSSON, T., VYNCK, K., GRISI, M., SAVO, R., BURRESI, M., AND WIERSMA, D. S. 2013. Holey random walks: Optics of heterogeneous turbid composites. *Physical Review E 87*, 2, 022120.

TOLAR JR, D. R., AND LARSEN, E. W. 2001. The moment condensed history algorithm for monte carlo electron transport simulations. In *Proceedings of the ANS Topical Meeting: International Conference on Mathematical Methods to Nuclear Applications, Salt Lake City, Utah, September*, 9–13.

TOLAR JR, D. R., AND LARSEN, E. W. 2001. A transport condensed history algorithm for electron monte carlo simulations. *Nucl. Sci. Eng. 139*, 1, 47–65.

TRAMONTANA, V., CASASANTA, G., GARRA, R., AND IANNARELLI, A. 2013. An application of wright functions to the photon propagation. *Journal of Quantitative Spectroscopy and Radiative Transfer*.

TSANG, L., AND ISHIMARU, A. 1984. Backscattering enhancement of random discrete scatterers. *JOSA A 1*, 8, 836–839.

TSANG, L., DING, K., SHIH, S., AND KONG, J. 1998. Scattering of electromagnetic waves from dense distributions of spheroidal particles based on monte carlo simulations. *JOSA A 15*, 10, 2660–2669.

TSANG, L., CHEN, C.-T., CHANG, A. T., GUO, J., AND DING, K.-H. 2000. Dense media radiative transfer theory based on quasicrystalline approximation with applications to passive microwave remote sensing of snow. *Radio Science 35*, 3, 731–749.

TUCHIN, V. 2007. *Tissue Optics: Light Scattering Methods and Instruments for Medical Diagnosis*, 2nd ed. SPIE Press.

VAN DE HULST, H. C., AND GRAAFF, R. 1996. Aspects of similarity in tissue optics with strong forward scattering. *Physics in Medicine and Biology 41*, 11, 2519.

VAN DE HULST, H. 1980. *Multiple light scattering*. Academic Press.

VASQUES, R., AND LARSEN, E. W. 2013. Non-classical transport with angular-dependent path-length distributions. 1: Theory. *arXiv preprint arXiv:1309.4817*.

WATSON, G. N. 1962. *A Treatise on the Theory of Bessel Functions*, 2nd ed. Cambridge University Press.

WEINBERG, A. M., AND WIGNER, E. P. 1958. *The physical theory of neutron Chain Reactors*. University of Chicago Press.

WERTHEIM, M. 1963. Exact solution of the percus-yevick integral equation for hard spheres. *Physical Review Letters 10*, 8, 321–323.

WEYRICH, T., MATUSIK, W., PFISTER, H., BICKEL, B., DONNER, C., TU, C., MCANDLESS, J., LEE, J., NGAN, A., JENSEN, H. W., AND GROSS, M. 2006. Analysis of human faces using a measurement-based skin reflectance model. *ACM Trans. Graphic. 25*, 1013–1024.

WIGNER, E. 1954. The Problem of Multiple Scattering. *Physical Review 94*, 1, 17.

WILLIAMS, M. M. R. 1971. *Mathematical methods in particle transport theory.* Wiley.

WILLIAMS, M. M. R. 1977. Comments on Particle Transport in Finite Slabs. *Nucl. Sci. Eng. 63*, 357–358.

WILLIAMS, M. M. R. 1992. A new model for describing the transport of radionuclides through fractured rock. *Annals of Nuclear Energy 19*, 10-12, 791–824.

WILLIAMS, M. M. R. 2006. The albedo problem with Fresnel reflection. *Journal of Quantitative Spectroscopy and Radiative Transfer 98*, 3, 358–378.

WING, G. 1962. *An introduction to transport theory*. Wiley.

WYMAN, D. R., AND PATTERSON, M. S. 1988. A discrete method for anisotropic angular sampling in monte carlo simulations. *Journal of Computational Physics 76*, 2, 414–425.

WYMAN, D. R., PATTERSON, M. S., AND WILSON, B. C. 1989. Similarity relations for anisotropic scattering in monte carlo simulations of deeply penetrating neutral particles. *J. Comput. Phys. 81*, 137–150.

XU, F., DAVIS, A. B., AND DINER, D. J. 2016. Markov chain formalism for generalized radiative transfer in a plane-parallel medium, accounting for polarization. *Journal of Quantitative Spectroscopy and Radiative Transfer*, –.

ZACCANTI, G., BIANCO, S. D., AND MARTELLI, F. 2003. Measurements of optical properties of high-density media. *Applied optics 42*, 19, 4023–4030.

ZHAO, S., RAMAMOORTHI, R., AND BALA, K. 2014. High-order similarity relations in radiative transfer. *ACM Transactions on Graphics (TOG) 33*, 4, 104.

ZIYA AKCASU, A., AND CORNGOLD, N. 2007. Strategies in stochastic transport. *Nucl. Sci. Eng. 156*, 1, 55–67.

ZOIA, A., DUMONTEIL, E., AND MAZZOLO, A. 2011. Collision densities and mean residence times for d-dimensional exponential flights. *Physical Review E 83*, 4, 041137.

ZOIA, A., DUMONTEIL, E., AND MAZZOLO, A. 2011. Collision statistics for random flights with anisotropic scattering and absorption. *Physical Review E 84*, 6, 061130.

ZOIA, A., DUMONTEIL, E., AND MAZZOLO, A. 2011. Residence time and collision statistics for exponential flights: the rod problem revisited. *Physical Review E 84*, 2, 021139.

ZURK, L., TSANG, L., DING, K., AND WINEBRENNER, D. 1995. Monte carlo simulations of the extinction rate of densely packed spheres with clustered and nonclustered geometries. *JOSA A 12*, 8, 1772–1781.